Inelastic Collisions of Fast Charged Particles with Atoms and Molecules—The Bethe Theory Revisited*

MITIO INOKUTI

Joint Institute for Laboratory Astrophysics† of the University of Colorado and of the National Bureau of Standards, Boulder, Colorado 80302
Argonne National Laboratory,‡ Argonne, Illinois 60439

The current understanding is summarized from a unified point of view, which Bethe initiated four decades ago and which enables one to put a variety of theoretical and experimental data into a coherent picture. Properties of the generalized oscillator strength, which plays the central role in the theory, are treated in detail. The integrated cross section for inelastic scattering and related quantities at the high-velocity limit also are discussed. The theory provides a series of criteria for testing the compatibility of cross-section data and atomic (or molecular) properties that may be obtained from theory or independent experiments.

CONTENTS

1. Introduction 297
2. The Differential Cross Section 298
 2.1 The Basic Formulas 298
 2.2 Commentary 299
 2.3 Relativistic Effects 303
 2.4 Conceptual Generalizations 304
3. The Generalized Oscillator Strength 305
 3.1 Experimental Studies 305
 3.2 The Bethe Surface 307
 3.3 The Sum Rules 313
 3.4 Atoms 316
 3.5 Molecules 321
4. The Integrated Cross Section 323
 4.1 The Basic Formulas 323
 4.2 The Fano Plot and Its Applications 328
 4.3 Total Cross Section for Inelastic Scattering and Stopping Power 330
 4.4 Relations to Other Theories 334
5. Concluding Remarks 337
 5.1 Areas for Further Studies within the Bethe Theory. 337
 5.2 Departures from the Bethe Theory at Lower Velocities 338
 5.3 Desirable Experiments 342
Acknowledgments 343
References 343

1. INTRODUCTION

Theoretical treatments of inelastic collisions of charged particles (regarded as structureless) with atoms and molecules may be conveniently classified into two kinds: those dealing with fast collisions and those dealing with slow ones. The criterion used in making this classification is that the particle velocity is "fast" or "slow" relative to a mean orbital velocity of atomic or molecular electrons in the shell (or subshell) that pertains to the inelastic process under consideration. Electrons of a few keV kinetic energy, for example, are "fast" with respect to any discrete-level excitation of He, whereas they are not fast with respect to the K-shell ionization of Ar.

For sufficiently fast collisions, the influence of the incident particle upon an atom or molecule may be regarded as a sudden and small external perturbation. This picture leads to elementary, though systematic, formulations. Early in the century, Bohr (B13, B15, B48) developed a theory of the stopping power of materials for fast particles in terms of an impulse approximation, which regards the collision as producing sudden transfer of energy and momentum to atomic electrons. Thus, the Bohr theory indeed gave the general structure of cross-section formulas correctly, but certain dynamical details remained "phenomenological" (i.e., not calculable within the scope of the theory) owing to the lack of quantum mechanics at that time. In 1930 Bethe (B30) established a quantum-mechanical theory based on the Born approximation, and thereby derived a number of important results (B32, B33, BJ68) concerning collision cross sections and the stopping power for fast particles.

An indication of some general characteristics of fast collisions may be in order at this point. The expression for the cross section for a process in which a fast particle transfers a given amount of energy and momentum consists of two distinct factors, one dealing with *the incident particle only* and the other dealing with *the target only*. The first factor is nearly trivial; the second, the generalized oscillator strength of an atom or molecule, constitutes the central object of study. In this sense, the study of fast collisions is, in essence, that of a target property, a kind of spectroscopy. Besides, a close relationship exists between fast collisions and photoabsorption, so that the theory of fast collisions provides a means of cross-checking data from these two independent sources, a procedure that proves valuable in many instances. The problem of slow collisions, on the other hand, is essentially concerned with a combined system of the incident particle plus the target in which the former has lost its mechanical individuality, at least for a short period of time. Thus, for example, a theory of slow-electron

* Work performed under the auspices of the U.S. Atomic Energy Commission.
† Visiting Fellow 1969-1970.
‡ Permanent address.

collisions with He deals with the dynamics of He^- in its excited continuum states. Obviously, the cross section of slow collisions, unlike that for fast collisions, permits no simple factorization.

Experimentation on detailed features of inelastic collisions dates back to the celebrated work of Franck and Hertz (FH14), who measured energy losses of electrons passing through gases and thereby demonstrated individual discrete excitations of atoms or molecules. Modern versions of the Frank–Hertz experiment by various groups (Lassettre and coworkers, and Simpson and coworkers, for example), are characterized by remarkably improved resolution both in electron energy and in beam collimation (K68, L69, KMC69, TRK70). These experiments are capable of providing precise differential cross-section data. Measurements of the total (or integrated) cross sections for excitation of a discrete level or for ionization have been carried out in numerous cases since the 1930's, but the results (KD66, MS68, MBG69, Ki69) still remain very incomplete and often discordant.

An important motivation for the study of inelastic collisions of charged particles, most notably of electrons, stems from the ever-increasing need for reliable cross-section data in such diverse fields as radiation physics, plasma physics, atmospheric physics, astrophysics, and electron microscopy. It should be strongly emphasized that most of these applications primarily require *absolute* cross sections over a wide energy region, as opposed to those relative variations of cross sections over a narrow energy region, which are of great significance in atomic physics *per se*. While no universal theory applicable to the entire energy region is likely to come forth in the near future, some restricted aspects of cross sections are amenable to rigorous theoretical analysis. An example of such an analysis is provided by the detailed-balancing relationship between the cross sections for inverse processes (p. 423 of WO62, p. 554 of LL65). Another such example is found in various dispersion relations (p. 447 of WO62, p. 557 of GW64). Although these theoretically rigorous relations alone do not suffice to determine cross sections, they often prove powerful as a control on cross-section data, obtained either theoretically or experimentally. The Bethe theory for fast collisions, when properly applied, should serve a similar end. As will be illustrated later, the theory can be utilized in many ways for testing the compatibility between high-velocity cross sections and independently obtained atomic properties, and sometimes even for making an educated guess about cross sections at lower velocities.

Though Bethe worked out the major theoretical consequences of his treatment, the physical content of the theory has not yet been fully appreciated. Besides, a systematic and detailed investigation of the generalized oscillator strength, both theoretical and experimental, still remains a goal of current study. The purpose of the present article is to summarize recent developments in the understanding of fast collisions and to indicate some worthwhile aims for future work on the subject. Its scope will be limited in the following respects. Neither elastic scattering nor molecular rotational and/or vibrational excitation will be discussed, because these subjects are significantly different from the main theme. Since this discussion is intended to be heuristic in nature, the coverage of the materials and references will be illustrative rather than exhaustive. In particular, no attempt is made to present pertinent cross-section data in a comprehensive way; discussion of such data is left to original references and to other reviews (KD66, MS68, Ki69, D69, KMC69, L69, MBG69, TRK70).

2. THE DIFFERENTIAL CROSS SECTION

2.1. The Basic Formulas

Consider a process in which a particle of velocity v, mass M_1, and charge ze (where $-e$ is the electron charge) collides with a stationary atom with mass M_2 in an initial state (most often the ground state) denoted hereafter as state 0, and gets deflected into the solid-angle element $d\omega$ along the direction with polar angles θ, φ measured in the center-of-mass system. Concomitantly, suppose the atom undergoes a transition to state n, discrete or continuum, at excitation energy E_n measured from state 0, and the kinetic energy associated with the relative translational motion is thereby reduced by E_n. When the particle is sufficiently fast but still nonrelativistic, the differential cross section $d\sigma_n$, calculated in the lowest order in the interaction V between the particle and the atom (i.e., in the first Born approximation), becomes (B30, p. 571 of LL65, and p. 294 of BJ68)

$$d\sigma_n=(2\pi)^{-2}M^2\hbar^{-4}(k'/k)\,|\int \exp(i\mathbf{K}\cdot\mathbf{r})u_n^*(\mathbf{r}_1,\cdots,\mathbf{r}_Z)\times Vu_0(\mathbf{r}_1,\cdots,\mathbf{r}_Z)d\mathbf{r}_1\cdots d\mathbf{r}_Z d\mathbf{r}\,|^2 d\omega, \quad (2.1)$$

where $M=M_1M_2/(M_1+M_2)$ is the reduced mass of the colliding system, $\mathbf{r}$ is the position of the particle relative to the center of the atom, $\hbar\mathbf{k}$ is the momentum of the particle before the collision, $\hbar\mathbf{k}'$ is the same after the collision, $\hbar\mathbf{K}=\hbar(\mathbf{k}-\mathbf{k}')$ is the momentum transfer, and u's are the eigenfunctions in the coordinates $\mathbf{r}_j$ of the atomic electrons, whose total number is Z. [The spin coordinates of the atomic electrons are suppressed in Eq. (2.1)].

When the interaction is Coulombic, i.e., when V is written as

$$V=-\sum_{j=1}^{Z}\frac{ze^2}{|\mathbf{r}-\mathbf{r}_j|}+\frac{zZ_Ne^2}{r}, \quad (2.2)$$

where Z_Ne is the charge on the atomic nucleus, Bethe recognized that it is advantageous to perform first

the integration over $\mathbf{r}$ by using the relation[1]

$$\int |\mathbf{r}-\mathbf{r}_j|^{-1} \exp(i\mathbf{K}\cdot\mathbf{r})\, d\mathbf{r} = 4\pi K^{-2} \exp(i\mathbf{K}\cdot\mathbf{r}_j). \quad (2.3)$$

Thus, Eq. (2.1) transforms into

$$d\sigma_n = 4z^2(Me^2/\hbar^2)^2(k'/k)K^{-4} |\epsilon_n(\mathbf{K})|^2 d\omega, \quad (2.4)$$

where $\epsilon_n(\mathbf{K})$ is an atomic matrix element

$$\epsilon_n(\mathbf{K}) = (n | \sum_{j=1}^{Z} \exp(i\mathbf{K}\cdot\mathbf{r}_j) | 0)$$

$$= \int u_n^* \sum_{j=1}^{Z} \exp(i\mathbf{K}\cdot\mathbf{r}_j) u_0 d\mathbf{r}_1 \cdots d\mathbf{r}_Z. \quad (2.5)$$

The nuclear interaction represented by the second term in Eq. (2.2) gives no contribution, owing to the orthogonality of states n and 0. Under most circumstances, one may consider $d\sigma_n$ as independent of φ, either because state 0 is spatially symmetric or because the atoms under study are oriented at random. In the latter case, the average over all atomic orientations is customarily implied, as is done throughout this article. Furthermore, one often uses the term "state n" to mean a set of all substates at E_n, in which case the sum over these degenerate substates is also implied in Eq. (2.4). [Exceptions arise in discussions on spin-polarized atoms (Ke68) or on the polarization of light resulting from excited atoms (MS68)]. Under these stipulations, $|\epsilon_n(\mathbf{K})|^2$ is a function of a *scalar variable* K, which actually is more convenient than θ for the classification of inelastic collisions. Therefore, one writes hereafter $|\epsilon_n(K)|^2$ instead of $|\epsilon_n(\mathbf{K})|^2$. Further, since K is independent of φ, one implies integration over φ when one expresses $d\sigma_n$ in terms of dK. One thus replaces $d\omega$ by $2\pi \sin\theta\, d\theta = \pi d(K^2)/kk'$ in Eq. (2.4) to obtain

$$d\sigma_n = 4\pi z^2(Me^2/\hbar^2)^2 k^{-2} K^{-4} |\epsilon_n(K)|^2 d(K^2). \quad (2.6)$$

Alternatively, one may use the variable $Q=(\hbar K)^2/2m$ with the dimension of energy, where m is the electron mass, and write

$$d\sigma_n = 2\pi z^2 e^4 (mv^2)^{-1} Q^{-1} |\epsilon_n(K)|^2 d(\ln Q). \quad (2.7)$$

This completes the derivation of the basic formula in the simple case of nonrelativistic collisions with an atom. Extensions to more general cases will be given in Secs. 2.2–2.4.

2.2 Commentary

Several remarks should be made about the Bethe differential cross section (2.7). First, for any incident particle, it explicitly contains v rather than the kinetic energy, and thus shows that v is the decisive variable. Second, the entity $d\sigma_n$ may be considered to consist of two factors of different nature. The factor $2\pi z^2 e^4 (mv^2)^{-1} \times Q^{-1} d(\ln Q)$ is evaluated from the observable quantities k, k', θ concerning the incident particle only. In fact, it is nothing more than the famous Rutherford cross section (R11) for the scattering of a particle with charge ze by a *free and initially stationary electron*, which upon the collision receives a recoil energy ranging from Q to $Q+dQ$. Notice that a given momentum transfer $\hbar K$ results in a unique value Q of energy transfer in this simplified situation. Because of the peculiar nature of the Coulomb force, the Rutherford cross section retains its form upon passing from classical to quantum mechanics (W45, B48). Actually, a definite amount of momentum transfer to the *atom as a whole* still leaves it with a choice of the resulting degree of internal excitation. The reason for this lack of unique correspondence between momentum transfer and energy transfer is that the atomic electrons responsible for internal excitation are initially bound rather than free and are moving around the nucleus. This situation is precisely described by the remaining factor $|\epsilon_n(K)|^2$ in Eq. (2.7), which gives the conditional probability that the atom makes the transition to a particular excited state n upon receiving a momentum transfer $\hbar K$ (B33, F63). The quantity $\epsilon_n(K)$ reflects the dynamics of the atom and is known as the inelastic-scattering form factor, a term widely used in nuclear and particle physics and sometimes in solid-state physics as well (Sec. 2.4).

In atomic physics, however, one more often uses a slightly different quantity, the generalized oscillator strength

$$f_n(K) = (E_n/Q) |\epsilon_n(K)|^2 \quad (2.8)$$

introduced by Bethe (B30). For convenience and ease of memory, one may use the Bohr radius $a_0=\hbar^2/me^2 = 0.52918\times10^{-8}$ cm and the Rydberg energy $R=me^4/2\hbar^2=13.606$ eV and put Eq. (2.8) in the form (MP57)

$$f_n(K) = (E_n/R)(Ka_0)^{-2} |\epsilon_n(K)|^2. \quad (2.9)$$

A reason for using $f_n(K)$ is that it is a straightforward generalization of a more familiar quantity, the optical (dipole) oscillator strength f_n, defined by

$$f_n = (E_n/R) M_n^2, \quad (2.10)$$

where

$$M_n^2 = |\int u_n^* \sum_{j=1}^{Z} x_j u_0 d\mathbf{r}_1 \cdots d\mathbf{r}_Z|^2/a_0^2 \quad (2.11)$$

is the dipole-matrix-element squared, and x_j is a component of $\mathbf{r}_j$. As long as the wavelength λ is sufficiently large compared to the atomic size, f_n is proportional to the cross section for absorption of a photon with energy $E_n=hc/\lambda$ by the atom, and the totality of f_n for all possible transitions embodies most

[1] Strictly speaking, the integral on the left-hand side of Eq. (2.3) is divergent, because the integrand behaves as $O(r^{-1})$ for $r\to\infty$. The replacement meant by Eq. (2.3) is justifiable, however, so long as it is used under another integration symbol, i.e., $\int d\mathbf{r}_j$ in the treatment of the text. For detailed discussions of this point, see pp. 332, 333 of B30, pp. 296, 297 of BJ68, and p. 333 of S68.

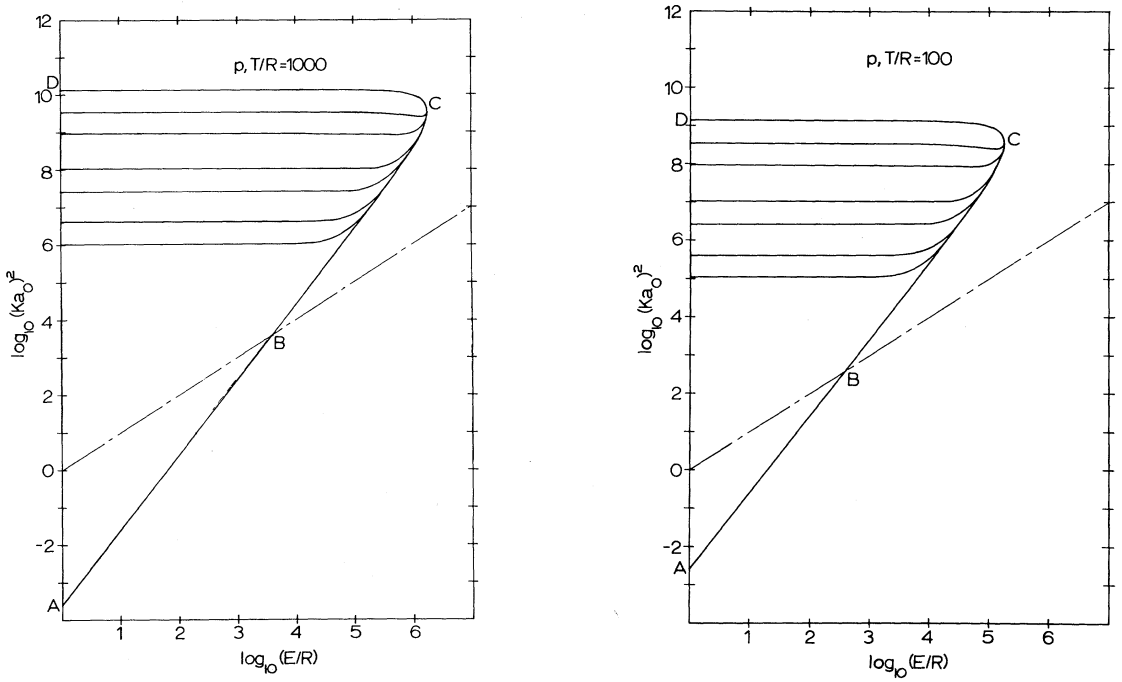

FIG. 1. Kinematics for proton impact. Plot (a) refers to $T/R=100$ (2.50 MeV kinetic energy) and plot (b) to $T/R=1000$ (25.0 MeV kinetic energy). The abscissa is E/R and the ordinate $(Ka_0)^2$, both on logarithmic scales. The curve ABC corresponds to $(Ka_0)_{\min}{}^2$, i.e., to $(Ka_0)^2$ at $\theta=0°$, and the curve DC corresponds to $(Ka_0)_{\max}{}^2$, i.e., to $(Ka_0)^2$ at $\theta=180°$. The intermediate curves correspond to $(Ka_0)^2$ at $\theta=1°$, 2°, 5°, 10°, 30°, and 60°, respectively, in order from bottom to top (Sec. 2.2). The chained line OB shows the position $(Ka_0)^2=E/R$ of the Bethe ridge discussed in Sec. 3.2. In reference to Sec. 4.3, the domain of integration pertinent to σ_{tot} or σ_{st} is $ABCD$, where the vertical line AD corresponds to the lowest excitation energy (which in the figures is set at $E/R=1$). The point B is defined as the intersection of the curve ABC with the position of the Bethe ridge. Then the major contributions to σ_{tot} arise from the region ABO, because the generalized oscillator strength nearly vanishes in the region BCD. Notice by comparing plot (a) and plot (b) with each other that the area $ABCD$ expands on going from $T/R=100$ to $T/R=1000$.

of the optical properties such as dispersion (FC68). Expanding the exponential of Eq. (2.5) into the familiar power series and noting the orthogonality of the atomic eigenstates 0 and n, one can easily show that

$$\lim_{K\to 0} f_n(K)=f_n, \tag{2.12}$$

an important relationship that connects the collision of fast charged particles with photoabsorption. As will be discussed in Sec. 3.1 in detail, the limit $K\to 0$ is closely approached for forward scattering ($\theta=0$) at high velocities [as can be seen from Eq. (2.17)].

Bohr (B13), in essence, arrived at Eq. (2.7) by an impulse approximation, but had no method of evaluating $|\epsilon_n(K)|^2$ or $f_n(K)$. Nevertheless, on the basis of his correspondence principle, he surmised certain crucial facts. For example, he argued that the average of the energy transfer to the atom over all modes of internal excitation for a given Q should be the same as the energy transfer to Z free electrons (B48, F63). In our notation, this means

$$\sum_n E_n |\epsilon_n(K)|^2/Q=\sum_n f_n(K)=Z, \tag{2.13}$$

where the summation is taken over all excited states n, discrete and continuum. Equation (2.13) is the Bethe sum rule (B30), one of the general properties of $f_n(K)$ that can be rigorously derived from its definition (2.8) (as will be shown in Sec. 3.3).

It is often convenient to use the variable $T=\frac{1}{2}mv^2$, which represents the kinetic energy if the incident particle is an electron or a positron, but which in general is m/M_1 times the kinetic energy in the laboratory system. Thus, T/R simply means the square of the velocity measured in units of the Bohr velocity $e^2/\hbar$. Then, Eq. (2.7) transforms (MP57) into

$$d\sigma_n=\frac{4\pi a_0{}^2z^2}{T/R}\frac{f_n(K)}{E_n/R}\,d[\ln (Ka_0)^2]. \tag{2.14}$$

For efficient handling of data, it is worth noting that $4\pi a_0{}^2R=4.788\times 10^{-15}$ cm²·eV.

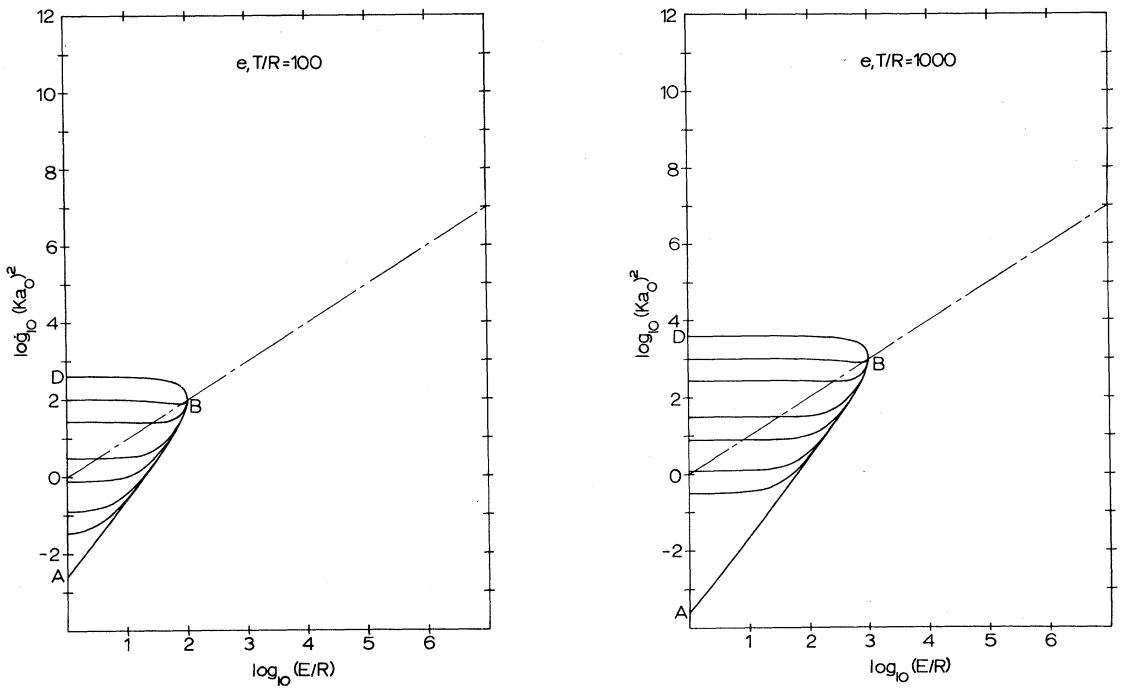

FIG. 2. Kinematics for electron impact. Plot (a) refers to $T/R=100$ (1.36 keV kinetic energy) and plot (b) to $T/R=1000$ (13.6 keV kinetic energy). The scale and the labeling are the same as in Fig. 1, except as noted below. The principal distinction from Fig. 1 is that the point B now coincides with the point C of Fig. 1 so that $(Ka_0)_{\max}{}^2=(\tilde{K}a_0)_{\max}{}^2=T/R$. The area $ABCD$ of Fig. 1 is much greater than the area ABC of Fig. 2 at the same incident velocity. Nevertheless, $\sigma_{\rm tot}$ for protons differs from $\sigma_{\rm tot}$ for electrons (or positrons) at the same velocity only by $O(R^2/T^2)$, because the generalized oscillator strength has substantial magnitude only in the optical region (near the lower left corner) and in the Bethe-ridge region. The difference in $\sigma_{\rm st}$ between protons and electrons (or positrons) at the same velocity is $O(R/T)$, because $\sigma_{\rm st}$ includes more significant contributions from the Bethe-ridge region (near the point B).

An additional remark concerns the kinematics of the collision. The energy-conservation relation

$$(\hbar k)^2=(\hbar k')^2+2ME_n \tag{2.15}$$

and the definition of $\mathbf{K}=\mathbf{k}-\mathbf{k}'$ lead to

$$(Ka_0)^2=2\left(\frac{T}{R}\right)\left(\frac{M}{m}\right)^2\left\{1-\tfrac{1}{2}\left(\frac{m}{M}\right)\left(\frac{E_n}{T}\right)-\left[1-\left(\frac{m}{M}\right)\left(\frac{E_n}{T}\right)\right]^{1/2}\cos\theta\right\}. \tag{2.16}$$

For a fixed value of E_n, the minimum value of $(Ka_0)^2$ occurs at θ, and the maximum value at $\theta=\pi$. For $E_n/T\ll 1$, for which the basic theoretical framework is valid, one obtains from Eq. (2.16)

$$(Ka_0)^2{}_{\min}=\tfrac{1}{4}\left(\frac{E_n{}^2}{RT}\right)\left\{1+\tfrac{1}{2}\left(\frac{mE_n}{MR}\right)+O\left(\left(\frac{mE_n}{MT}\right)^2\right)\right\}, \tag{2.17}$$

$$(Ka_0)^2{}_{\max}=4\left(\frac{T}{R}\right)\left(\frac{M}{m}\right)^2\left\{1-\tfrac{1}{2}\left(\frac{mE_n}{MT}\right)+O\left(\left(\frac{mE_n}{MT}\right)^2\right)\right\}. \tag{2.18}$$

The interval of permissible $(Ka_0)^2$ values expands both upwards and downwards as the velocity increases. Further, for a fixed $E_n/R\ll(M/m)(T/R)$, the value of $(Ka_0)^2$ increases very rapidly with θ near $\theta=0$. The behavior of $(Ka_0)^2$ as a function of E_n/R and θ is displayed in Figs. 1 and 2 for typical cases of proton impact and of electron impact, respectively. These figures will be quoted often in later stages of discussion.

Whereas the above $(Ka_0)^2{}_{\max}$ of Eq. (2.18) is correct for the collisions resulting in a specified value of energy transfer E_n, a different upper limit $(\tilde{K}a_0)^2{}_{\max}$ applies in practice when one deals with the totality of inelastic collisions for a given incident velocity, e.g., in evaluations of stopping power (B30, B33, F63) and of the total inelastic-scattering cross section (discussed in Sec. 4.3).

Consider all inelastic collisions with given values of K and k. Then, the smallest possible k', therefore the largest possible E_n, occurs for $\theta=0$, in which case $k'=k-K$ and

$$E_n=(\hbar^2/2M)(2kK-K^2)$$

according to Eq. (2.15). The kinematics of the col-

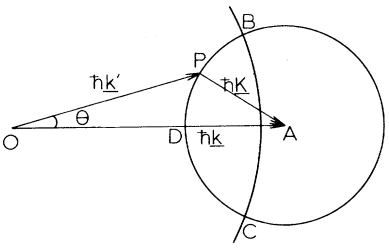

FIG. 3. Diagram for kinematics. The fixed initial momentum $\hbar\mathbf{k}$ of the relative motion is represented by the vector $[OA]$. Given the magnitude $\hbar K$ of momentum transfer, draw a circle with its center at A and its radius $\hbar K$. Draw another circle with its center at O and its radius equal to the largest possible magnitude $\hbar k'$ of the final momentum, namely $(\hbar^2k^2-2ME_1)^{1/2}$, where E_1 is the lowest excitation energy. Call the intersections of the circles B and C. Any point P on the arc BDC of the circle around A represents a possible end point of vector $\hbar\mathbf{k}'=[OP]$, and θ=angle POA is the scattering angle. The largest energy transfer, thus the smallest $\hbar k'=(\hbar^2k^2-2ME_n)^{1/2}$, occurs when P coincides with the intersection D of the arc BDC and the line OA.

lision is displayed in Fig. 3. Suppose, for a moment, that the binding of an atomic electron to the nucleus is insignificant when one considers a large energy transfer, as is actually the case for excitation of outer-shell electrons. Then $Q=(\hbar K)^2/2M$ is the approximate value of the energy transfer, which must not exceed the energy E_n derived above, i.e.,

$$(\hbar^2/2M)\,(2kK-K^2)\geq(\hbar K)^2/2m.$$

This inequality leads to $K\leq 2km/(M+m)$, and hence to

$$(Ka_0)^2\leq(\tilde{K}a_0)^2_{\max}=4(T/R)[1+(m/M)]^{-2}, \quad (2.19)$$

a limit far more restrictive than that given by Eq. (2.16) for $M\gg m$.

Collisions with K values such that $(Ka_0)^2_{\max}>(Ka_0)^2>(\tilde{K}a_0)^2_{\max}$ can take place nevertheless, provided that electrons pertinent to the inelastic process are subject to sufficiently strong binding. For example, a proton with 1.84 MeV kinetic energy in the center-of-mass system, for which $(\tilde{K}a_0)^2_{\max}=(4/R)$ keV according to Eq. (2.19), does actually have fair probabilities (M68) of exciting those K-shell electrons of heavier atoms ($Z\gtrsim 30$) whose binding energies are roughly $Z^2R\gtrsim 10$ keV.

When one deals with excitation to continua (i.e., with ionization), the excitation energy is no longer a discrete variable, but is a continuous variable E taking all real values greater than the first ionization threshold I_1. Then it is appropriate to consider, in place of σ_n, the density[2] $d\sigma/dE$ of the cross section per unit range of E. Thus, an adaptation of Eq. (2.14) to this case gives the differential of $d\sigma/dE$ as

$$d\left(\frac{d\sigma}{dE}\right)=\frac{4\pi a_0^2z^2}{T/R}\frac{R}{E}\frac{df(K,E)}{dE}\,d[\ln(Ka_0)^2]. \quad (2.20)$$

Here $df(K,E)/dE$, the density of the generalized oscillator strength per unit range of E, may be defined by

$$df(K,E)/dE=(E/R)\,(Ka_0)^{-2}\sum_{\Omega}|\,\epsilon_{E,\Omega}(K)\,|^2, \quad (2.21)$$

with

$$\epsilon_{E,\Omega}(K)=(E,\Omega\,|\sum_{j=1}^{Z}\exp(i\mathbf{K}\cdot\mathbf{r}_j)\,|\,0),$$

where the final continuum state is specified by E and a set Ω of all the other quantum numbers (such as the angular momentum or the direction of electron ejection) and is normalized as

$$(E,\Omega\,|\,E',\Omega')=\delta(E-E')\delta(\Omega-\Omega').$$

An equivalent but more compact definition is

$$df(K,E)/dE=\sum_n(E_n/R)[|\,\epsilon_n(K)\,|^2/(Ka_0)^2]\delta(E_n-E), \quad (2.22)$$

where the summation, like that in Eq. (2.13), runs over all excited states—discrete as well as continuum. Equation (2.22) may be considered to be a formal definition of $df(K,E)/dE$ also in the discrete spectrum (as will be discussed further in Secs. 2.4 and 3.3).

So far the target has been called "an atom," but the discussions are equally applicable to a molecule, except that one should consider all of its internal degrees of freedom when one specifies the states 0 and n. Thus, the symbol 0 or n now represents a set of quantum numbers (electronic, vibrational, and rotational) that designates a molecular state. Then, the differential cross section $d\sigma_n$ [Eq. (2.7) or Eq. (2.14)] is given in terms of $|\,\epsilon_n(K)\,|^2$ of Eq. (2.5) or $f_n(K)$ of Eq. (2.9). Further, one usually treats quantities $d\sigma_{n'}$, $|\,\epsilon_n(K)\,|^2$, or $f_n(K)$ as averaged over effectively degenerate initial substates and summed over effectively degenerate final substates. The precise meaning of the term "effectively degenerate" depends on the individual physical situation of interest. Except for H_2, rotational-level spacings of molecules are much smaller than the energy resolution width of current collision experiments and also smaller than the thermal energy at room temperature. Therefore, rotational levels are usually considered as effectively degenerate. Alternatively, one can treat molecular rotation as adiabatic (i.e., slow compared to the duration of collision), which is a good approximation for fast collisions. One then computes $|\,\epsilon_n(K)\,|^2$ for alternative fixed molecular orientations and takes the average of the results.

[2] To avoid confusion, one may paraphrase the definition of $d\sigma/dE$. The cross section (as a fixed T) for excitation to continuum states between E and $E+dE$ is $(d\sigma/dE)dE$. Alternatively, one may interpret $\sigma(E)$ as the cross section for excitation to all states up to E and hence $d\sigma/dE$ as the derivative of $\sigma(E)$. The use of "d/dE" in $df(K,E)/dE$ and other continuum properties are to be understood in similar ways.

The application to molecules will be discussed more fully in Sec. 3.5. (See also p. 827 of MBG69.)

The last point of the commentary concerns the spin multiplicity of the states 0 and n. For light atoms in which the spin–orbit coupling is negligible, the atomic eigenfunction may be written in the LS coupling scheme. Since the operator in the matrix element $\epsilon_n(K)$ of Eq. (2.5) deals exclusively with the configuration space and thus commutes with the electron-spin operator, $\epsilon_n(K)$ vanishes for all transitions between states with different spin multiplicities and so does $f_n(K)$. For example, $f_n(K)=0$ for a singlet–triplet transition in He to a good approximation. When one takes into account the spin–orbit coupling, $f_n(K)$ for such a transition is finite, as is especially true with heavy atoms or molecules containing heavy atoms.

When the incident particle is an *electron*, it is in principle indistinguishable from the atomic electrons. Consideration of this situation leads to "electron-exchange effects," which are not included in the first Born approximation as treated here. It is commonly believed (MS68) that these effects are unimportant at sufficiently high velocities. Atomic transitions between states with different spin multiplicities, mentioned in the previous paragraph, are made possible as a result of the electron-exchange effects also, but the probability of such transitions for fast collisions is known to be small on both theoretical and experimental grounds. The electron-exchange effects will be discussed further in Secs. 4.4 and 5.2.

2.3. Relativistic Effects

When the ratio $\beta=v/c$ of v to the light velocity c approaches unity, relativistic modifications of the formula for $d\sigma_n$ and on the kinematics are required. Since $T/R=(\hbar v/e^2)^2=(\beta/\alpha)^2$, where $\alpha^{-1}=\hbar c/e^2=137.04$, one sees, for example, that $\beta^2=0.053$ for $T=10^3$ $R=1.36\times10^4$ eV. One thus anticipates that relativistic effects may amount to several percent around $T\approx10^4$ eV and be greater at higher velocities.

In the following brief sketch of the relativistic effects, it is presupposed that the incident kinetic energy is still low enough to permit neglect of radiative effects (such as coupling with bremsstrahlung), i.e., that the processes involved are not extremely relativistic (BS57, R59, MOK64, BG70). It should be emphasized, however, that this situation actually prevails over a wide energy region $T\lesssim10^9$ eV, and that the theory in this region is well established.

As Bethe has shown (B32, B33), the relativistic version of Eq. (2.4) is

$$d\sigma_n=4z^2e^4\hbar^{-4}c^{-4}WW'(k'/k)\,|\,\eta_n(K)\,|^2 \times[K^2-(W-W')^2\hbar^{-2}c^{-2}]^{-2}d\omega, \quad (2.23)$$

where W and W' represent total energy inclusive of the rest energy Mc^2 of the incident particle, before and after the collision, respectively. (In this section, one takes the atom as infinitely heavy so that $M=M_1$.) That is, we have

$$W=(M^2c^4+c^2\hbar^2k^2)^{1/2}, \quad (2.24)$$

$$W'=(M^2c^4+c^2\hbar^2k'^2)^{1/2}=W-E_n. \quad (2.25)$$

The relativistic form factor $\eta_n(K)$ is defined by Eq. (50.2) of B33. In the nonrelativistic limit, $WW'\to(Mc^2)^2$ and $|\,\eta_n(K)\,|^2\to|\,\epsilon_n(K)\,|^2$, so that one recovers Eq. (2.4). The factor $c^{-4}WW'$ arises because of relativistic kinematics, and the quantity $(W-W')^2\hbar^{-2}c^{-2}$ appears in the bracket because of the relativistic retardation of the interactions.

In order to cast Eq. (2.23) in a form similar to Eq. (2.7), one must define a variable Q that tends to $(\hbar K)^2/2m$ in the nonrelativistic limit, a procedure that is not unique. (Hereafter m always represents the rest mass of an electron.) Bethe (B33) defines

$$Q=(\hbar^2K^2-E_n^2c^{-2})/2m, \quad (2.26)$$

so that $dQ=(\hbar^2/2m)d(K^2)$. Then replacing $d\omega$ by $\pi d(K^2)/kk'$ under the same stipulations as in Sec. 2.1, one rewrites Eq. (2.23) as

$$d\sigma_n=2\pi z^2e^4(mv^2)^{-1}(W'/W)\,|\,\eta_n(K)\,|^2Q^{-1}d(\ln Q) \quad (2.27)$$

in close analogy to Eq. (2.7). The ratio W'/W tends to unity both for $v/c\ll1$ and for $v/c\to1$, and may be set equal to unity without appreciable errors in most physical situations. Thus, the interpretation given to Eq. (2.7) in the beginning of Sec. 2.2 largely applies to Eq. (2.27) also. A subtle distinction concerns the meaning of Q defined by Eq. (2.26). First, the above Q contains E_n and thus is no longer a variable independent of E_n. Second, in the simplified situation in which a free and initially stationary electron receives momentum $\hbar K$, the energy transferred to the electron is not quite Q except when Q is large and is nearly equal to E_n. The exact amount Q_r of the recoil kinetic energy is

$$Q_r=(m^2c^4+c^2\hbar^2K^2)^{1/2}-mc^2. \quad (2.28)$$

Fano (F63) uses this variable rather than Q, though the differential cross section $d\sigma_n$ takes a slightly more involved form [Eq. (16) of F63] when expressed in terms of Q_r instead of Q.

As to the relativistic form factor $\eta_n(K)$, only those properties essential to the theme of this article will be commented upon. For detailed discussions, the reader is referred to Refs. B32, B33, F54, F56a, and F63. The precise evaluation of $\eta_n(K)$ requires the relativistic eigenfunctions for states n and 0, but Bethe (B32, B33) showed that, to a good approximntion, $\eta_n(K)$ may be related to the nonrelativistic form factor $\epsilon_n(K)$ in the following way. For $Ka_0\gtrsim1$, one may neglect relativistic effects and set

$$|\,\eta_n(K)\,|^2\cong|\,\epsilon_n(K)\,|^2 \quad (2.29)$$

so long as $E_n \ll mc^2 = 0.5110$ MeV, a condition satisfied in most excitations of not very heavy atoms. For $Ka_0 \ll 1$, in contrast, one should put

$$|\eta_n(K)|^2 \cong |\epsilon_n(K)|^2 - M_n^2(1-\beta^2)E_n^2/(2Rmc^2), \quad (2.30)$$

where M_n^2 is the nonrelativistic dipole-matrix-element squared, as defined by Eq. (2.11). Equations (2.29) and (2.30) show that the dynamics of the atom or molecule with respect to collisions at relativistic velocities is still mainly described in terms of $|\epsilon_n(K)|^2$, a fact that makes $|\epsilon_n(K)|^2$ or $f_n(K)$ of basic importance beyond the nonrelativistic region.

An analysis by Fano (F56a, F63) shows that $|\eta_n(K)|^2$ consists of two distinct parts, one that results from the Coulomb force acting parallel to $\mathbf{K}$, and another that stems from virtual photons giving rise to forces perpendicular to $\mathbf{K}$. These two parts excite atomic states of different parity, and give additive contributions, no interference between them being present.

Although Bethe (B32, B33) gave Eqs. (2.27), (2.29), and (2.30) specifically for electron collisions, these results (as well as their consequences such as the integrated cross section discussed in Sec. 4.1) apply to collisions of any charged particle (regarded as structureless). This point is apparent from the treatment of Fano (F56a, F63).

The kinematical limits for $(Ka_0)^2$ again follow from the energy conservation, Eq. (2.25). The results are

$$(Ka_0)^2_{\min} = (k-k')^2 a_0^2 \cong E_n^2/(2mv^2R), \quad (2.31)$$

$$(Ka_0)^2_{\max} = (k+k')^2 a_0^2 \cong (2mv^2/R)(M/m)^2[(1-\beta^2)]^{-1} \quad (2.32)$$

for collisions with a fixed value of E_n. These limits obviously reduce to the nonrelativistic ones given in Eqs. (2.17) and (2.18). The upper limit $(\tilde{K}a_0)^2$ that effectively applies to the totality of inelastic collisions at a given v turns out to be

$$(\tilde{K}a_0)^2_{\max} = 2mv^2/[R(1-\beta^2)], \quad (2.33)$$

from the same argument as in the nonrelativistic case [Eq. (2.19) and the passage above it].

2.4. Conceptual Generalizations

The concept of the generalized oscillator strength may be adapted to a variety of physical situations such as charged-particle interactions with condensed phases. A heuristic starting point for consideration is to rewrite the expression (2.22) for $df(K, E)/dE$ in a different form. [Equation (2.22) was introduced specifically for transitions into continua, but is formally applicable to a discrete spectrum as well. Since, except for atomic hydrogen, significant values of $df(K, E)/dE$ occur mostly in continua ($E > I_1$), it is advantageous to consider discrete spectra as a secondary and exceptional case.]

The alternative form is

$$\frac{df(K, E)}{dE} = \frac{E/R}{(Ka_0)^2}(2\pi\hbar)^{-1}\int_{-\infty}^{\infty}\phi(K, t) \times \exp(-Et/\hbar)\,dt, \quad (2.34)$$

where $\phi(K, t)$ is defined by initial-state expectation values (denoted by angular parentheses) through the expression

$$\phi(K, t) = \sum_j \sum_k \langle \exp(-i\mathbf{K}\cdot\mathbf{r}_j) \exp[i\mathbf{K}\cdot\mathbf{r}_k(t)] \rangle - |\sum_j \langle \exp(i\mathbf{K}\cdot\mathbf{r}_j) \rangle|^2, \quad (2.35)$$

$\mathbf{r}_k(t)$ being the Heisenberg position operator at time t for the kth electron in the atom described by the Hamiltonian H, i.e.,

$$\mathbf{r}_k(t) = \exp(iHt/\hbar)\,\mathbf{r}_k \exp(-iHt/\hbar). \quad (2.36)$$

The equivalence of Eq. (2.34) with Eq. (2.22) is readily verified by insertion of the completeness relation $\sum_n |n\rangle\langle n| = 1$ for atomic eigenstates $|n\rangle$ between the two exponentials on the right-hand side of Eq. (2.35). The expression (2.34) is a special case of the Kubo general formula for the linear response of a system at equilibrium to a small external perturbation (V54, K59, K63, N64); the function $\phi(K, t)$ then may be called the time correlation of electron-density fluctuations associated with the propagation vector $\mathbf{K}$, and $df(K, E)/dE$ is $(E/R)\,(Ka_0)^{-2}$ times its Fourier component with angular frequency $E/\hbar$. Notice that $df(K, E)/dE$ of Eq. (2.34) is given as an expectation value in the initial state (most often the ground state) rather than in terms of an off-diagonal matrix element $|\epsilon_n(K)|^2$ of Eq. (2.21), a fact that makes Eq. (2.34) useful for considerations of some general properties of the generalized oscillator strength (as in Secs. 3.2, 3.3, and 4.4). Equation (2.34) also might serve as the starting point for numerical evaluation in certain cases; this possibility is beginning to be explored (Sc70).

A more important aspect of Eq. (2.34) arises from its extended interpretation. Because Eqs. (2.34)–(2.36) contain no explicit specification as to the description of the target, they are readily applicable to an aggregate of atoms or molecules as well as to an isolated atom or molecule. A particular mode of description of the physical system under consideration, i.e., a model, becomes explicit only upon evaluating the initial-state expectation value in Eq. (2.35). Fano (F56b) has shown that $df(K, E)/dE$ as given in Eq. (2.34) is virtually equal to $\mathrm{Im}[-1/\epsilon(\mathbf{K}, E)]$, where $\epsilon(\mathbf{K}, E)$ is a generalized complex dielectric constant describing the response of any medium to a small electromagnetic disturbance with angular frequency $E/\hbar$ and propagation vector $\mathbf{K}$. This relationship between charged-particle scattering and $\epsilon(\mathbf{K}, E)$ is utilized in the treatment of the density effect on stopping

power (F40, F56b, F63, CF70), as well as in the interpretation of electron energy losses in solids (R65, Po67, Ge68). In the limit $K \to 0$, the quantity $\epsilon(\mathbf{K}, E)$ reduces to the optical dielectric constant that is often studied in solid-state spectroscopy.

The notion of the (elastic and inelastic) form factor applies to a wide class of physical phenomena, well beyond those associated with charged-particle interactions. Indeed, the term "form factor" was first introduced in x-ray scattering. Whenever one tries to use collisions of a fast projectile to learn about *the structure of any physical object* the primary information to be obtained is described in terms of an appropriately defined form factor as a function of momentum transfer, and of energy transfer if the collisions are inelastic. A classic example is the famous experiment on α-particle scattering by Geiger and Marsden (GM9), which led Rutherford (R11) to the recognition that the sufficiently frequent occurrence of large-angle scattering (i.e., large momentum transfers) must arise from the presence of the atomic nucleus—i.e., the presence of a positive charge concentrated within a volume much smaller than the atomic dimension already known to him at that time. A modern version of the same experiment is the nucleon-structure study by means of electron and proton scattering at very high energies, where the data are most conveniently expressed in terms of form factors (DZ61). A subject more similar to our present theme is Coulomb excitation, by which one investigates the scattering of fast charged particles associated with excitations of nuclear energy levels (BB65, DW66). Finally, the scattering of neutrons by solids, particularly by magnetic materials, provides knowledge of the crystal structure via form factors (P52, V54, K63, N64). All these examples indicate the fundamental importance of the study of form factors. And the form factor, or equivalently the generalized oscillator strength, of an isolated atom or molecule is probably the most precisely understood property in such phenomena.

It may be added that the generalized oscillator strength also governs the Compton scattering of photons by atoms, when the photon energy is much smaller than mc^2 but is much greater than the binding energy of atomic electrons (W29, B34, EP70).

3. THE GENERALIZED OSCILLATOR STRENGTH

3.1. Experimental Studies

Despite its conceptual simplicity, the generalized oscillator strength is difficult to evaluate theoretically by means of Eq. (2.8) because a sufficiently accurate eigenfunction of an atomic or molecular system in its ground state and especially in its excited states is seldom available. For the quantitative knowledge of the generalized oscillator strength of individual atoms and molecules, one actually owes much more to experiment than to any theory.

How does one learn about the generalized oscillator strength from experiment? An answer is provided by the phenomenological introduction of an apparent generalized oscillator strength $\mathrm{f}_n(K, T)$, a procedure initiated by Lassettre and coworkers in their extensive investigation of electron scattering (LF64).

Suppose an experiment determines the differential cross section $d\sigma_n/d\omega$, expressed in the center-of-mass system, for collisions of a charged particle with an atom or molecule. One defines

$$\mathrm{f}_n(K, T) = \frac{(m/M)^2}{4z^2a_0^2}\left(1-\frac{m}{M}\frac{E_n}{T}\right)^{-1/2}(Ka_0)^2\frac{E_n}{R}\frac{d\sigma_n}{d\omega}, \tag{3.1}$$

where all the quantities on the right-hand side can be determined experimentally. For sufficiently large $T=\frac{1}{2}mv^2$, where the first Born approximation is valid, the above $\mathrm{f}_n(K, T)$ should be equal to the Bethe generalized oscillator strength $f_n(K)$ defined by Eq. (2.8), as one may easily see by inserting $d\sigma_n/d\omega$ of Eq. (2.4) into Eq. (3.1); that is,

$$\mathrm{f}_n(K, T) \to f_n(K) \qquad \text{(for large } T\text{)}. \tag{3.2}$$

An important implication of this statement is the following. A necessary, though not sufficient, condition for the validity of the first Born approximation is that experimental values of $d\sigma_n/d\omega$ at different T should produce the same K dependence of $\mathrm{f}_n(K, T)$, independent of T. This criterion does not assume theoretical knowledge of $f_n(K)$, and thus can be used entirely operationally as soon as experimental data are at hand. In contrast, experimental $d\sigma_n/d\omega$ at smaller T may in fact yield $\mathrm{f}_n(K, T)$ that depends on T, in which case a departure from the first Born approximation is evident.

Although Eq. (3.1) defines $\mathrm{f}_n(K, T)$ for collisions of any (structureless) charged particle, in practice it has been utilized only for electron impact. The reason for this is twofold: first, it is only for electron beams that the feasible energy resolution and angular collimation are sharp enough to make the resulting data significantly precise; second, owing to their small mass, electrons afford an ample opportunity to scan $\mathrm{f}_n(K, T)$ over a substantial interval of $(Ka_0)^2$ values by measuring $d\sigma_n/d\omega$ at different θ even with a relatively modest angular resolution. In contrast, for collisions of heavy particles, the variation of $(Ka_0)^2$ with θ near $\theta=0$ is very rapid (as seen in Fig. 1) so that an extremely fine angular resolution is required to bring out significant data of $\mathrm{f}_n(K, T)$. Nevertheless, the use of proton impact is beginning to be explored (PS69) in this respect also.

Another advantage of electron scattering in the study of $\mathrm{f}_n(K, T)$ is that the difference between the center-of-mass system and the laboratory system usually is negligibly small, again owing to the small

electron mass. Thus, one can safely insert the laboratory differential cross section in place of $d\sigma_n/d\omega$ on the right-hand side of Eq. (3.1) and can identify T with the laboratory kinetic energy.

The procedure of defining $\mathfrak{f}_n(K, T)$ can be generalized readily to relativistic particles by means of Eqs. (2.27), (2.29), and (2.30). For efficient handling of data, a tabulation of relativistic kinematics (MMH56) is helpful.

It should be emphasized that the determination of $\mathfrak{f}_n(K, T)$ in general requires a highly precise experimental determination of the energy and direction of the incident and scattered beams, because the ratio E_n/T and the scattering angle involved in interesting cases are often quite small. It is beyond the scope of this article to discuss the technology necessary to meet this requirement, and the reader is referred to excellent reviews (K68, KMC69, TRK70) for detailed treatments of this aspect.

The analysis in terms of $\mathfrak{f}_n(K, T)$ evidently assumes a data set of $d\sigma_n/d\omega$ at various θ for fixed E_n and T. However, experimental data for electron scattering usually are taken in a different way. For a fixed T, the intensity of scattered electrons emerging in the vicinity of a fixed angle θ with kinetic energy $T-E_n$ is recorded. This (usually relative) intensity, considered as a function of E_n, is called the *electron energy-loss spectrum* measured at θ and T. In general, it exhibits level structures of the atom or molecule as the photoabsorption spectrum does. Within the validity of the first Born approximation, the electron energy-loss spectrum is proportional to $d\sigma_n/d\omega$ as given by Eq. (2.4). In particular, the same spectrum taken for forward scattering ($\theta=0$) is proportional to

$$\left.\frac{d\sigma_n}{d\omega}\right|_{\theta=0}=4a_0^2\left(1-\frac{E_n}{T}\right)^{1/2}\frac{f_n(K_{\min})}{(Ka_0)^2_{\min}\,(E_n/R)}. \quad (3.3)$$

By use of Eqs. (2.12) and (2.17) one can easily show that

$$d\sigma_n/d\omega\,|_{\theta=0}=16a_0^2R^2TE_n^{-3}f_n \qquad (\text{for } E_n\ll T), \quad (3.4)$$

where f_n is the optical oscillator strength. In other words, the electron energy-loss spectrum for forward scattering and for $E_n\ll T$ is equal to E_n^{-3} times the optical spectrum (i.e., f_n considered as a function of E_n).

Although Relation (3.4) is often useful for quick comparison of electron scattering with photoabsorption, the influence of a finite angular resolution upon the forward energy-loss spectrum sometimes becomes appreciable on closer examination (GW65, GS68). Suppose that an experiment measures the intensity of electrons that are inelastically scattered into the small cone defined by the interval $0<\theta<\hat{\theta}\ll 1$ of the scattering angle θ. Then, the result of the measurement is the ratio $\Delta\sigma_n/\Delta\omega$, where

$$\Delta\sigma_n=\int_{0<\theta<\hat{\theta}}d\sigma_n,$$

$$\Delta\omega=\int_{0<\theta<\hat{\theta}}d\omega=2\pi\int_0^{\hat{\theta}}\sin\theta\,d\theta=4\pi\sin^2(\hat{\theta}/2).$$

In order to evaluate $\Delta\sigma_n$ by use of Eqs. (2.14) and (2.16), one may assume that

$$f_n(K)=f_n+(Ka_0)^2f_n^{(1)}+\cdots$$

for sufficiently small $(Ka_0)^2$, where $f_n^{(1)}$ is a property of the target treated in detail in the passage below Eq. (3.13).

The result of an elementary calculation is then

$$\Delta\sigma_n/\Delta\omega=16a_0^2R^2TE_n^{-3}[f_n\zeta^{-1}\ln(1+\zeta)+(E_n/4RT)f_n^{(1)}] \qquad (\text{for } E_n\ll T), \quad (3.5)$$

where the aperture angle $\hat{\theta}$ enters only through

$$\zeta=4(\hat{\theta}E_n/T)^2.$$

Usually the departure of the function $\zeta^{-1}\ln(1+\zeta)$ from unity is the primary portion of the correction to the idealized relation (3.4). Notice also that $\zeta^{-1}\ln(1+\zeta)$ is a monotonically decreasing function of $\zeta>0$. The second term in the bracket of Eq. (3.5) is independent of $\hat{\theta}$ and is usually less important so long as $f_n^{(1)}$ and f_n are comparable to each other. (The treatment of GW65, justifiably in its context, neglects this term.) In general, however, due attention should be paid to the second term, because the magnitude of $f_n^{(1)}$ is only poorly known in advance for most cases.

A remark on the practical application of Eq. (3.1) in electron scattering may be useful. The computation of $(Ka_0)^2$ by means of Eq. (2.16) usually is inconvenient because of the high precision necessary to maintain sufficient accuracy of data handling. In the practically important cases in which θ and $\xi\equiv(m/M)\times(E_n/T)$ are small, evaluation of the function

$$\chi(\xi,\theta)=1-\tfrac{1}{2}\xi-(1-\xi)^{1/2}\cos\theta \quad (3.6)$$

on the right-hand side of Eq. (2.16) suffers from near cancellation. To avoid this difficulty, it is advantageous to transform Eq. (3.6), for example, into

$$\chi(\xi,\theta)=\tfrac{1}{2}\xi^2[1+(1-\xi)^{1/2}]^{-2}+2(1-\xi)^{1/2}\sin^2(\theta/2). \quad (3.7)$$

[This transformation was pointed out to the writer by Dr. G. E. Chamberlain. Other similar transformations are given by Eq. (2) of LF64 and by Eq. (1.1.20) of K68.]

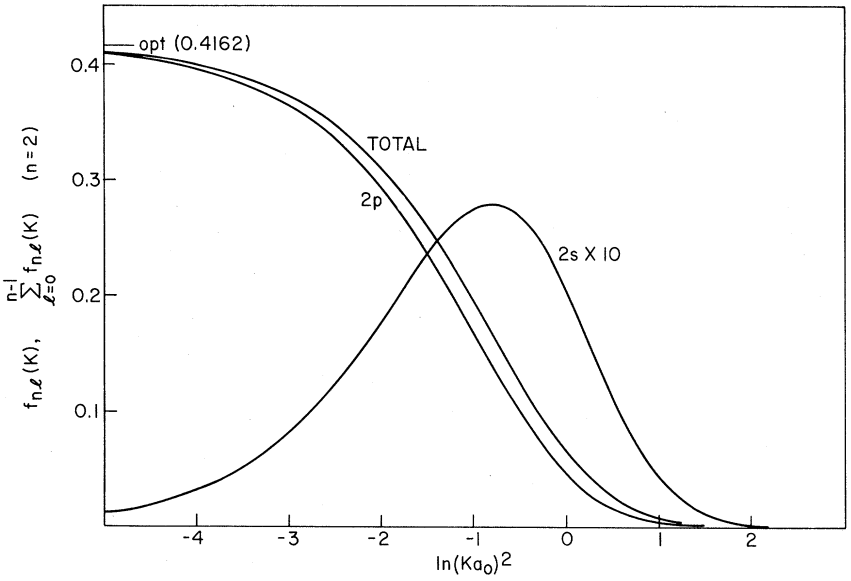

FIG. 4. Generalized oscillator strengths for the transitions from the ground state to the $n=2$ level of H (I66). The abscissa represents ln $(Ka_0)^2$. The curve labeled "TOTAL" represents the sum $f_2(K)=f_{2s}(K)+f_{2p}(K)$. The line labeled "opt" shows the optical oscillator strength $f_{2p}=0.4162$. These remarks apply, with obvious modifications, to Figs. 5-7 as well.

3.2. The Bethe Surface

Because atomic hydrogen is the only system for which the generalized oscillator strength for every transition is rigorously known, one may utilize this simplest case to exemplify and illustrate the general understanding. Some of the properties discussed below are indeed valid for any atom or molecule, but others are peculiar to atomic hydrogen. In what follows, efforts will be made to distinguish these two kinds of properties as clearly as possible.

The literature abounds in mathematical expressions related to the generalized oscillator strength of atomic hydrogen, both in the ground state and in some excited states (B30, B33, MM31, W51, W52, W56, E55, S61, LLS61, Om65a, Om65b, KM66a, KM66b, BK67, H69b, to name only representative references). For the discrete excitations from the ground state, the standard references are MM65 (p. 480) and B30. Some numerical data are given in I63 and I66. For excitation from a spherically symmetric state (an S state) of any atom, the treatment of the generalized oscillator strength becomes easiest if one chooses the axis of orientational quantization of the atom along the vector $\mathbf{K}$. Then, the dependence of the matrix element of $\sum_j \exp(i\mathbf{K}\cdot\mathbf{r}_j)$ upon the azimuthal quantum number M_L of the excited state is simple: only the substate with $M_L=0$ gives a nonvanishing value, whose absolute square is identical to the sum $|\epsilon_n(K)|^2$ of absolute squares of the matrix elements over M_L when the axis of quantization is chosen arbitrarily. For instance, Eq. (92) on p. 480 of MM65, originally derived by Massey and Mohr (MM31) for atomic hydrogen, should be understood in the above context.

Figure 4 shows the generalized oscillator strength for the excitation of the $2s$ and $2p$ state from H($1s$), plotted in a suitable way introduced by Miller and Platzman (MP57). The abscissa variable $\ln[(Ka_0)^2]$ is so chosen that the area under the curve between the kinematical limits given by Eqs. (2.17) and (2.18) measures to the (integrated) cross section $\sigma_n=\int d\sigma_n$ for excitation of the respective state, apart from the factor $4\pi a_0^2 z^2(R/T)(R/E_n)$, as seen from Eq. (2.14). First, notice the difference between an optically allowed transition ($2p\leftarrow 1s$) and an optically forbidden transition ($2s\leftarrow 1s$), with respect to both the magnitude and the behavior at the optical limit $K\rightarrow 0$. The fact that $f_n(K)$ is finite and greatest at $K\rightarrow 0$ for lower allowed excitations, indicates the efficiency of collisions with large impact parameters in exciting allowed transitions.[3] (The precise connection between the variable K and the impact parameter will be

[3] Another way of interpreting the difference between an optically allowed transition and an optically forbidden transition is to consider the matrix element $V_{n0}(\mathbf{r})=(n\mid V\mid 0)=\int u_n^* V u_0 d\mathbf{r}_1\cdots d\mathbf{r}_Z$ of the interaction V [Eq. (2.2)] taken between atomic eigenstates n and 0. One may regard this function $V_{n0}(\mathbf{r})$ as a "potential" seen by the incident particle at position $\mathbf{r}$ when it undergoes inelastic scattering. Then the essential factor of Eq. (2.1) is a squared matrix element of $V_{n0}(\mathbf{r})$ now taken with respect to the plane-wave states of the incident particle. For brevity of discussion, one may take the atom as neutral (i.e., $Z=Z_N$). By use of the standard multipole expansion of V, it is easy to examine the asymptotic behavior of $V_{n0}(\mathbf{r})$ for large r. If the transition $n\leftarrow 0$ is allowed, one immediately obtains

$$V_{n0}(\mathbf{r})\sim ze^2(n\mid \sum_j x_j\mid 0)r^{-2},$$

where $x_j=(\mathbf{r}_j\cdot\mathbf{r})/r$. If the transition $n\leftarrow 0$ is forbidden, $V_{n0}(\mathbf{r})$ is of shorter range; $V_{n0}(\mathbf{r})$ varies as r^{-3} for a quadrupole transition, and as a decaying exponential for an $S\leftarrow S$ transition (cf. p. 103 of BFM50).

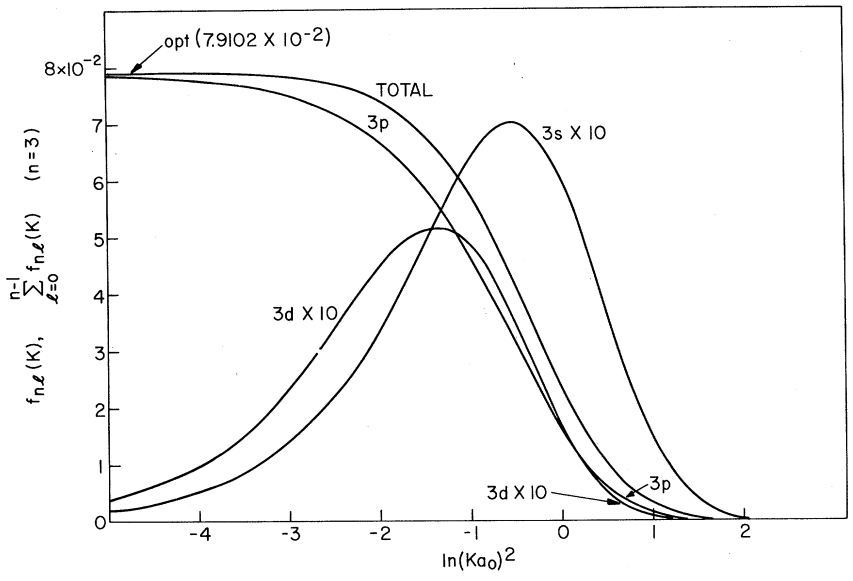

FIG. 5. Generalized oscillator strength for the transitions from the ground state to the $n=3$ level of H(I66).

discussed in Sec. 4.4.) Second, the generalized oscillator strength decreases rapidly for large $(Ka_0)^2$ for the following reason. An atom or molecule under a weak external perturbation can receive a momentum transfer $\hbar K$ because momentum fluctuations of its electrons, governed by the uncertainty principle, respond to the perturbation in a manner described precisely by Eqs. (2.34)–(2.36). Since atomic electrons are never completely localized, their momenta cannot fluctuate excessively beyond a limit set by their binding, so that they cannot receive a correspondingly large momentum transfer without recoiling out of the atom. The asymptotic behavior of $f_n(K)$ for $K\to\infty$ is given by

$$f_n(K)\sim K^{-2(l+l'+5)}, \tag{3.8}$$

where l and l' are the angular-momentum quantum numbers of the active electron's orbitals for the initial and final atomic states, respectively (RF67).

Figures 5–7 show the same situations for the transitions to the states with principal quantum numbers $n=3$, 4, and 5, respectively. These are not very different from the $n=2$ excitation, as far as the allowed np excitations are concerned. It is important at this point to distinguish between the generalized oscillator strength $f_{nl}(K)$ for the transition to the state nl, l being the angular-momentum quantum number, and the sum $f_{E_n}(K)$ at fixed excitation energy $E_n=(1-n^{-2})R$. [Notice that $f_{E_n}(K)$ corresponds to the concept of Eqs. (2.22) and (2.34).] Bethe (B30) derived

$$f_{E_n}(K)=2^8n^5(n^2-1)[\tfrac{1}{3}(n^2-1)+(nK_0)^2]\times[(n-1)^2+(nKa_0)^2]^{n-3}[(n+1)^2+(nKa_0)^2]^{-n-3}. \tag{3.9}$$

In Figs. 4–7, $f_{E_n}(K)$ is represented by the curve

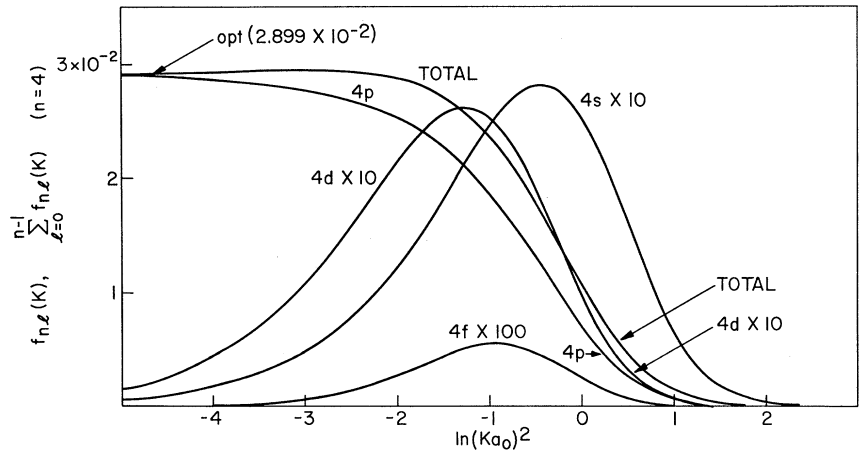

FIG. 6. Generalized oscillator strengths for the transitions from the ground state to the $n=4$ level of H (I66).

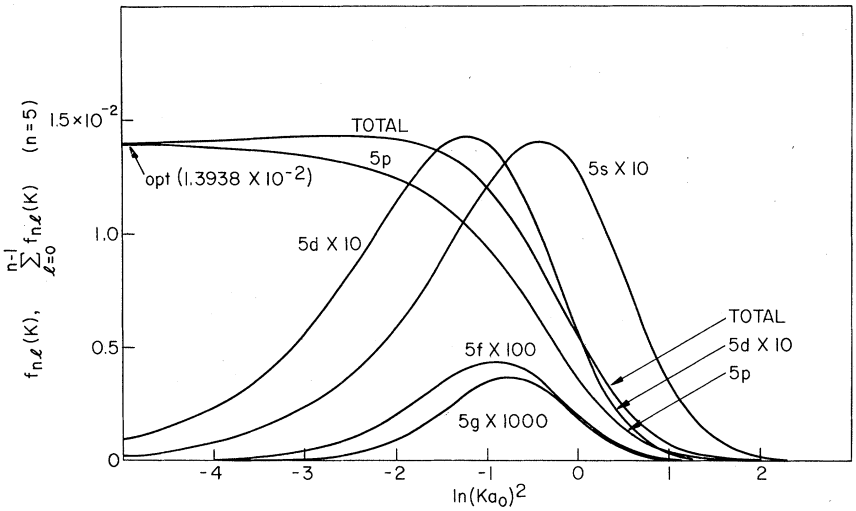

FIG. 7. Generalized oscillator strengths for the transitions from the ground state to the $n=5$ level of H (I66).

labeled "TOTAL." While $f_{E_n}(K)$ for $n=2$ and 3 are monotonically decreasing, $f_{E_n}(K)$ for $n\geq 4$ exhibits a broad maximum that becomes increasingly more discernible for larger n, as verified by logarithmic differentiation of Eq. (3.9).

For the transitions into the continuum of H, which occur whenever the energy transfer E is greater than the ionization threshold energy $I_1=R$, an expression corresponding to Eq. (3.9) is

$$\frac{df(K,E)}{dE}=\frac{2^7[(Ka_0)^2+(E/3R)]ER^{-2}}{[(K+\kappa)^2a_0^2+1]^3[(K-\kappa)^2a_0^2+1]^3}\times\{1-\exp[-2\pi/(\kappa a_0)]\}^{-1}\times\exp\left\{-\frac{2}{ka_0}\arctan\left[\frac{2\kappa a_0}{(Ka_0)^2-(\kappa a_0)^2+1}\right]\right\},\quad(3.10)$$

where $\hbar\kappa$ is the magnitude of the momentum of the ejected electron, and thus is related to E by

$$\kappa a_0=[(E/R)-1]^{1/2}.\quad(3.10')$$

This result was derived by Bethe (B30) and by Massey and Mohr (MM31). Examination of the derivation readily reveals that in Eq. (3.10) one should use the branch of the multivalued arctangent function that lies between 0 and π (W52, H69b). Notice that $df(K,E)/dE$ of Eq. (3.10) corresponds to the definition of Eq. (2.21) and includes contributions from all angular-momentum states at given E.

Figure 8 shows the behavior of $df(K,E)/dE$ for $1\leq E/R\leq 4$. The curve at the ionization threshold $E/R=1$ still is similar to that of $f_{E_n}(K)$ for $n\geq 4$ (Figs. 6 and 7), but the curve at $E/R=1.5$ already exhibits a significantly different shape, characterized by a clearly discernible maximum at about $(Ka_0)^2=0.6$. This maximum becomes more and more distinct with increasing E. The limiting value of $df(K,E)/dE$ as $K\to 0$ (i.e., the differential dipole oscillator strength) diminishes fairly rapidly with increasing E. The behavior for $4\leq E/R\leq 50$ shown in Fig. 9 confirms the above-mentioned trend. This whole situation is interpreted in the following elementary way.

First, consider a process with energy transfer (say $E/R=50$) much greater than the binding energy ($I_1=R$ for atomic hydrogen) of the atomic electron. Then, the role of the binding must be relatively insignificant, and the atomic electron will receive the energy transfer in nearly the same way as if it were free. In this "free-electron" limit, conservation of energy and momentum permits only those collisions in which the recoil energy Q of Eq. (2.7) is equal to E, or equivalently $(Ka_0)^2=E/R$. According to the meaning of the generalized oscillator strength discussed in the beginning of Sec. 2.2, the $df(K,E)/dE$ in this case is nonvanishing only at $(Ka_0)^2=E/R$.

Because the atomic electron in reality is bound and its momentum undergoes quantum-mechanical fluctuations, collisions with $(Ka_0)^2$ values unequal but close to E/R do take place. Therefore, the peaks in Fig. 9 have finite widths, which are largely attributable to the electron binding. In this connection, it may be instructive to inspect the behavior of $df(K,E)/dE$ given by Eq. (3.10) when $(Ka_0)^2\approx E/R\gg 1$. It is easy to see that the peak mathematically stems from the denominator factor

$$[(K+\kappa)^2a_0^2+1]^3[(K-\kappa)^2a_0^2+1]^3=\{[(Ka_0)^2-(E/R)]^2+4(Ka_0)^2\}^3\approx\{[(Ka_0)^2-(E/R)]^2+4(E/R)\}^3$$

because all the other factors are slowly varying functions of $(Ka_0)^2$. Thus, $df(K,E)/dE$ is appreciable only if

$$|(Ka_0)^2-(E/R)|<\xi(E/R)^{1/2},\quad(3.11)$$

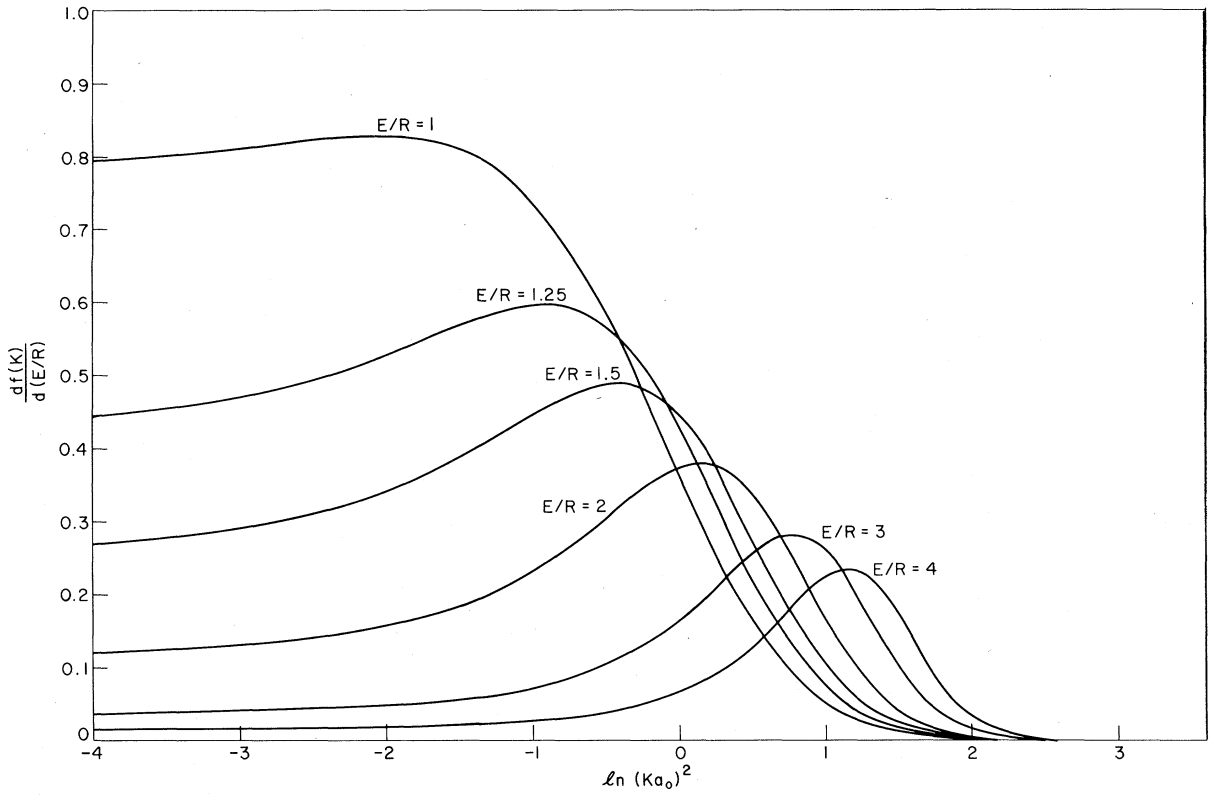

FIG. 8. Density of the generalized oscillator strength per unit range of excitation energy E for the transitions with $1 \leq E/R \leq 4$ from the ground state into the continuum of H (I66).

where ξ is a constant of the order of magnitude of unity. In other words, *$df(K, E)/dE$, when considered as a function of* $(Ka_0)^2$, has a peak with the width $\xi(E/R)^{1/2}$, which slowly increases as E/R. For a discussion about the cross section $d\sigma_n$ [Eq. (2.14)], however, it is more appropriate to consider *$df(K, E)/dE$ as a function of* $\ln (Ka_0)^2$. Then one may recast the inequality (3.11) as

$$| \ln (Ka_0)^2 - \ln (E/R) | < \xi(R/E)^{1/2}, \quad (3.11')$$

and state that the width in the $\ln (Ka_0)^2$ scale is $\xi(R/E)^{1/2}$. In this way one understands why peaks in Fig. 9 become sharper and sharper as E/R increases. For excitation from a shell of any atom or molecule with the binding energy B, the width of the peak is of the order of magnitude of $(B/E)^{1/2}$ in the $\ln (Ka_0)^2$ scale [as will be seen in Eq. (4.83)].

For smaller values of E/R, the simple picture discussed above breaks down because the initial binding becomes decisive. In particular, the electron, upon ejection, feels the attractive Coulomb field of the residual ion.

The generalized oscillator strength is represented comprehensively by a three-dimensional plot of $df(K, E)/dE$ as a function of $\ln (Ka_0)^2$ and E. Such a plot, a composite of the curves in Figs. 4–9, is the surface shown in Fig. 10, which we call *the Bethe surface* (IP65).

Concerning the definition of the Bethe surface, it is most advantageous to treat the discrete spectrum in the following manner. To represent $f_n(K)$ for a discrete excitation to a state at E_n, one plots a block with height $f_n(K)(dn/dE_n)$ and having as base the energy interval $E_n - \Delta E_n \leq E \leq E_n + \Delta E_n$, where $\Delta E_n = \frac{1}{2} dE_n/dn$. Then the discrete portion of the surface smoothly joins the continuum portion (Sec. 2.4 of FC68, p. 218 of BJ68, and Footnote 20 of KI69a).[4]

[4] For any atom or molecule, suppose one can identify a Rydberg series characterized by a set s of quantum numbers such as angular momenta. Each state belonging to the series is specified by the effective quantum number $n_s^* = n - \mu_s$, where n is the principal quantum number and μ_s is the quantum defect for the series s. As $n \to \infty$, the series converges to its limit, i.e., the ionization threshold I_s at which the continuum characterized by the same s begins. Let $f_{n_s*}(K)$ be the generalized oscillator strength for state n_s^*, and let $df_s(K, E)/dE$ be the density of the generalized oscillator strength for the continuum s. Then, according to the basic concept of the quantum-defect theory (Se70 and references therein), one expects the continuity in the sense that

$$\lim_{n \to \infty} [(n_s^*)^3/2R] f_{n_s*}(K) = df_s(K, E)/dE \,|_{E=I_s}.$$

(One must restate the continuity relation, however, when the series interacts with another series, i.e., with a series having a different s.)

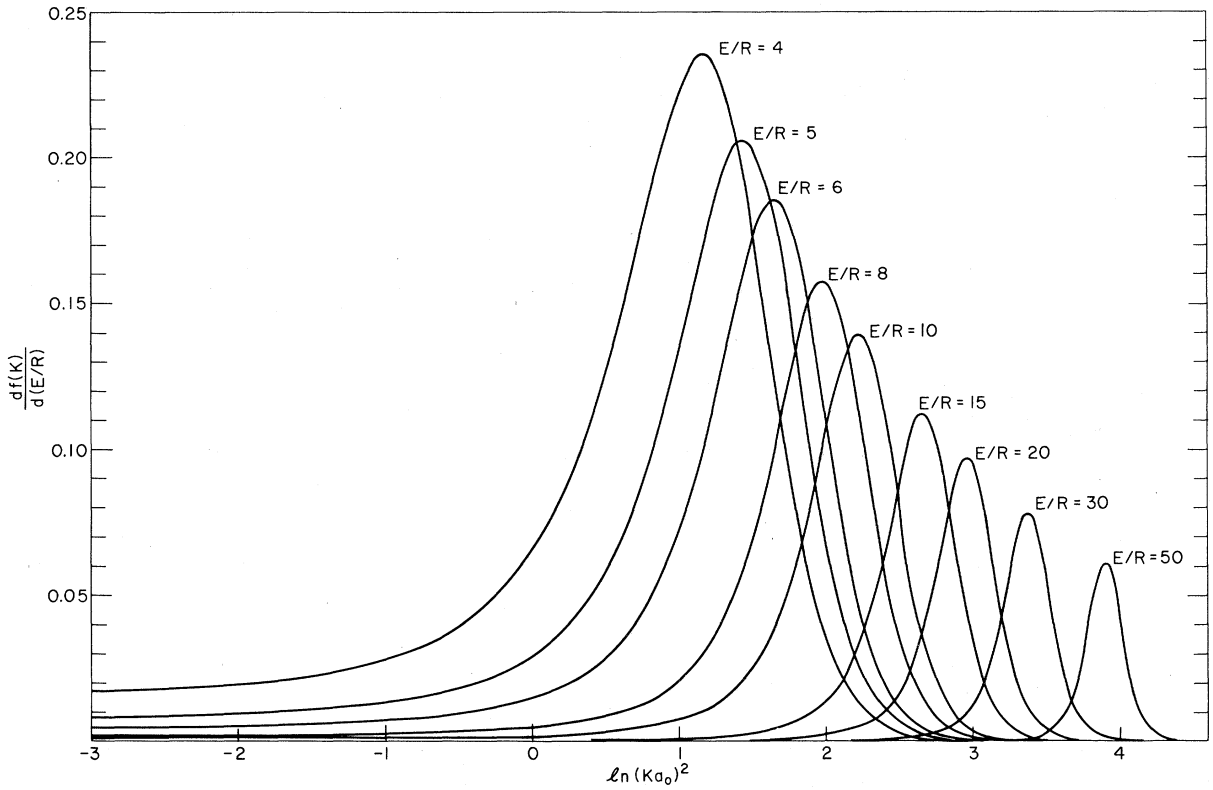

FIG. 9. Density of the generalized oscillator strength per unit range of excitation energy E for the transitions with $4 \leq E/R \leq 50$ from the ground state into the continuum of H (I66). Note the change of vertical scale from that of Fig. 8.

For H, for which $E_n = (1-n^{-2})R$, this situation becomes clear when one verifies that

$$\lim_{n\to\infty} (n^3/2R) f_n(K) = df(K, E)/dE\,|_{E=R}, \quad (3.12)$$

where the left-hand side is evaluated by Eq. (3.9) and the right-hand side by Eq. (3.10).

The Bethe surface embodies all information concerning the inelastic scattering of charged particles by an atom or molecule within the first Born approximation. Experimental investigations of the kind discussed in Sec. 3.1, as well as theoretical calculations of the generalized oscillator strength, may be regarded as a topographical survey of this surface, which plays a role in our present subject similar to that of the better-known Fermi surface in the electronic structure of crystals.

The Bethe surface gives one a clear perspective of the entirety of inelastic collisions. Therefore, it is especially useful for an analysis of quantities such as the stopping power and the total inelastic-scattering cross section (Sec. 4.3). For example, the stopping cross section $\sum_n E_n \int d\sigma_n$ (where the summation includes the integration over continua) is equal to the volume under the surface above a domain of ln $(Ka_0)^2$ and E determined by kinematics (as seen in Figs. 1 and 2), apart from the factor $4\pi z^2 a_0^2 R^2/T$.

In Fig. 10, View (a), the curve on the left vertical plane, which corresponds to the intersection of the surface at a small value of $(Ka_0)^2$, approximately represents the density of the optical oscillator strength per unit E, i.e., the photoabsorption cross section (apart from a universal constant) for photon energy E. The energy-loss spectrum in the forward scattering of fast electrons [Eq. (3.4)] closely approximates that curve for small E except for the kinematical factor (roughly E^{-3}). As E increases, $(Ka_0)^2_{\min}$ of Eq. (2.17) becomes more and more appreciable and the correspondence between the energy-loss spectrum for forward scattering and the photoabsorption cross section becomes looser and looser (cf. Figs. 1 and 2).

Figure 10 immediately shows that two distinct domains are important. The first domain where E/R is small or moderate and $(Ka_0)^2$ is small represents "soft" collisions, classically associated with large impact parameters (as noted in Sec. 4.4). These collisions largely depend on the dipole property, which governs the photoabsorption and which is sensitive to the electronic structure of an individual atom or molecule, especially for lower E. The second domain where both E/R and

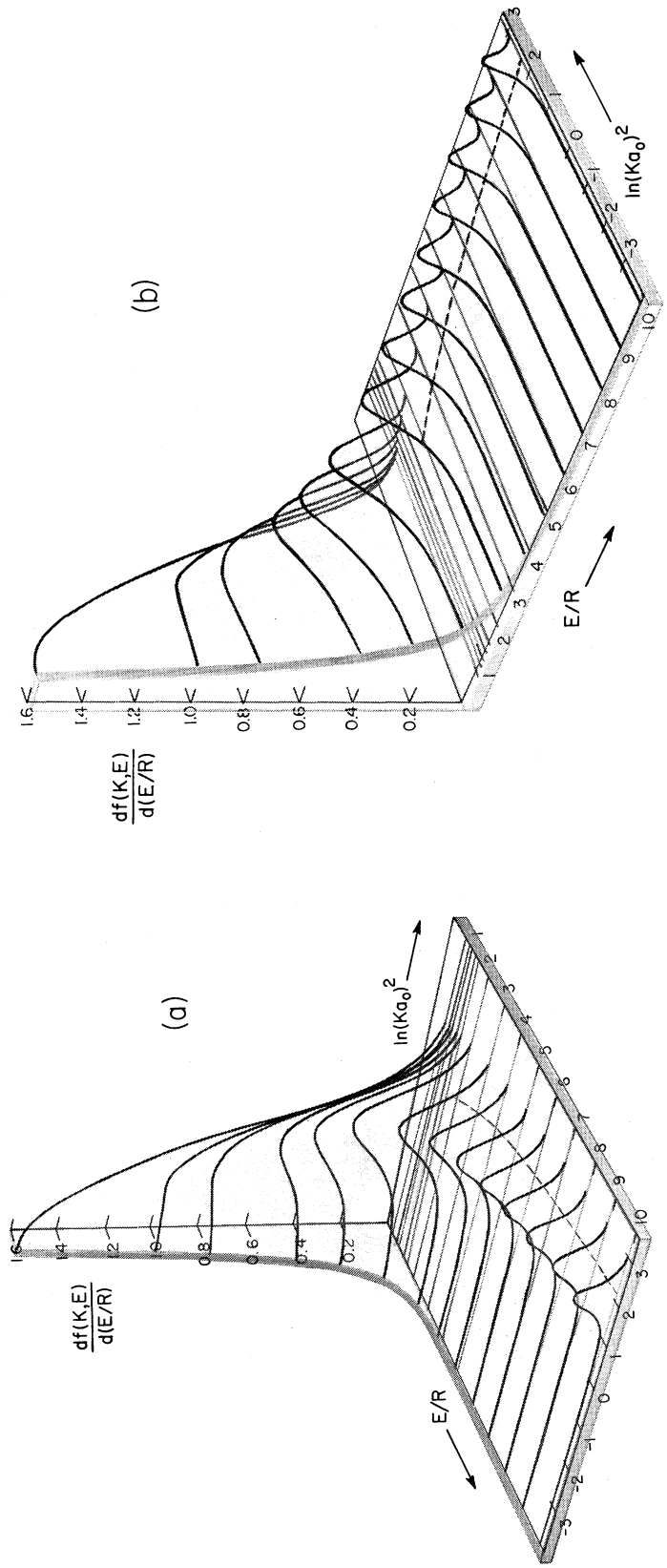

FIG. 10. Photographs of a plastic model of the Bethe surface for atomic hydrogen. The horizontal axes for E/R and $\ln (Ka_0)^2$ define the base plane. The vertical axis represents $Rdf(K, E)/dE$. The fourteen plates are placed at $E/R = 3/4, 8/9, 1, 5/4, 3/2, 2, 3, 4, 5, 6, 7, 8, 9$, and 10. The first two plates represent the discrete spectrum, in which case the vertical scale corresponds to $\frac{1}{2}n^3 f_n(K)$, n being the principal quantum number. While the model shows the major portion $-4 \leq \ln (Ka_0)^2 \leq 3.6$, the surface indefinitely extends as a plateau toward smaller $\ln (Ka_0)^2$. The dotted curve on the base plane shows the location $(Ka_0)^2 = E/R$ of the Bethe ridge, which is the main feature for large E/R. View (a) shows the spreading of the Bethe ridge with decreasing E/R. The optical region $(Ka_0)^2 \ll 1$ develops conspicuously for small E/R. View (b) shows in front a cut at $\ln (Ka_0)^2 = -4$, a curve that closely approximates the photoabsorption spectrum Rdf/dE. The author cordially thanks Mr. Allen L. Harlow for building the model.

$(Ka_0)^2$ are large is characterized by *the Bethe ridge*, which peaks around the curve $(Ka_0)^2=E/R$. This latter feature of the Bethe surface is common to all atoms and molecules, as seen from the interpretation given earlier, and is decisive in the theory of stopping power (B30, B33, F63).

The behavior of the generalized oscillator strength at small values of $(Ka_0)^2$ deserves particular attention, because it is equivalent to the differential cross section at small scattering angles, which often is studied experimentally. Straightforward Taylor expansion of the exponential in Eq. (2.5) results (S58, IP65) in

$$f_n(K)=\sum_{\lambda=0}^{\infty}(Ka_0)^{2\lambda}f_n^{(\lambda)}/\lambda!, \tag{3.13}$$

where

$$f_n^{(\lambda)}=[d/d(Ka_0)^2]^{\lambda}f_n(K)\,|_{K=0}$$

$$=\lambda!\frac{E_n}{R}\sum_{\kappa=1}^{2\lambda+1}\frac{(-1)^{\lambda-\kappa+1}}{\kappa!(2\lambda+2-\kappa)!}X_n^{(\kappa)}X_n^{(2\lambda+2-\kappa)*}, \tag{3.14}$$

$$X_n^{(\kappa)}=(n\,|\sum_j x_j^{\kappa}\,|\,0)/a_0^{\kappa}, \tag{3.15}$$

and $x_j=(\mathbf{K}\cdot\mathbf{r}_j)/K$. In Eq. (3.14), $X_n^{(2\lambda+2-\kappa)*}$ means the complex conjugate of $X_n^{(2\lambda+2-\kappa)}$. The first expansion coefficient $f_n^{(0)}$ is the optical oscillator strength f_n of Eq. (2.10). The absence of terms with odd powers of Ka_0 is a consequence of the definite parity of any atomic eigenstate. Furthermore, for optically allowed transitions, $X_n^{(\kappa)}$ vanishes for all even κ; for optically forbidden transitions, it vanishes for all odd or all even κ depending upon the parities of states 0 and n.

Properties of the coefficients $f_n^{(\lambda)}$ are of considerable importance in several respects. First, when one attempts to determine the optical oscillator strength f_n from electron-scattering data, one encounters the need for an extrapolation of $f_n(K, T)$ to the limit $K=0$, which never is physically attained for any inelastic collision [Eq. (2.17)]. Our present knowledge about $f_n^{(\lambda)}$ for $\lambda\geq 1$ is too limited to be of use in the extrapolation. Theoretical data on $f_n^{(\lambda)}$ for H (IP65, I66) and for He (KI68, KI69a, KI69b) may serve as a guideline for future work. Second, $f_n^{(\lambda)}$ for $\lambda\geq 1$ contains matrix elements $X_n^{(\kappa)}$ which are in general related to higher-multipole optical transitions (G66, G88). For example, a value of $X_n^{(2)}$ deduced from $f_n^{(1)}$ for an $S\leftrightarrow D$ transition immediately yields the electric-quadrupole moment of the same transition. Notice, however, that $X_n^{(\kappa)}$ itself is different from a multipole matrix element. In this connection, the following two instances are illustrative. For an $S\leftrightarrow P$ transition, $X_n^{(3)}$ in general is finite, but the octopole-moment matrix element vanishes owing to the symmetry. Further, for an $S\leftrightarrow S$ transition, which is optically forbidden with any multipole, $X_n^{(2)}$ in general is finite.

Whereas the existence of $f_n(K)$ as given by the integral of Eq. (2.5) is ensured for all real K, the power-series expansion (3.13) converges only for sufficiently small $(Ka_0)^2$. For the transitions into the continuum the domain of convergence is given by the excitation energy E involved via the inequality $(Ka_0)^2<E/R$ (W51, W52), as can be verified in the case of H by use of Eq. (3.10). The radius of convergence in general is governed by the asymptotic behavior of the atomic wave functions involved (L65, V67).

Lassettre (L65) pointed out that the generalized oscillator strength can be expressed by a power series in a variable $(Ka)^2/[(Ka_0)^2+\zeta^2]$, where ζ is a constant determined from the energies of the atomic states, and that this power series, unlike Eq. (3.13), is convergent for all real $(Ka_0)^2$. For discrete excitations in atomic hydrogen in particular, the series happens to terminate after a finite number of terms. In general, the Lassettre series, with appropriate truncation [Eq. (3.44)], often is useful for fitting experimental or theoretical data. Vriens (V67) and Crothers (Cr70) have extended Lassettre's analysis and have given numerical applications (see also VC70). It may be added that another representation of $f_n(K)$, in terms of a linear combination of exponential functions of $(Ka_0)^2$, has been suggested (Gr66, GD67). In contrast to the Lassettre series, this representation lacks a firm theoretical basis, and therefore must be considered merely as a means of summarizing empirical data for numerical work.

3.3. The Sum Rules

In contrast to the local spectral properties discussed in Sec. 3.2, the following sum rules represent global properties of the Bethe surface. Consider the μth (energy) moment of the distribution of the generalized oscillator strength

$$S(\mu, K)=\sum_n (E_n/R)^{\mu}f_n(K), \tag{3.16}$$

where the summation extends over all excited states. The portion corresponding to continua should be understood as the integral

$$\int (E/R)^{\mu}[df(K, E)/dE]dE.$$

Some of the moments $S(\mu, K)$ can be expressed in terms of remarkably simple formulas.

For $\mu=-1$, the derivation is simplest; from Eqs. (2.5), (2.9), and (3.16), together with the completeness relation, one immediately obtains

$$S(-1, K)=[\sum_j\sum_k\langle\exp[i\mathbf{K}\cdot(\mathbf{r}_k-\mathbf{r}_j)]\rangle$$

$$-|\sum_j\langle\exp(i\mathbf{K}\cdot\mathbf{r}_j)\rangle|^2]/(Ka_0)^2, \tag{3.17}$$

where the angle brackets $\langle\ \rangle$ denote the expectation value in the initial state (most often the ground state). The right-hand side of Eq. (3.17) may be written as $ZS_{\mathrm{inc}}(K)/(Ka_0)^2$, where Z is the total

number of atomic electrons and $S_{\rm inc}(K)$ is the incoherent-scattering function well known in x-ray physics (Cu69, Hu69). In the limit $K\to 0$, Eq. (3.17) reduces to

$$S(-1,0)=\sum_j\sum_k\langle x_j x_k\rangle/a_0^2, \tag{3.18}$$

which is the sum of M_n^2 defined by Eq. (2.11) and thus may be called the total dipole-matrix-element squared, $M_{\rm tot}^2$. In Eqs. (3.17) and (3.18) the cross terms with $j\neq k$ explicitly indicate the role of electron correlation (IKP67).

The calculation of $S(0,K)$ leads to the Bethe sum rule (B30)

$$S(0,K)=Z \qquad \text{(for any } K\text{)}, \tag{3.19}$$

standard proofs of which appear in many references (B30, p. 303 of BJ68, p. 581 of LL65). Equation (3.19) is a remarkable generalization of the Thomas–Reiche–Kuhn sum rule that corresponds to the limit $K\to 0$. For illustration of a general point of view appropriate to the treatment of sum rules (P52, K59, FT64), a slightly formal derivation is given below. The insertion of Eqs. (2.34)–(2.36) into Eq. (3.16) followed by the interchange of integrations with respect to E and t yields

$$S(\mu,K)=(-i\hbar/R)^{\mu+1}(Ka_0)^{-2}\phi^{(\mu+1)}(K,0), \tag{3.20}$$

an expression showing that $S(\mu,K)$ is in essence the $(\mu+1)$th time derivative of the correlation function $\phi(K,t)$ evaluated at $t=0$, in agreement with a general theorem (K59). For $\mu=0$, one must compute $\phi^{(1)}(K,0)$. For brevity, denote the Heisenberg operator $\sum_j \exp[i\mathbf{K}\cdot\mathbf{r}_j(t)]$ by $A(t)$ and denote its time derivative by

$$A^{(1)}(t)=(i/\hbar)[H,A(t)], \tag{3.21}$$

where the symbol $[,]$ stands for a commutator. [For the definition of $\mathbf{r}_j(t)$, see Eq. (2.36).] Then from Eq. (2.35) one obtains

$$\phi^{(1)}(K,0)=\partial\langle A^*A(t)\rangle/\partial t\,|_{t=0}=\langle A^*A^{(1)}\rangle, \tag{3.22}$$

where $A^{(1)}\equiv A^{(1)}(0)$, and A^* denotes the Hermitian conjugate of $A\equiv A(0)$. So long as the eigenfunction may be taken as real, i.e., unless magnetic fields are present, one can easily see that $(n'\mid A\mid n)=(n\mid A\mid n')$ and $(n'\mid A^{(1)}\mid n)=-(n\mid A^{(1)}\mid n')$ for any operator A which is a function of $\mathbf{r}_j$ but not of momentum $\mathbf{p}_j$. Therefore, we find $\langle A^*A^{(1)}\rangle=-\langle A^{(1)}A^*\rangle$, the use of which in Eq. (3.22) results in

$$\phi^{(1)}(K,0)=\tfrac{1}{2}\langle[A^*,A^{(1)}]\rangle. \tag{3.23}$$

If the Hamiltonian H is of the usual (nonrelativistic) form

$$H=(2m)^{-1}\sum_j \mathbf{p}_j^2+U(\mathbf{r}_1,\cdots,\mathbf{r}_Z), \tag{3.24}$$

explicit evaluation of Eq. (3.23) gives

$$\phi^{(1)}(K,0)=(i\hbar/2m)K^2Z, \tag{3.25}$$

which leads to the desired result, Eq. (3.19).

The evaluation of $S(1,K)$ requires

$$\begin{aligned}\phi^{(2)}(K,0)&=(\partial^2/\partial t^2)\langle A^*A(t)\rangle\,|_{t=0}=(\partial/\partial t)\langle A^*A^{(1)}(t)\rangle\,|_{t=0}\\&=(\partial/\partial t)\langle A^*(-t)A^{(1)}\rangle\,|_{t=0}=-\langle A^{*(1)}A^{(1)}\rangle.\end{aligned} \tag{3.26}$$

[Alternative expressions $\langle A^*A^{(2)}\rangle$ and $\langle A^{*(2)}A\rangle$ are disadvantageous for evaluation because they lead to double commutators.] By working out the commutator of Eq. (3.21), one arrives at

$$\begin{aligned}S(1,K)&=-(\hbar/R)^2(Ka_0)^{-2}\phi^{(2)}(K,0)\\&=(2mR)^{-1}\langle\,|\sum_j p_{x_j}\exp(iKx_j)\\&\qquad+\exp(iKx_j)p_{x_j}\,|^2\rangle,\end{aligned} \tag{3.27}$$

where $x_j=(\mathbf{K}\cdot\mathbf{r}_j)/K$, and p_{x_j} is the x component of the momentum of the jth electron. Equation (3.27) can be further reduced to

$$\begin{aligned}S(1,K)&=(Ka_0)^2\sum_j\sum_k\langle\exp[iK(x_k-x_j)]\rangle\\&\quad+(2/mR)\sum_j\sum_{k(j\neq k)}\langle\exp[iK(x_k-x_j)]p_{xk}p_{xj}\rangle\\&\qquad+(4/3R)\sum_j\langle\mathbf{p}_j^2/2m\rangle.\end{aligned} \tag{3.28}$$

The last term is equal to $4/3R$ times the total kinetic energy, which by virtue of the virial theorem may be equated to the negative of the energy eigenvalue of the initial state if the potential U in Eq. (3.24) is entirely Coulombic. In the optical limit, Eq. (3.28) becomes

$$S(1,0)=(4/3R)\sum_j\sum_k\langle\mathbf{p}_j\cdot\mathbf{p}_k)/2m\rangle, \tag{3.29}$$

which still contains cross terms ($j\neq k$).

A similar but more tedious calculation gives [cf. Eq. (32) of FT64]

$$\begin{aligned}S(2,K)&=Z(Ka_0)^4+(4/R)(Ka_0)^2\sum_j\langle\mathbf{p}_j^2/2m\rangle\\&\quad+8a_0^3\sum_j\sum_{k(j\neq k)}\langle\,|\mathbf{r}_j-\mathbf{r}_k|^{-3}j_2(K\,|\mathbf{r}_j-\mathbf{r}_k|)\rangle\\&\qquad+(16\pi a_0^3/3)Z_N\sum_j\langle\delta(\mathbf{r}_j)\rangle,\end{aligned} \tag{3.30}$$

where j_2 is the spherical Bessel function of the first kind and Z_Ne is the charge on the atomic nucleus. (For molecules, the last term must be summed over all nuclei.) Notice also that only the last term survives in the limit $K\to 0$.

The moment $S(\mu,K)$ for $\mu\geq 3$ can be formally

treated in a similar way, but actually the result will contain a divergent term for practically any atom or molecule. Mathematically, the asymptotic behavior of $df(K, E)/dE$ is given (RF67) as

$$df(K, E)/dE \sim E^{-3.5} \quad \text{(for } E\to\infty \text{ and fixed finite } K\text{)}, \tag{3.31}$$

so that $S(\mu, K)$ as a function of the continuous variable μ is logarithmically divergent at $\mu=2.5$, a fact well known for $K\to 0$ (p. 217 of BJ68). A physical interpretation is as follows: As μ increases, $S(\mu, K)$ calculated as above will include higher and higher derivatives of A, and these include more and more contributions arising from the region near the nucleus where the motion of the atomic electrons is most violent. Indeed, $S(2, K)$ of Eq. (3.30) contains a δ-function term, which is still integrable, but $S(3, K)$ formally contains such terms as $\langle r_j^{-4}\rangle$, which are divergent for an atom or molecule that has a finite electron density at a nucleus.

When the initial atomic state is *the ground state*, E_n and $f_n(K)$ are invariably nonnegative. Then, for any real ξ, the expression

$$\sum_n [\xi(E_n/R)^{\nu/2}+(R/E_n)^{\nu/2}]^2(E_n/R)^{\mu}f_n(K)$$

is nonnegative. Therefore, one obtains an inequality

$$S^2(\mu, K)\le S(\mu-\nu, K)S(\mu+\nu, K) \quad \text{(for any real } \nu\text{)}, \tag{3.32}$$

where the equality occurs only if the distribution $f_n(K)$ is concentrated at a particular energy. Although the inequality (3.32) is nearly trivial, it is sometimes useful for a check of numerical data. It may be added that the equality in (3.32) is approached in the limit $Ka_0\to\infty$. From Eqs. (3.19), (3.28), and (3.30), one sees that $S(1, K)\to Z(Ka_0)^2$, $S(2, K)\to Z(Ka_0)^4$, and therefore $S^2(1, K)/[S(2, K)S(0, K)]\to 1$, as $Ka_0\to\infty$. This result is another manifestation of the Bethe ridge discussed in Sec. 3.2 in connection with Fig. 10.

For illustration, four moments for the ground-state hydrogen atom are

$$S(-1, K)=(Ka_0)^{-2}\{1-[1+\tfrac{1}{4}(Ka_0)^2]^{-4}\}, \tag{3.33}$$

$$S(0, K)=1, \tag{3.34}$$

$$S(1, K)=(Ka_0)^2+4/3, \tag{3.35}$$

$$S(2, K)=(Ka_0)^4+4(Ka_0)^2+16/3. \tag{3.36}$$

Sometimes it is useful to consider the moment

$$S^{(\lambda)}(\mu)=\sum_n (E_n/R)^{\mu}f_n^{(\lambda)}, \tag{3.37}$$

where $f_n^{(\lambda)}$ is the λth derivative of $f_n(K)$ evaluated at $K=0$ [Eq. (3.14)]. As long as $S(\mu, K)$ is well defined and well behaved ($\mu\le 2.5$), one may write

$$S^{(\lambda)}(\mu)=[d/d(Ka_0)^2]^{\lambda}S(\mu, K)\,|_{K=0}. \tag{3.38}$$

Some properties of $S^{(\lambda)}(\mu)$ are known and useful for applications. For example the Bethe sum rule [Eq. (3.19)] immediately implies (S58, IP65)

$$S^{(\lambda)}(0)=0 \quad \text{(for } \lambda=1, 2, \cdots\text{)}, \tag{3.39}$$

which is a remarkably strong restriction on $f_n^{(\lambda)}$. A case of interest in a later application (Sec. 4.3) is

$$S^{(1)}(1)=Z-4\hbar^{-2}\sum_j\sum_{k(j\neq k)}\langle x_j p_{xj} x_k p_{xk}\rangle, \tag{3.40}$$

which is derived by differentiation of Eq. (3.28). The second term in Eq. (3.40) arises from electron correlation and is expected to be small compared to Z. (See KI71 for data on two-electron atoms.) For any one-electron atom, $S^{(1)}(1)=1$ since the second term in Eq. (3.40) is absent.

Although $S(\mu, K)$ is divergent for $\mu\ge 2.5$, $S^{(\lambda)}(\mu)$ as defined by Eq. (3.37) exists for integer $\mu\ge 3$, provided that λ is made correspondingly large; the precise criterion for finite $S^{(\lambda)}(\mu)$ is $\mu-\lambda<2.5$, as seen from the analysis of Rau and Fano (RF67; see also KI71). Actually $S^{(2)}(4)$, for example, is used in the stopping-power theory (FT64). Qualitatively, the above situation may be interpreted in the following way. On one hand, larger and larger μ values weight contributions from higher and higher E that stem from an inner region of the atomic system where the electron density is greater. Thus, $S^{(\lambda)}(\mu)$ for any fixed λ diverges for excessively large values of μ. For a fixed μ, on the other hand, larger and larger λ values render contributions from the inner region of the atomic system less and less important [as may be understood from Eq. (3.14)]. These two trends tend to balance out, as μ and λ increase together.

No simple general formula for $S(\mu, K)$ for $\mu\le -2$ seems to be known. In the optical limit $K\to 0$, however, $S(-2, 0)$ is expressed in terms of the dipole polarizability α_d as

$$S(-2, 0)=\alpha_d/(4a_0^3), \tag{3.41}$$

and other moments for $\mu\le -3$ also are related to various physical properties (FC68, HBE64).

While the sum rules cannot completely determine the Bethe surface, they provide a powerful control on experimental or theoretical data for the generalized oscillator strength. By virtue of the sum rules, knowledge of the Bethe surface over a limited region of excitation energies allows one to infer some properties of the surface over the remaining region.

Considerations of the nuclear motion, so far disregarded, give rise to corrections to the sum rules, which apparently have not been studied except in the optical limit (HBE64).

It should be emphasized that the sum rules discussed above apply to the entire atomic system. Actually an atom or molecule with many electrons possesses shell structures, which among other properties manifest themselves in the generalized oscillator strength. Thus, a portion of its distribution may be assigned to a definite shell, but only approximately, because the notion of the shell stems from an independent-particle model, which never is exact. For example, "the total generalized oscillator strength for excitation from the K shell of Ne" is a convenient and useful concept, but its imprecise nature should be borne in mind upon every application. (A value for the above "quantity" is somewhat less than 2 and should depend on the momentum transfer $\hbar K$ in a way not well understood.) No clear-cut formulation of shellwise sum rules, even in the optical limit, seems to have been achieved (FC68).

The quantity

$$L(\mu)=\sum_n (E_n/R)^\mu f_n \ln (E_n/R) \qquad (3.42)$$

appears in several applications; $L(-1)$ concerns the total inelastic-scattering cross section (Sec. 4.3), $L(0)$ the stopping power (Sec. 4.3), $L(1)$ the straggling [i.e., statistical fluctuations in the energy loss of charged particles (F63)], and $L(2)$ the Lamb shift of energy levels (BS57). While $L(\mu)$, unlike $S(\mu, 0)$, does not seem to be expressible in terms of simple initial-expectation values, there is a useful relationship between $L(\mu)$ and $S(\mu, 0)$. If $S(\mu, 0)$ is regarded as a function of a continuous variable μ, then $L(\mu)$ is simply the derivative $\partial S(\mu, 0)/\partial\mu$. Therefore, in order to estimate $L(\mu)$, one may sometimes use $S(\mu, 0)$ values at several integral values of μ and take the derivative either graphically or by means of an analytical fit (P59, D60). This procedure may succeed in giving a trustworthy value of $L(\mu)$ if the variation of $S(\mu, 0)$ near the particular value of μ is sufficiently mild and well determined.

A mathematical relation, sometimes used in the evaluation of $f_n(K)$, may be indicated here. Taking the matrix element of the commutator $[H, A]$ between eigenstates n and 0, one readily sees that

$$(n \mid [H, A] \mid 0)=E_n(n \mid A \mid 0),$$

where E_n is by definition the difference between the eigenenergies of n and 0. From Eq. (3.21), the left-hand side is equal to $(\hbar/i)(n \mid A^{(1)} \mid 0)$, and thus in effect represents the matrix element of the time derivative of A in the Heisenberg picture. If one works out the commutator with H given by Eq. (3.24) and uses the result in Eqs. (2.5) and (2.9), one obtains

$$f_n(K)=(R/E_n)\,a_0^2 \mid \sum_j \int \exp(iKx_j) \times (u_0 \partial u_n^*/\partial x_j - u_n^* \partial u_0/\partial x_j)\, d\mathbf{r}_1, \cdots, d\mathbf{r}_Z \mid^2, \qquad (3.43)$$

an expression alternative to Eq. (2.9). Because the operators in Eq. (2.9) and (3.43) reduce for $K\to 0$ to $\sum_j \mathbf{r}_j$ and $\sum_j \dot{\mathbf{r}}_j$, respectively, these expressions are called somewhat loosely the "length" formula and the "velocity" formula (BFM50).

Although the two formulas are equivalent for exact atomic eigenfunctions, they differ in the weights with which the contributions from different portions of the configuration space are included. For example, at least for $K\to 0$, the major contributions to Eq. (3.43) arise from an inner region of the atomic system, while those to Eq. (2.9) arise from an outer region. Therefore, when approximate eigenfunctions are used, the two formulas usually give different numerical results, and the difference between them provides *a measure of consistency*. However, a close agreement between the two numerical results by no means should be taken as a proof of their *reliability*. In fact, one can devise a scheme of constructing approximate u_0 and u_n in such a way that the two formulas give identical results; an independent-particle model in which all the atomic electrons move in a single local potential is an example. (Similarly, the Bethe sum rule may be satisfied with $f_n(K)$ computed from the set of exact eigenfunctions associated with that highly idealized model.)

Recently Starace (S71) has given a detailed discussion on the two formulas, specifically in the optical limit $K\to 0$. Thus he has identified a class of approximations to atomic eigenfunctions for which the "length" formula is logically more consistent. His conclusion appears to be valid for finite K also, possibly after minor modifications.

Also, one may consider the matrix element of the double commutator $[H, [H, A]]$ to obtain

$$(n \mid [H, [H, A]] \mid 0)=E_n^2(n \mid A \mid 0),$$

which will lead to another alternative expression for $f_n(K)$ that may be called the "acceleration" formula. This formula weighs the contributions from an innermost region of the atomic system even more heavily than the "velocity" formula does. Inasmuch as standard variational methods are inadequate for accurately determining the behavior of wave functions in the innermost region, the "acceleration" formula seldom is advantageous for numerical evaluation of $f_n(K)$.

3.4. Atoms

The purpose of this and the succeeding section is to discuss specific atoms and molecules that bring out some significant aspects of the understanding of the Bethe surface.

Apart from the hydrogen atom for which theoretical knowledge is virtually complete but presently available experimental data (BGR61, W69) appear provisional, the helium atom is the best understood with

respect to the Bethe surface. Chiefly owing to a series of investigations by Lassettre and coworkers (L69 and references therein), the major portion of the Bethe surface for He is known within several percent.

As early measurements (V31, WT34, WW35) already showed, the $2^1P \leftarrow 1^1S$ excitation gives rise to the most intense peak in the electron energy-loss spectrum at small scattering angles. The generalized oscillator strength $f_{2^1P}(K)$ for this transition has been repeatedly studied both experimentally and theoretically and thus offers a "case history" as sketched below.

The first calculation by Massey and Mohr (MM31, M33) used hydrogenlike wave functions in the "length" formula, Eq. (2.5). Miller and Platzman (MP57) pointed out that the result of this calculation was seriously in error; in the optical limit $K \to 0$, the Masse–Mohr result was $f_{2^1P}=0.19$, while Miller and Platzman had concluded from an analysis of optical sum rules that the correct value should be about 0.277. They also suggested that the results of Altshuler (A52), who had used the same pair of wave functions but evaluated the "velocity" formula, Eq. (3.43), must be more reliable. The calculation by Jones (J48, LJ64) used a pair of considerably more accurate wave functions explicitly including electron correlation in the "length" formula. Lassettre and coworkers (SL58, LKS64 and SL64) justifiably regarded this result as adequately accurate for normalization of experimental data on He as well as on all other atoms and molecules. In fact, the pair of wave functions used by Jones had given the optical oscillator strength $f_{2^1P}=0.268$ (W33). As a result of pre-eminent studies on the two-electron atoms by Pekeris and coworkers, a conclusively accurate value $f_{2^1P}=0.27616\pm0.00001$ became available later (SP64). Thus, the Jones result turned out to be too small by 3% at $K \to 0$.

The remarkably high precision claimed for modern measurements (K68, KMC69, L69) indicated the need for an improved calculation. [The sensitivity of $f_{2^1P}(K)$ to different approximate wave functions is well known from studies in the optical limit (W67) and is demonstrated by numerous calculations (e.g., BKK68a, BKK68b, KK68, VdB69a, V70).] Kim and Inokuti (KI68) thus computed $f_{2^1P}(K)$ from the Weiss wave functions, which are nearly as accurate as the Pekeris wave functions, by use of the "length" and "velocity" formulas as well as of the expansion formula, Eq. (3.13). Their result is probably accurate to about 1% for $(Ka_0)^2 \leq 2$. An independent and equivalent calculation (BKK69) confirmed their "length" result.

The experimental situation up to 1968 is best summarized in L69. Briefly speaking, all measurements at that time were "relative" in the sense that they determined the differential cross section $d\sigma_{2^1P}/d\omega$ at different θ within a multiplicative constant only; the resulting data therefore had to be normalized against theory in one way or another. Thus, the comparison at this point with calculation was in essence a test of the *shape* of the apparent $\mathfrak{f}_{2^1P}(K, T)$ [Eq. (3.1)]. The data of Lassettre and coworkers (LKS64 for $T=511$ eV, SL64 for $T=500$ eV, LSM66 for $T=400$ eV) agree with the calculation (KI68), the average deviation for $(Ka_0)^2 \leq 2$ being about 3%. [Further, these data are normalized to the Jones theoretical result in the neighborhood of $(Ka_0)^2 \approx 0.3$, where it happens to be virtually the same as the new result of KI68. Therefore, renormalization against the latter result does not modify the conclusion.] The measurements of Vriens, Simpson, and Mielczarek (VSM68) for $T \leq 400$ eV, however, show a trend somewhat different from the measurements of Lassettre and coworkers. The data of VSM68 are normalized by fit to a truncated Lassettre series (L65, V67)

$$\mathfrak{f}_{2^1P}(K, T)/f_{2^1P} = (1+x)^{-6}[1+gx/(1+x)], \quad (3.44)$$

where f_{2^1P} is set at the accurate value of Schiff and Pekeris (SP64), g is a constant, and $x=(Ka_0)^2/3.391$. Under this normalization, the $\mathfrak{f}_{2^1P}(K, T)$ of VSM68 at $T=400$ eV declines with an increase of $(Ka_0)^2$ somewhat more steeply than the Lassettre data and is systematically smaller than the calculation of KI68. Later remeasurements with higher precision (SM69) at $T=400$ eV and at 511 eV confirm the shape of $\mathfrak{f}_{2^1P}(K, T)$ reported in VSM68. Thus, these measurements may suggest that there is an appreciable departure from the Born approximation for $T \lesssim 400$ eV. The data of Geiger (G63) verify the validity of the Born approximation at $T=25$ keV, though within an understandably modest precision owing to the photographic technique used in this experiment.

Lassettre, Skerbele, and Dillon (LSD69), using an improved apparatus, extended relative measurements at $T=500$ eV to the region of small momentum transfers, $0.08 \leq (Ka_0)^2 \leq 0.41$. They normalized their data through extrapolation to $(Ka_0)^2 \to 0$ by use of the fitting formula, Eq. (3.44). The result shows good agreement with the calculation of KI68, the average deviation of 2.3% being smaller than the claimed experimental precision. However, the deviation is systematic in the sense that the experimental data are slightly larger than theory.

The same paper (LSD69) presents, as a theoretical justification of the normalization procedure, the theorem of the limiting oscillator strength, namely,

$$\lim_{K \to 0} \mathfrak{f}_n(K, T) = f_n \qquad \text{(at any } T\text{)}. \quad (3.45)$$

The content of the theorem should be sharply distinguished from Eq. (3.2), which is based on the first Born approximation. The proof assumes only a finite radius of convergence for the Born series as a function of the interaction strength, and this remarkable theorem should apply to every transition in any atom

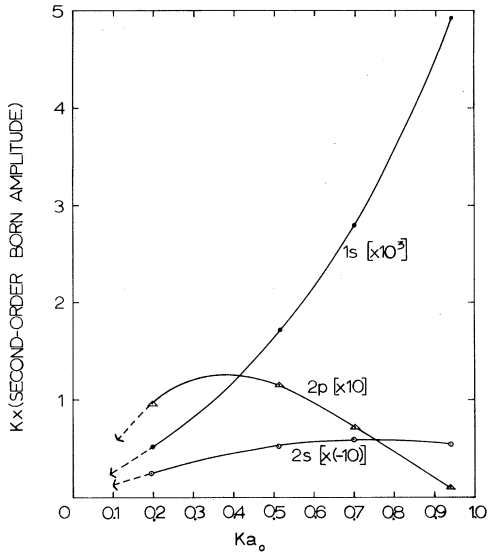

FIG. 11. Test of the calculated second-order Born amplitude with the theorem of the limiting oscillator strength. The abscissa represents Ka_0, and the ordinate represents K times the contribution of the respective labeled intermediate state to the second-order Born amplitude. Further, the ordinate quantity has been multiplied by the scaling factor shown in the square bracket. The data have been taken from KMS60.

or molecule. A qualification should, however, be borne in mind in the interpretation and application: the limit $K\to 0$ is never physically attained for any inelastic collision. The smallest momentum transfer for a given E_n and T [Eq. (2.17)] becomes appreciable for small T. Then, a check with the theorem will require an extrapolation of experimental data over the sizable unphysical region $0<(Ka_0)^2<(Ka_0)^2_{\min}$, a procedure that may prevent a unique conclusion. (In the particular application in LSD69, the unphysical region is comfortably small and the extrapolation is thus quite convincing.)

An illustration of the content of the theorem may be in order. Equation (3.45) follows immediately if the μth-order term in the Born expansion of the scattering amplitude[5] is bounded (after analytic continuation) at $K=0$ for every $\mu\geq 2$. (In contrast, the first-order Born amplitude behaves as K^{-1} near $K=0$.) It is of interest then to see if theoretical results (e.g., for the second-order Born amplitude) reveal the above property. Figure 11 illustrates such a test in the case of the $2s\leftarrow 1s$ excitation of the hydrogen atom by moderately slow electrons ($T/R=4$). The three curves depict as functions of K the contributions from the specified intermediate state to the second-order Born amplitude multiplied by K. Every curve should then extrapolate to the origin, in order to be consistent with the theorem. The $1s$ and $2s$ contributions clearly show this trend, while the behavior of the $2p$ contribution is somewhat inconclusive though apparently compatible with the theorem. Similar theoretical data for the $2p\leftarrow 1s$, $3p\leftarrow 1s$, and $3s\leftarrow 2s$ excitations of the hydrogen atom likewise conform to the theorem (H69a).

The latest development in the case history of the He 2^1P excitation is the advent of absolute measurements of the differential cross section $d\sigma_{2^1P}/d\omega$ (CMK70, LSD70, cf. K69 for a summary. By the term "absolute measurements" one means here determinations based solely upon experimental parameters without recourse to normalization to any theoretical result. Lassettre, Skerbele, and Dillon (LSD70) made their previous data (LSD69) "absolute" in the following manner. In the same laboratory Bromberg (Br69) had measured absolutely the differential cross section $d\sigma_{el}/d\omega$ for elastic scattering of 500-eV electrons by the helium atom, using an independent apparatus especially designed for this purpose. The Bromberg result combined with the ratio $(d\sigma_{2^1P}/d\omega)/(d\sigma_{el}/d\omega)$, which was determined from electron energy-loss spectra (including the elastic peak), readily leads to absolute $d\sigma_{2^1P}/d\omega$. The apparent generalized oscillator strength $f_{2^1P}(K, 500\text{ eV})$ thereby derived agrees well with the calculation of KI68. The average deviation of 1.2% is well within the experimental uncertainties.

Chamberlain, Mielczarek, and Kuyatt (CMK70) independently made absolute measurements for the 2^1P (and 2^1S) excitation as well as for the elastic scattering of electrons at $\theta=5°$ and $T=50$—400 eV. The resulting $d\sigma_{2^1P}/d\omega$ at $T=400$ eV is smaller by 9.5% than the calculation of KI68, and the trend of the data leads the authors to suggest that an asymptotic approach within 1% of the Born-approximation result will occur around $T=1$ keV. Further, the more recent result (unpublished) for $d\sigma_{2^1P}/d\omega$ at $\theta=5°$ and $T=500$ eV is again smaller by 6% than the calculation of KI68. Thus, the conclusion of CMK70 as to the validity of the Born approximation is different from that of Lassettre and coworkers (LSD69, LSD70) although the discrepancy between the two sets of data may barely exceed the combined estimates of systematic errors of the experiments involved.

One should consider the agreement within less than 10% between results of independent investigators as a remarkable accomplishment of the state of art, especially when one recalls far more serious discrepancies often found in the integrated excitation cross sections and total ionization cross sections (Sec. 4.2 and 4.3). At the same time, the same difference illustrates the extreme difficulty of absolute measurements with high precision. Clearly the case history of the $2^1P\leftarrow 1^1S$ excitation is still not closed.

The excitation $2^1S\leftarrow 1^1S$ exemplifies the situation

[5] The scattering amplitude $a_n(\theta, \varphi; T)$ is a function of θ, φ, and T, in general complexed valued, and is related to the differential cross section $d\sigma_n$ by $d\sigma_n=(k'/k)|a_n(\theta, \varphi; T)|^2 d\omega$, as explained on p. 551 of LL65 and p. 328 of MM65. Thus, the apparent generalized oscillator strength $f_n(K, T)$ of Eq. (3.1) may be expressed as $f_n(K, T)=(4z^2a_0^2)^{-1}(M/m)(E_n/R)(Ka_0)^2|a_n(\theta, \varphi; T)|^2$.

with an optically forbidden transition. The theoretical calculation is more sensitive to the choice of approximate wave functions, in part owing to the same symmetry of the atomic states involved (A53, VdB69a, V70). The calculation of KI68 for this case is, however, just as definitive as for the $2^1P \leftarrow 1^1S$ transition. The experimental study is more difficult than for the 2^1P excitation, simply because the cross section in the pertinent velocity region is much smaller. Comparison of theory (KI68) with experiment (LKS64, SL66, BGS67, VSM68, CMK70) apparently indicates that the Born-approximation limit is attained at higher electron velocities than for the 2^1P excitation. (This point will be discussed further in Sec. 5.2.)

The experimental study of other individual discrete excitations in He encounters a stringent requirement of electron-energy resolution. For example, the apparent generalized oscillator strength "for the 3^1P excitation" reported in LKS64 and in G63 actually corresponds to the sum $f_{3^1P}(K, T)+f_{3^1S}(K, T)+f_{3^1D}(K, T)$ because neither of the two experiments had enough resolution to separate the three states (KI69b). Having achieved with 25-keV electrons a resolution width of about 5 meV, Boersch, Geiger, and Schröder (BGS67) obtained remarkable forward electron energy-loss spectra, which show the peaks for the n^1P excitations up to $n=11$ and which lead to relative values of optical oscillator strength f_{n^1P} in satisfactory agreement with theory. Experimental data concerning the K dependence of $f_n(K, T)$, however, are meager, while reliable theoretical results are available for several important transitions (O68b, KI68, KI69b, BKK69).

The transition to continua (i.e., the ionization) of He has been studied experimentally (LKS64, SL64) as well as theoretically (O69, BK70). Because the continuum wave function is very hard to evaluate with high accuracy, the agreement of theory with experiment within several percent should be considered as satisfactory at present. A notable feature in the continuum transition, already detected in an early experiment (WP34), concerns the double-electron excitation—e.g., to the $2s\,2p\ ^1P$ state, which is not quite stationary but is subject to autoionization into the $1s\,Ep\ ^1P$ continuum, where Ep denotes a continuum one-electron orbital at excitation energy E measured from the ground state. The electron energy-loss spectrum in the region around $E=60$ eV (SL64, BGS67) clearly exhibits an interference pattern due to the configuration interaction between the quasidiscrete state and the underlying continuum (F61).

The transitions from the metastable 2^1S and 2^3S states of He to other discrete states exhibit another notable aspect of the generalized oscillator strength. While the experimental study for these cases is still in an exploratory stage (BGT69), definitive calculations (KI69a) resulted in the recognition that the generalized oscillator strength can sometimes possess a zero-value minimum when plotted as a function of $(Ka_0)^2$, as shown in Fig. 12.

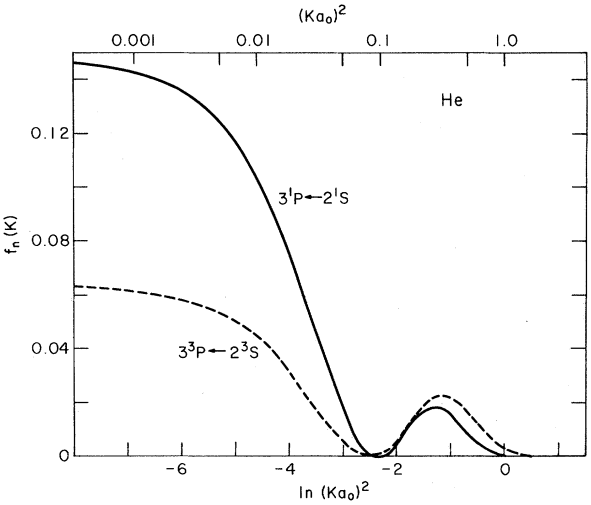

FIG. 12. The generalized oscillator strengths for the $3^1P \leftarrow 2^1S$ and $3^3P \leftarrow 2^3S$ transitions in He. The minima in these cases are exact zeros according to the first Born approximation. The data have been taken from KI69a.

The discussion from this point on will concern atoms in general rather than He.

The minimum of the generalized oscillator strength is significant in several respects (KICM68). First, when the matrix element $\epsilon_n(K)$ defined by Eq. (2.5), presumably a continuous function of K, changes its sign, a zero-value minimum of $f_n(K)$ occurs. A departure from exact zero in the measured $f_n(K, T)$ therefore may indicate failure of the first Born approximation. Otherwise, it may reveal certain interesting subtleties of atomic wave functions as will be described later. Second, within the validity of the Born approximation, the position of the minimum is related to the node of the orbitals of the electron active in the transition and therefore provides a stringent test of calculated wave functions that is hardly possible otherwise (KICM68). Third, minima of a similar origin occur frequently in atoms (B62, Ma69, Mc69, SL70a, Ma71) and in molecules as well (LW58, M69, MMK69). Finally, one may appreciate the generality of this phenomenon by noting that its analog has been observed in inelastic-scattering form factors for nuclear Coulomb excitations (DW66).

The values of $(Ka_0)^2$ at which a minimum occurs depend among other factors upon the excitation energy E. The presumably continuous succession of such minima for different E thus forms a trajectory on the plane with axes representing E/R and $\ln[(Ka_0)^2]$, above which the Bethe surface spans. The trajectory may (though not always) reach the $K=0$ plane (the optical limit) at certain values of E, in which case one finds the better-understood Cooper minimum—i.e., a minimum of the optical oscillator strength as

a function of E (S51, C62, Sec. 4.5 of FC68). Therefore, the minima will appear as a trough of the Bethe surface, a feature which is absent in Fig. 10 for H($1s$) but which is quite common for many-electron atoms (KICM68, Ma69, Ma71).

The relationship of the minima to the atomic wave functions can be studied explicitly with a specific atomic model. For example, Shimamura (Sh71) and Miller (M71) have examined the minima for a variety of atomic transitions in the case of the hydrogenlike model. Although these authors point out certain interesting systematics, it is unclear to what extent the results of the hydrogenlike model should apply to real atoms, in which the potential field seen by an active electron usually is known to be substantially non-Coulombic (FC68).

In general, the minimum is not necessarily a zero even within the first Born approximation. Notice that $|\epsilon_n(K)|^2$ usually implies a sum

$$\sum_{\Omega} |(n\Omega|\sum_j \exp(i\mathbf{K}\cdot\mathbf{r}_j)|0)|^2,$$

where Ω is a set of quantum numbers precisely describing degenerate channels for the final state. For example, in a continuum, Ω may designate the angular momentum or the direction of the ejected electron, in the same way as in Eq. (2.21). Each individual term in the sum will not vanish simultaneously at the same K and therefore $|\epsilon_n(K)|^2$ should be finite everywhere. If one of the terms dominates in a certain range of $(Ka_0)^2$ values and changes its sign, then $|\epsilon_n(K)|^2$ should show a near-zero minimum.

This cause for the nonzero minimum may be best illustrated in the following example. The spin–orbit coupling makes the radial functions for the final states different for different j, the quantum number for the total angular momentum (S51). Since the position of a minimum depends upon details of the radial wave functions for each j, the zero-value minimum occurs at different $(Ka_0)^2$ for different j. The combined contributions from different j at a particular E thus can never quite vanish in the continuum. Also, the intensity of the electrons ejected as a result of excitation near a minimum should be strongly dependent upon j, and therefore one expects marked spin polarization of these electrons (F69), an effect that has actually been confirmed in the optical limit (KL70).

Our knowledge of the Bethe surfaces for atoms other than H and He is still distressingly incomplete, for reasons that will be apparent below.

Experimental studies have so far been limited to those several atoms which can be put in isolation for a sufficiently long period of time and in a sufficiently large quantity. The valence-shell excitation of the rare-gas atoms has been studied occasionally (G64a, KS64, KICM68), but by no means in complete possible detail. Study on the inner-shell excitation is in the exploratory stage (AGLS68, VdW70, VW71).

The valence-shell excitation of alkali atoms is probably the case most systematically studied so far (HR68a, HR68b, HR69a, HR69b). However, the data normalization again beclouds comparison with theory (HR69b, Ma69). A serious discrepancy between experiment and theory exists for the $4^2F \leftarrow 4^2S$ transition in potassium (G68) and clearly indicates the need for future study. For small $(Ka_0)^2$, the generalized oscillator strength in this case should behave as $(Ka_0)^4$ [as seen from Eq. (3.14)], the constant of proportionality being related to the octopole transition probability. The experimental data (HR68a) show a $(Ka_0)^2$ dependence and a magnitude far greater than theoretically expected (G68) although the discrepancy may be in part attributable to a departure from the first Born approximation.

Skerbele and Lassettre (SL70a) experimentally studied the $6^1P_1 \leftarrow 6^1S_0$ transition of mercury and observed with incident electrons of 500 eV a shallow minimum of its apparent generalized oscillator strength between $(Ka_0)^2 = 1.1$ and 1.5. This location of the minimum is significantly different from that of a theoretical prediction by Mc69, i.e., $(Ka_0)^2 = 2.3$—3.3 depending upon the atomic models used. [The statement of SL70a about agreement with theory appears to stem from a misunderstanding of the result of Mc69. This discrepancy was kindly pointed out to the writer by Dr. S. T. Manson and Dr. Y.-K. Kim.] Clearly, the situation calls for further study, both experimental and theoretical.

The theoretical calculation of the generalized oscillator strength for many-electron atoms is invariably obstructed by lack of sufficiently accurate wave functions. The defect of hydrogenlike approximations is now well recognized at least in the optical limit and calls for the use of more realistic atomic models (FC68). Systematic studies (Ma69, ACS70, A71, Ma71, Mc71), which represent an initial but substantial step toward sound understanding, are based on an independent-electron model that includes an effective potential for the active electron derived from a self-consistent-field theory. However, the limitations of this approach again are already known in the optical limit (FC68). In particular, the importance of electron correlations, both in the initial and final atomic eigenstates, is now very well appreciated (A71). Only for small atoms such as Li and Be does there seem to be an immediate hope for calculations nearly as accurate as those for He.

Numerous publications on the excitation of atoms, as summarized in Secs. I 4–8 of MS68, report only the integrated cross sections, thus bypassing a discussion of the differential cross section, or the generalized oscillator strength. Inasmuch as the differential cross section provides a far more stringent test of both theory and experiment, it is hoped that future investigators will publish the differential-cross-section data in as great detail as possible.

3.5. Molecules

As compared to studies on atoms, studies on molecules with respect to generalized oscillator strength have so far been conducted largely with a different emphasis. An immediate objective of studies on molecules often has been focused on the spectroscopic aspect, i.e., on the elucidation of the nature of energy levels, as opposed to the more ambitious task of exploring the Bethe surface. Since at present there remains much to be learned about molecular energy levels—far more than about atomic energy levels, the difference in emphasis is inevitable and the discussion of this section accordingly will reflect these circumstances.

Yet there is a considerable amount of experimental data on the generalized oscillator strength for at least lower excitations of commonly occurring stable molecules (B69, L69). In contrast, only sporadic attempts have been made toward theoretical calculations, evidently because of the difficulty of obtaining molecular wave functions. For a general reference, the treatise by Massey, Burhop, and Gilbody (MBG69, Chapters 12 and 13) may be consulted. Only a sketch of the basic theoretical aspects will be presented below.

By far the best theoretically studied system is the hydrogen molecular ion H_2^+ that contains only one electron and permits exact solution for the electronic wave functions, so long as the nuclei are taken as stationary. A series of investigations by Peek (P64, P65a, P65b, P67, P69) illustrates the complexities of the molecular generalized oscillator strength, apparent even in this simplest case. Unfortunately, no experimental data appear to be available concerning the generalized oscillator strength of H_2^+, however.

As has been indicated near the end of Sec. 2.2, the explicit calculation of the generalized oscillator strength, or of the squared form factor $|\epsilon_n(K)|^2$, now requires a specification of the internal degrees of freedom. At the outset, one usually assumes the Born–Oppenheimer separation between the electronic and nuclear motions simply because of lack of better alternatives. The assumption is perhaps justifiable for the ground electronic state, but is in general questionable for excited electronic states, especially for higher states that involve near crossings of different molecular terms. Therefore, the schematic nature of the treatment below should be always borne in mind (M65).

For simplicity of the presentation, the discussion below will explicitly deal with a diatomic molecule; generalization to polyatomic molecules is straightforward in principle.

For a *diatomic molecule*, one may specify a final state by a set of electronic quantum numbers n, vibrational quantum number v, and rotational quantum numbers J and M. Also, one designates an initial state by corresponding quantum numbers n_0, v_0, J_0, M_0. (Spin quantum numbers are irrelevant for the discussion here, and are thus suppressed.) Let Θ, Φ be the polar angles of the internuclear axis, and ρ the internuclear distance. Assuming the Born–Oppenheimer separation and neglecting the rotational–vibrational coupling, one writes the wave functions of the final state as

$$Y_{JM}(\Theta, \Phi) X_{nv}(\rho) w_n(\mathbf{r}_1, \cdots, \mathbf{r}_Z; \boldsymbol{\varrho})$$

and that for the initial state as

$$Y_{J_0M_0}(\Theta, \Phi) X_{n_0v_0}(\rho) w_0(\mathbf{r}_1, \cdots, \mathbf{r}_Z; \boldsymbol{\varrho}),$$

where the Y's are spherical harmonics, the X's are vibrational wave functions, and the w's are electronic wave functions depending upon the coordinates $\mathbf{r}_1, \cdots, \mathbf{r}_Z$ of all the molecular electrons and upon the nuclear coordinates $\boldsymbol{\varrho}(\rho, \Theta, \Phi)$. The form factor for the transition is then given by

$$\begin{aligned}\epsilon(K; n, v, J, M \leftarrow n_0, v_0, J_0, M_0) &= \int\int\int Y_{JM}^*(\Theta, \Phi) X_{nv}^*(\rho) \epsilon_n(K; \rho, \Theta, \Phi) \\ &\times Y_{J_0M_0}(\Theta, \Phi) X_{n_0v_0}(\rho) \rho^2 d\rho d(\cos\Theta) d\Phi, \quad (3.46)\end{aligned}$$

where $\epsilon_n(K; \rho, \Theta, \Phi)$ is the electronic part defined by

$$\begin{aligned}\epsilon_n(K; \rho, \Theta, \Phi) = \int w_n^*(\mathbf{r}_1, \cdots, \mathbf{r}_Z; \boldsymbol{\varrho}) \sum_{j=1}^{Z} \exp(i\mathbf{K}\cdot\mathbf{r}_j) \\ \times w_{n_0}(\mathbf{r}_1, \cdots, \mathbf{r}_Z; \boldsymbol{\varrho}) d\mathbf{r}_1 \cdots d\mathbf{r}_Z. \quad (3.47)\end{aligned}$$

While $|\epsilon(K; n, v, J, M \leftarrow n_0, v_0, J_0, M_0)|^2$ provides the most precise description of the individual transition, one is seldom interested in this much detail. Since rotational levels are not usually resolved in current experiments, one treats them as effectively degenerate. Thus, one sums

$$|\epsilon(K; n, v, J, M \leftarrow n_0, v_0, J_0, M_0)|^2$$

over all J and M and takes the average over J_0 and M_0. The result may be written as $|\epsilon_n(K; v \leftarrow v_0)|^2$ and called the squared form factor for the transition from the vibrational level v_0 in the initial electronic state n_0 to the vibrational level v in the final electronic state n. In this procedure, one usually neglects the very slight dependence of K upon J and J_0 that results from the kinematics [as seen in Eq. (2.16)] and uses a representative unique value of K. Then, the closure property of spherical harmonics leads to

$$\begin{aligned}|\epsilon_n(K; v \leftarrow v_0)|^2 &= (4\pi)^{-1} \int\int d(\cos\Theta) d\Phi \\ &\times \left| \int X_{nv}^*(\rho) \epsilon_n(K; \rho, \Theta, \Phi) X_{n_0v_0}(\rho) \rho^2 d\rho \right|^2 \quad (3.48)\end{aligned}$$

The result agrees with the expectation from the adiabatic nature of molecular rotation; $|\epsilon_n(K; v \leftarrow v_0)|^2$ is equal to the average of the squared form factor evaluated for all the possible molecular orientations.

A further simplification is introduced by recognizing that $\epsilon_n(K; \rho, \Theta, \Phi)$ defined by Eq. (3.47) is in general a more slowly varying function of ρ than are the vibrational wave functions, $X_{n_0v_0}(\rho)$ and $X_{nv}(\rho)$. This

is especially true when v_0 or v is small. Then, $\epsilon_n(K;\rho,\Theta,\Phi)$ may be replaced by its value $\epsilon_n(K;\bar{\rho},\Theta,\Phi)$ at a representative ρ value $\bar{\rho}$, which may be taken as the equilibrium internuclear distance ρ_e if $v_0=0$. The physical argument for this assertion is that, because the nuclei are so much heavier than an electron, they do not move appreciably in the period during which electrons undergo a transition under the influence of the incident particle. One thus reduces Eq. (3.48) to

$$|\epsilon_n(K;v\leftarrow v_0)|^2 = (4\pi)^{-1}\int\int d(\cos\Theta)d\Phi\,|\epsilon_n(K;\bar{\rho},\Theta,\Phi)|^2 \times\left|\int X_{nv}^*(\rho)X_{n0v_0}(\rho)\rho^2 d\rho\right|^2. \quad (3.49)$$

This expression consists of two factors. The first deals primarily with the electronic motion, and thus may be called the electronic form factor squared. The second deals exclusively with the nuclear vibration and is identical to the Franck–Condon factor well known in molecular spectroscopy. An immediate corollary of Eq. (3.49) is that the peak height in the electron energy-loss spectrum (as discussed in Sec. 3.1) within a single electronic transition is governed almost entirely by the Franck–Condon factor, a fact that has been very well borne out from a number of measurements (B69, L69).

One should also recognize certain qualifications to the validity of Eq. (3.49). As explicit calculations for H_2^+ (P64, P65) and for H_2 (MK67) demonstrate, $\epsilon_n(K;\rho,\Theta,\Phi)$ is not always a slowly varying function of ρ, and therefore the choice of an appropriate representative value $\bar{\rho}$ is not always easy. In particular, the representative $\bar{\rho}$ in general depends upon K.

The work by Miller and Krauss (MK67) on low-lying excitations of H_2 exemplifies moderately accurate calculations that are feasible at present. The result shows fair agreement with experiment (GS69a). Exceptionally accurate results, however, are available for a few excitations for H_2, but only at the optical limit (RD67, Wo69).

The role of the Franck–Condon factor in electron energy-loss spectra seems to deserve special attention. Whereas Eq. (3.49) has been derived under quite restrictive assumptions, including the first Born approximation, the Born–Oppenheimer separation, and the insensitivity of the electronic matrix element to the nuclear coordinates, Lassettre and coworkers (MSL65a, LSDR68) point out experimental evidence strongly suggesting that the Franck–Condon factor is significant beyond these limitations. The relative intensities for vibrational peaks belonging to the *same* electronic transition are found to be remarkably independent of the scattering angle and of the incident electron energy down to some 30 eV for a number of molecular transitions with excitation energies about 10 eV (LSDR68), a situation in which the first Born approximation is clearly inappropriate. Moreover, the same relative intensities turn out to be very closely proportional to the respective Franck–Condon factors.

Lassettre and coworkers (MSL65a, LSDR68) advance a theoretical explanation of the above-mentioned fact. They argue that, because the period of nuclear motion is much longer than the duration of a collision of an electron having kinetic energies of some 30 eV or higher, a "sudden" approximation should be applicable to the nuclear vibration. Thus, the probability of exciting a vibrational level belonging to an electronic manifold should split into two factors, one representing the probability of the electronic excitation and the other representing the conditional probability that the molecule thereby ends up in the particular vibrational level. Because of the rapidity of the electronic excitation, the latter factor should be obtained as the square of the inner product of the vibrational wave functions (i.e., the Franck–Condon factor) according to the general prescription of the sudden approximation. This argument is admittedly plausible, but seems to call for a more quantitative justification.

The Franck–Condon principle in the above sense has been extensively utilized in the spectroscopic study of molecular energy levels. For example, Lassettre and coworkers (LSDR68) were able to ascertain that the benzene molecule has two different electronic levels $^1E_{2g}$ and $^1B_{1u}$ in the region of excitation energy between 6.0 and 6.5 eV. A distinct advantage of electron energy-loss spectra over the more conventional photoabsorption spectra is that the former permit a more detailed study by way of the dependence upon the scattering angle, or equivalently upon the momentum transfer (RW63, R64, RW65).

An important theme in the spectroscopic study of electron energy-loss spectra is their comparison with photoabsorption spectra. As one expects from Eq. (2.12), electron energy-loss spectra, taken at small scattering angles and at incident kinetic energies much higher than the excitation energies involved, agree quite well with photoabsorption spectra of the same molecule in most of the cases studied (L69). However, several notable exceptions have been observed. For example, the highest peak in the electron energy-loss spectrum of N_2 of the forward scattering at high incident energies occurs at an excitation energy of 12.93 eV, while the apparently most intense transition in the photoabsorption spectrum according to its earlier measurements occurs at 12.74 eV (LGMS65, GS65, GS69b). This discrepancy was first attributed to a failure of the first Born approximation, but was later resolved in terms of a difficulty in the photoabsorption measurement (MSL65b). Actually, a later, improved measurement (LMD68) of the photoabsorption by N_2 gave a result closely agreeing to the

electron energy-loss spectrum. The resolution in the electron energy-loss spectrum is fixed by the combined energy spread of the initial beam and of the energy analyzer for the scattered beam, and the resulting spectrum corresponds to the electron-energy distribution convoluted with the "real" spectrum that would be obtained with an ideal apparatus with infinitely fine resolution. Therefore, even if every structure is not completely resolved, the relative integrated intensities of different bands in the electron energy-loss spectra approximate true intensities of the bands, the precision evidently being dependent upon the resolution and sensitivity of detection. The basic reason for this advantage is that the energy-loss process is insensitive by its own nature to the primary kinetic energy of the electrons.

In contrast, the photoabsorption is a resonant process, which requires that the energy of a photon to be absorbed be exactly equal to an excitation energy of an atom or molecule, according to the Bohr frequency condition. Therefore, when the atom or molecule possesses sharp spectral lines, photons with exactly the corresponding energies are absorbed strongly, while photons with only slightly different energies may be transmitted unabsorbed. If one works with a finite resolution in the photoabsorption study, the resulting spectrum represents a weighted average over unresolved lines. These weights are extremely sensitive to the target density, the optical path, and the instrumental transmission function in each experimental setup, as treated in detail in H71. Thus, the intensities obtained for the unresolved lines in the photoabsorption spectrum are too small (MSL65b, GS69b). Similar situations occur for H_2 (G64b, GT66), O_2, (GS68), and other cases.

An additional remark in this connection concerns intensities of a Rydberg series near its convergence limit. Occasionally in a measured photoabsorption spectrum, a Rydberg series, when followed with increasing photon energy, shows an abrupt rise in intensity at the limit, as seen, for example, in HTL63a and HTL63b. This rise is a result of the instrumental effect discussed in the previous paragraph (CS66). One expects in general that a corresponding electron energy-loss spectrum, like the "true" spectrum, should be continuous across the series limit.[4]

Another advantage of the electron energy-loss spectrum for spectroscopic purposes concerns identification of the nature of forbidden transitions. By comparing the dependence of the spectrum upon the incident electron energy and upon the scattering angle, one can sometimes establish, for example, whether a transition is of the electric quadrupole type or of the singlet–triplet type (ML65, LS65, ML66, RL66, LSM66, SDL67, LSDR68, L69).

The minima of the generalized oscillator strength discussed in Sec. 3.4 appear to be even more common to molecules than to atoms (LW58, KM69, M69, MMK69). For molecules as opposed to atoms, the nodes of the wave functions for the initial and final electronic states causing the minima belong not necessarily to the radial part, but sometimes to the angular part. For polyatomic molecules, the minima (and possibly also the maxima) of the generalized oscillator strength may sometimes be useful for the determination of the symmetry property of an excited-state wave function. The possibility of such spectroscopic applications has been discussed in the literature (K61).

In concluding this section, one must emphasize that much remains to be done in the study of molecular generalized oscillator strength, especially in the experimental determination of its absolute magnitude. In this connection it may be heuristic to note—though by no means implying a criticism, that the foremost pioneers, Lassettre and coworkers (SL70b), have recently uncovered a correction factor of 0.754 to be applied to all their own earlier data except for those on He and H_2.

4. THE INTEGRATED CROSS SECTION

4.1. The Basic Formulas

By the integrated cross section σ_n one means the cross section for excitation to a specified state n, discrete or continuum, of an atom or molecule, regardless of the angle of scattering of an incident particle. In the nonrelativistic case, σ_n is simply an integral of $d\sigma_n$ given by Eq. (2.14) over all kinematically possible values of the momentum transfer $\hbar K$, i.e.,

$$\sigma_n = \frac{4\pi a_0^2 z^2}{T/R} \int_{(Ka_0)_{\min}^2}^{(Ka_0)_{\max}^2} \frac{f_n(K)}{E_n/R} \frac{d(Ka_0)^2}{(Ka_0)^2}, \qquad (4.1)$$

where $(Ka_0)^2_{\min}$ and $(Ka_0)^2_{\max}$ are given by Eqs. (2.17) and (2.18) respectively.

Bethe (B30, B33) recognized that it is advantageous to express σ_n in terms of an asymptotic expansion in inverse powers to $T=\frac{1}{2}mv^2$ because the basic theoretical framework for $d\sigma_n$ assumes sufficiently large T. The resulting expression then contains coefficients that are determined uniquely from the generalized oscillator strength $f_n(K)$. (The discussion below pertains to any charged particle. However, m in the definition of T always is electron mass.)

In order to illustrate the nature of the asymptotic expansion, one may treat an example that can be worked out analytically. For the $2p \leftarrow 1s$ excitation of atomic hydrogen, one has (p. 480 of MM65)

$$f_{2p}(K) = 2^{13}3^{-9}[1+(4/9)(Ka_0)^2]^{-6} \qquad (4.2)$$

and

$$E_{2p}/R = 3/4. \qquad (4.3)$$

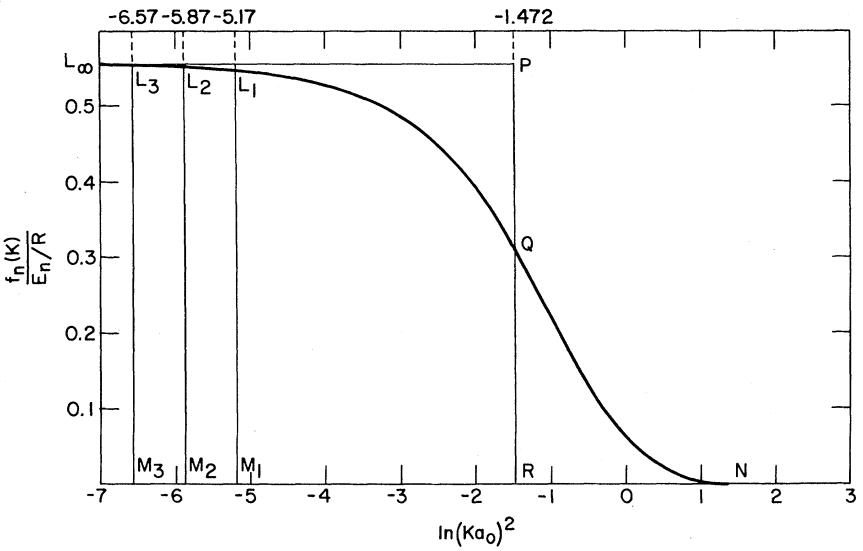

FIG. 13. Illustration of the Bethe procedure. The ordinate represents $(R/E_n)f_n(K)$, and the abscissa $\ln (Ka_0)^2$. The plotted curve corresponds to the $2p\leftarrow 1s$ excitation in H [Eq. (4.2)]. The height of the limiting value for $\ln (Ka_0)^2\rightarrow -\infty$, indicated by the point L_∞, is M_n^2 [Eq. (4.5)]. The vertical lines L_1M_1, L_2M_2, and L_3M_3 show the lower limit $\ln (Ka_0)_{\min}^2$ of the integration when $T/R=25$, 50, and 100, respectively. Notice in contrast that $(R/E_n)f_n(K)$ is utterly negligible at the upper limit $(Ka_0)^2_{\max}$ of the integration; from Eq. (2.18) one obtains $\ln (Ka_0)^2_{\max}=4.6$, even when $T/R=25$ and $M=m$. Thus, the integral A_n on the right-hand side of Eq. (4.1) corresponds, for example when $T/R=100$, to the area NL_3M_3, $L_\infty P$ being parallel to the horizontal axis. In the example one thus places the line PQR at $\ln (Ka_0)^2=-1.472$, which is the abscissa of the point R. Then the required integral A_n is given by the area L_3M_3RP [Eq. (4.13)]. Notice that the ordinate of L_3 is practically indistinguishable from that of L_∞. As T decreases, the lower limit moves to the right so that the points L_2 and L_1 on the curve progressively depart from the horizontal line $L_\infty P$.

Thus, the integral on the right-hand side of Eq. (4.1) is

$$A_{2p}=M_{2p}^2\int_{(Ka_0)_{\min}^2}^{(Ka_0)_{\max}^2}\frac{d\xi}{\xi(1+4\xi/9)^6}, \tag{4.4}$$

where

$$M_{2p}^2=f_{2p}R/E_{2p}=2^{15}3^{-10}=0.55493 \tag{4.5}$$

is the dipole-matrix-element squared for the transition [Eqs. (2.10) and (2.11)]. Elementary integration of Eq. (4.4) leads to

$$A_{2p}=M_{2p}^2\left[\ln\left(\frac{4\xi/9}{1+4\xi/9}\right)+\sum_{j=1}^{5}\frac{1}{j(1+4\xi/9)^j}\right]_{\xi=(Ka_0)_{\min}^2}^{\xi=(Ka_0)_{\max}^2}. \tag{4.6}$$

Notice first that, for large T, $(Ka_0)^2_{\max}\approx 4(M/m)^2\times(T/R)$ is a large number. Through straightforward expansion into inverse powers of $(Ka_0)^2_{\max}$, one finds that the term with $\xi=(Ka_0)^2_{\max}$ in Eq. (4.6) amounts to $O((Ka_0)^{-12}_{\max})=O((mR/MT)^6)$ only, the contributions of greater magnitude vanishing after cancellation. Second, $(Ka_0)^2_{\min}$ is small for large T; in the present example, it is given by

$$(Ka_0)^2_{\min}=3^24^{-3}\frac{R}{T}\left[1+\frac{3}{8}\frac{mR}{MT}+O\left(\left(\frac{mR}{MT}\right)^2\right)\right] \tag{4.7}$$

according to Eqs. (2.17) and (4.3). The term with $(Ka_0)^2_{\min}$ therefore dominates in Eq. (4.6). Again, straightforward expansion gives

$$A_{2p}=M_{2p}^2\left[-\ln\left[\tfrac{9}{4}(Ka_0)^2_{\min}\right]-\sum_{j=1}^{5}j^{-1}+\tfrac{8}{3}(Ka_0)^2_{\min}+O((Ka_0)^4_{\min})\right]. \tag{4.8}$$

Inserting Eq. (4.7) into Eq. (4.8) and recalling Eq. (4.1), one obtains the (integrated) cross section σ_{2p} in the form

$$\sigma_{2p}=\frac{4\pi a_0^2z^2}{T/R}\left[M_{2p}^2\ln\left(\frac{4c_{2p}T}{R}\right)+\frac{\gamma_{2p}}{T/R}+O\left(\frac{R^2}{T^2}\right)\right], \tag{4.9}$$

where one defines

$$\ln c_{2p}=2\ln 2-\sum_{j=1}^{5}j^{-1}=-0.89704, \tag{4.10}$$

$$\gamma_{2p}=2^{12}3^{-9}[1-(m/M)]=0.20810[1-(m/M)], \tag{4.11}$$

and M_{2p}^2 is given by Eq. (4.5). [The argument of the logarithm in Eq. (4.9) contains a factor of 4 solely for a traditional reason that will be apparent later.] The expression only with the leading term in the bracket in Eq. (4.9) is known as *the Bethe asymptotic cross section*. For T sufficiently large that the first Born approximation is adequate, the second term in the bracket usually is a small correction; for an incident proton with $T/R=25$ (or with the kinetic energy of 0.624 MeV), the second term amounts to 0.40% compared to the leading term. (The vanishing

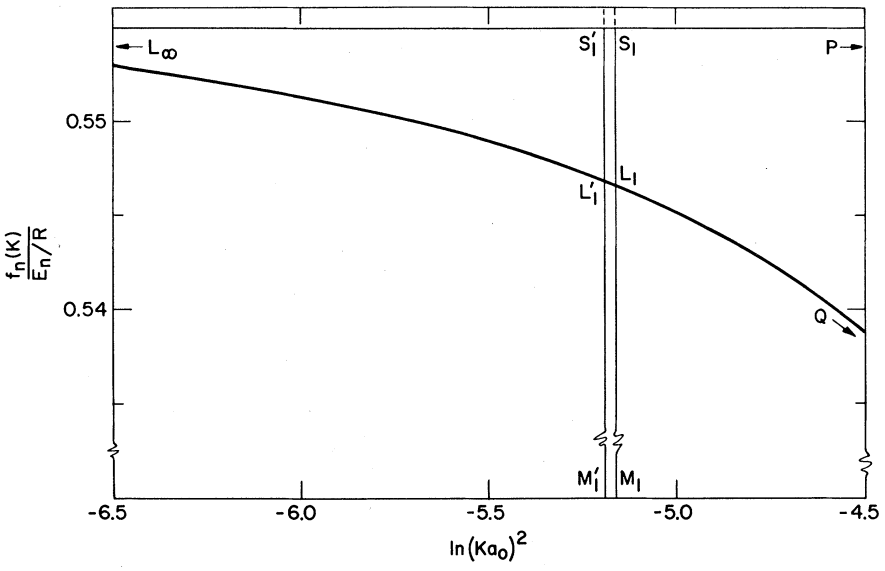

FIG. 14. Illustration of the corrections to the Bethe asymptotic formula. This figure shows in detail the region near the upper left corner of Fig. 13. While both the abscissa and the ordinate represent the same quantities as in Fig. 13, the zero on the vertical scale is suppressed. The corrections arise in two ways. First, the area $L_\infty L_1 S_1$, tacitly included in the earlier determination of the value $(Ka_0)^2$ (corresponding to the position of the vertical line PQR in Fig. 13), should be dropped. In other words, more precise determination of $(\bar{K}a_0)^2$ should stem from the requirement that the area PS_1L_1Q be equal to the area NQR in Fig. 13. This revision causes the correction to A_n as given by Eq. (4.16). Second, the vertical line L_1M_1 corresponds to the exact value of $(Ka_0)^2_{\min}$ [which in this figure is shown for electron collision $(M/m=1)$ at $T/R=25$], while the line $L_1'M_1'$ corresponds to its approximate value $E_n^2/(4RT)$ used in the derivation of the Bethe asymptote [Eq. (4.15)]. The area $L_1'M_1L_1$ should therefore be excluded [Eq. (4.17)].

of γ_{2p} for $M/m=1$, which approximately applies to electrons, is peculiar to the example and should be taken as accidental.)

A general procedure of the asymptotic expansion, which does not presume an analytical form for $f_n(K)$, is best explained with reference to Fig. 13, which shows a typical situation with a low-lying optically allowed excitation (MP57). The integral A_n on the right-hand side of Eq. (4.1) is represented by the area under the curve limited by $\ln(Ka_0)^2_{\min}$ and $\ln(Ka_0)^2_{\max}$. First of all, because the integrand decreases rapidly for large values of $(Ka_0)^2$, as seen from Eq. (3.8), the upper limit of the integration is so large when T is large that it may be replaced by infinity without an appreciable error, as has been verified in the example. Second, $(Ka_0)^2_{\min}$ is in general small and decreases with increasing T (cf. Figs. 1 and 2 for kinematics). Therefore, the required area is given in the limit of large T as the product of $\ln(\bar{K}a_0)^2 - \ln(Ka_0)^2_{\min}$ and the dipole-matrix-element squared $M_n^2=f_nR/E_n$ defined by Eqs. (2.10) and (2.11), if $(\bar{K}a_0)^2$ is so chosen that the areas $L_\infty QP$ and QNR on Fig. 13 are equal. When analytically expressed, this choice amounts to

$$\ln(\bar{K}a_0)^2=\int_0^\infty \frac{f_n(K)}{f_n}[\ln(Ka_0)^2] - \int_{-\infty}^0 \left[1-\frac{f_n(K)}{f_n}\right] d[\ln(Ka_0)^2]. \quad (4.12)$$

Thus, $(\bar{K}a_0)^2$ is independent of T and the integral A_n becomes

$$\begin{aligned} A_n &= \int_{\ln(Ka_0)_{\min^2}}^{\ln(Ka_0)_{\max}^2} \frac{f_n(K)}{E_n/R}(d\ln(Ka_0)^2] \\ &= M_n^2 \ln[(\bar{K}a_0)^2/(Ka_0)^2_{\min}] + O(E_n/T) \\ &= M_n^2 \ln[(\bar{K}a_0)^2(4RT/E_n^2)] + O(E_n/T), \end{aligned} \quad (4.13)$$

where the last equality follows from Eq. (2.17). Following Bethe (B30), one usually expresses the argument of the logarithm in the last line of Eq. (4.13) by $4c_nT/R$, thereby defining

$$\ln c_n = \ln[(\bar{K}a_0)^2(R/E_n)^2]. \quad (4.14)$$

Consequently, one arrives at the Bethe asymptotic formula

$$\sigma_n = \frac{4\pi a_0^2 z^2}{T/R}\left[M_n^2 \ln\left(\frac{4c_nT}{R}\right) + O\left(\frac{E_n}{T}\right)\right]. \quad (4.15)$$

The nature of this result may be clarified further by the following examination of the next-higher-order term $O(E_n/T)$ in the bracket of Eq. (4.15). For this purpose, one refers to Fig. 14, where the region of small $(Ka_0)^2$ in Fig. 13 is shown under great magnification. First, the choice of $(\bar{K}a_0)^2$ according to Eq. (4.12) is not quite precise, unless $f_n(K)$ is constant in the interval $0<(Ka_0)^2<(Ka_0)_{\min}^2$. More precisely, one should revise Eq. (4.12) through replacing the lower limit $-\infty$ of the second integral by $\ln(Ka_0)_{\min}^2$.

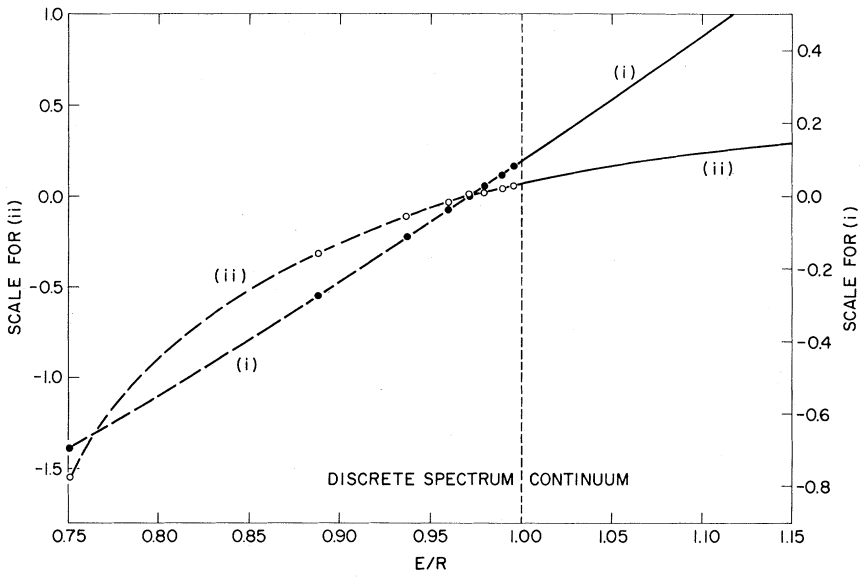

FIG. 15. The parameter ln c_E for excitation and ionization from H(1s) as a function of E. The data are taken from I63 and I66. The abscissa is E/R, so that the interval $0.75<E/R<1$ corresponds to the discrete spectrum and the interval $1<E/R$ to the continuum. The points shown on curve (i) represent ln c_n in the discrete spectrum for $n=2$, 3, 4, 5, 6, 7, 10, and 15. Curve (i) in the continuum shows ln c_E. Notice the smooth continuation at the ionization threshold $E/R=1$, where $\lim_{n\to\infty}$ ln $c_n=0.092955$. Curve (ii) represents (R^2/E) (df/dE) ln c_E in the continuum, and the open circles on curve (2) show $\frac{1}{2}n^3M_n^2$ ln c_n in the discrete spectrum again for $n=2$, 3, 4, 5, 6, 7, 10, and 15. The plot is also smoothly continuous at $E/R=1$, where $\lim_{n\to\infty}\frac{1}{2}n^3M_n^2$ ln $c_n=0.07264$.

The modified $(\bar{K}a_0)^2$ will slightly depend upon T. This correction to A_n is shown by the area $L_\infty L_1 L_2$ and is given by

$$-\int_{-\infty}^{\ln(Ka_0)^2_{\min}}\left[\frac{f_n(K)-f_n}{E_n/R}\right]d[\ln(Ka_0)^2]$$

$$=-\frac{f_n^{(1)}}{E_n/R}\frac{E_n^2}{4RT}+O\left(\frac{E_n^2}{T^2}\right), \quad (4.16)$$

where $f_n^{(1)}$ is $df_n(K)/d(Ka_0)^2$ evaluated at $K=0$ [as defined by Eqs. (3.13)–(3.15)]. Second, the replacement of $(Ka_0)^2_{\min}$ by its asymptotic value $E_n^2/(4RT)$ also caused the inclusion of the excess area $L_1'M_1'M_1L_1$ that amounts to

$$\frac{f_n}{E_n/R}\ln\left[\frac{(Ka_0)^2_{\min}}{E_n^2/4RT}\right]=\frac{f_n}{E_n/R}\frac{m}{2M}\frac{E_n}{T}+O\left(\frac{E_n^2}{T^2}\right). \quad (4.17)$$

Finally, the error due to the replacement of $(Ka_0)^2_{\max}$ by infinity is easily verified to be smaller than $O(E_n^2/T^2)$. Thus, combining Eqs. (4.16) and (4.17), one writes

$$\sigma_n=\frac{4\pi a_0^2z^2}{T/R}\left[M_n^2\ln\left(\frac{4c_nT}{R}\right)+\frac{\gamma_n}{T/R}+O\left(\frac{E_n^2}{T^2}\right)\right], \quad (4.18)$$

where γ_n is defined by

$$\gamma_n=-(m/2M)f_n-(E_n/4R)f_n^{(1)}. \quad (4.19)$$

For an analytical derivation of this result, the reader is referred to the Appendix of KI68.

The optically forbidden excitation, for which $f_n=0$, is easier to treat. The asymptotic cross section σ_n in this case is simply

$$\sigma_n=\frac{4\pi a_0^2z^2}{T/R}\left[b_n+\frac{\gamma_n}{T/R}+O\left(\frac{E_n^2}{T^2}\right)\right], \quad (4.20)$$

where b_n is defined by

$$b_n=\int_{-\infty}^{\infty}\frac{f_n(K)}{E_n/R}\,d\ln(Ka_0)^2 \quad (4.21)$$

and γ_n is again given by Eq. (4.19), the first term there vanishing because f_n is zero by definition (KI68).

A further extension of the foregoing treatment to terms of still higher orders in E_n/T is formally straightforward, but is of questionable value because effects disregarded in the first Born approximation must influence such higher-order terms in the true cross section (cf. Secs. 4.3 and 5.2). In other words, as far as σ_n is concerned, the essentially meaningful content of the first Born approximation is embodied in a few parameters, which thus obviate the need for tabulation of σ_n at different T.

Much too often the meaning of the Bethe asymptotic cross section is misunderstood, and the term "Bethe approximation" is used somewhat loosely in the literature (MS68, MBG69). The "Bethe approximation" usually implies a more or less arbitrary choice of $(\bar{K}a_0)^2$ for an estimation of the order of magnitude of σ_n; the causal suggestion to set $(\bar{K}a_0)^2=1$ on p. 377 of B30 is an origin. In the foregoing discussion, as in more fundamental treatment by Bethe (B30, B33), the quantity $(\bar{K}a_0)^2$ is precisely defined in terms of $f_n(K)/f_n$ (or the angular distribution of inelastic scattering). Thus, $(\bar{K}a_0)^2$, or ln c_n in turn, is a property of the transition to state n and depends upon E_n.

For transitions into continua (usually resulting in ionization in the case of atoms), the integrated cross section[2] $d\sigma/dE$ per unit range of excitation energy E may be defined by an equation which is similar to Eq. (4.1) but in which the differential generalized oscillator strength $df(K,E)/dE$ appears in place of $f_n(K)$ [as in Eqs. (2.20)–(2.22)]. The Bethe procedure

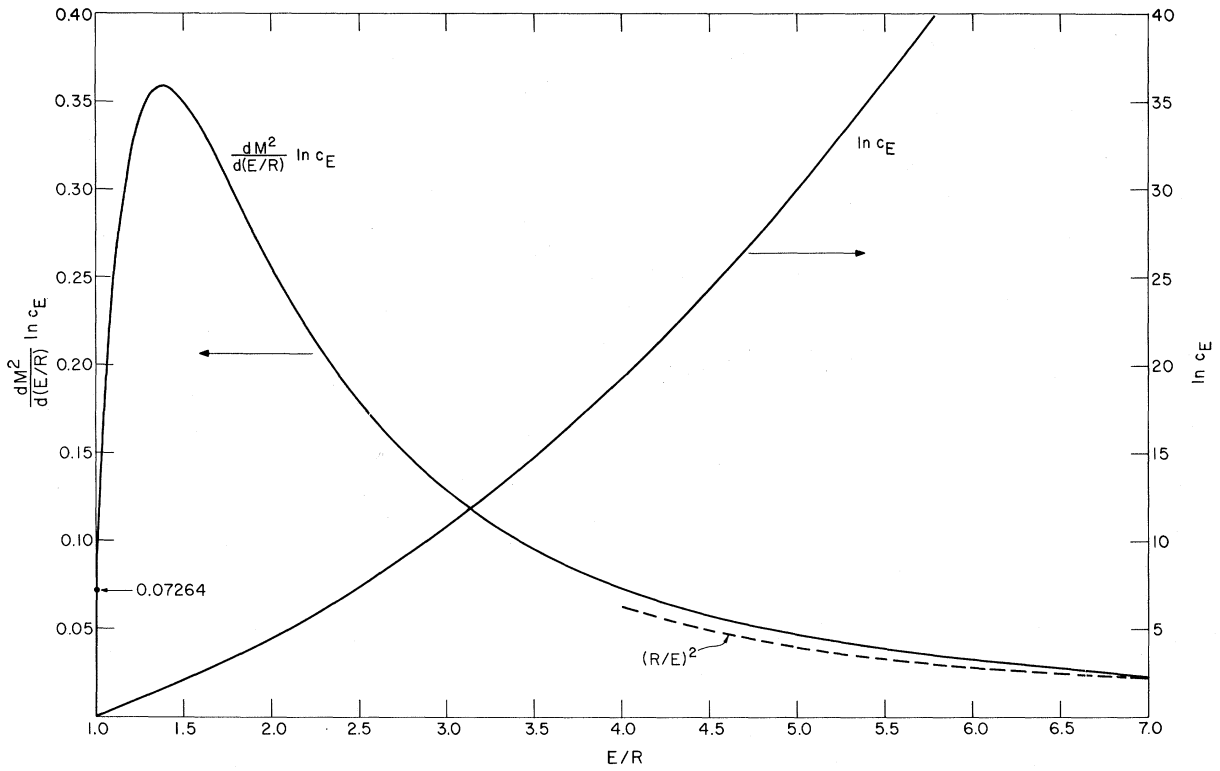

FIG. 16. The parameter ln c_E for ionization from H(1s) as a function of E. The figure is taken from I66. The curve labeled ln c_E corresponds to extending curve (i) of Fig. 15 to greater E/R. Notice the rapid enhancement of ln c_E with increase in E. The curve labeled $dM^2/d(E/R)\cdot\ln c_E$ corresponds to extending curve (ii) of Fig. 15. The quantity $dM^2/d(E/R)$ is equal to $(R^2/E)df/dE$ in the notation of the text [Eqs. (4.22) and (4.25)]. The broken curve represents the asymptotic behavior given by Eq. (4.25).

is applicable as well and leads to

$$\frac{d\sigma}{dE}=\frac{4\pi a_0^2 z^2}{T/R}\left[\frac{R}{E}\frac{df}{dE}\ln\left(\frac{4c_E T}{R}\right)+\frac{d\gamma}{dE}\frac{R}{T}+O\left(\frac{E^2}{T^2}\right)\right], \tag{4.22}$$

where $df/dE=[df(K,E)/dE]_{K=0}$ is the differential optical oscillator strength, and c_E and $d\gamma/dE$ are defined by Eqs. (4.12), (4.14), and (4.19) after replacement of $f_n(K)$ by $df(K,E)/dE$.

As the foregoing discussion shows, all the parameters characterizing the asymptotic cross sections [Eqs. (4.18), (4.20), and (4.22)] are uniquely determined in principle from the Bethe surface. In practice, however, the knowledge of the Bethe surface of individual atoms and molecules is limited at present, as seen in Secs. 3.4 and 3.5. Only in such exceptional cases as H and He can precise evaluation of the parameters for various transitions be carried out rigorously. Alternatively, when experimental cross sections in the asymptotic region are available, one may deduce therefrom these parameters (through a plot discussed in the next section) and regard their values as a source of information on the Bethe surface. A search for systematics of these parameters of many atoms and molecules will continue to be a major task in the coming years. Certain general properties of the parameters are now indicated below.

The parameter usually most decisive in the integrated cross section is the distribution of the dipole-matrix-element squared, M_n^2 in discrete spectra and $(R/E)df/dE$ in continuous spectra. The distribution is smooth at the ionization threshold $E=I$, i.e.,

$$\lim_{n\to\infty}\tfrac{1}{2}n^3 M_n^2=[(R/E)(df/dE)]_{E=I}. \tag{4.23}$$

Similarly, the secondary parameter ln c_n in discrete spectra and ln c_E in continuous spectra connect smoothly:

$$\lim_{n\to\infty}\ln c_n=[\ln c_E]_{E=I}, \tag{4.24}$$

provided that ln c_n includes contributions from all degenerate angular-momentum states (as discussed in the passage near the beginning of p. 58 of IKP67). This situation is exemplified in Figs. 15 and 16. Figure 16 also shows the behavior of ln c_E for large values of E.

Strictly speaking, Eqs. (4.23) and (4.24) literally apply to the hydrogen atom, in which case n is taken as the principal quantum number. For any other atom or molecule, however, they must be reinterpreted. One considers a Rydberg series and the continuum associated with it. Then the relations (4.23) and (4.24) are expected to hold for the Rydberg series, when n is taken as the effective quantum number including the quantum defect.[4]

As explained in detail later [Eq. (4.89)], $\ln c_E$ asymptotically behaves as

$$(R^2/E)\,(df/dE)\,\ln c_E \sim Z(R/E)^2, \qquad (4.25)$$

for large E, where Z is the number of electrons in the atom or molecule. Equation (4.25) is an important consequence of the Bethe ridge (Fig. 10). In contrast, the coefficient $(R/E)df/dE$ of the $T^{-1}\ln T$ term of Eq. (4.22) declines much faster with E, i.e., as $E^{-4.5}$ [cf. Eq. (3.31)].

For relativistic velocities ($T \gtrsim 10^4$ eV), the asymptotic cross section [Eqs. (4.18) and (4.20)] needs modifications. As shown by Bethe (B32, B33) and explained in detail by Fano (F54, F56a, F63), the cross section is again given in terms of the same basic parameters as in the nonrelativistic case. The treatment is based upon Eqs. (2.29) and (2.30), and the result is as follows: For an optically allowed excitation to state n, one has

$$\sigma_n = \frac{8\pi a_0^2 z^2}{mv^2/R}\left\{M_n^2\left[\ln\left(\frac{\beta^2}{1-\beta^2}\right)-\beta^2\right]+C_n\right\}, \qquad (4.26)$$

where m is the electron rest mass and C_n is given by

$$C_n = M_n^2[\ln c_n + \ln (2mc^2/R)] = M_n^2[\ln c_n + 11.2268]. \qquad (4.27)$$

For a forbidden excitation to state n, one has simply

$$\sigma_n = 8\pi a_0^2 z^2 (R/mv^2) b_n. \qquad (4.28)$$

For small velocity, Eqs. (4.26) and (4.28) reduce to the leading terms of Eqs. (4.18) and (4.20), respectively, as they should. According to Fano's analysis (F56a) the structure of Eq. (4.26) may be interpreted as follows: The portion

$$8\pi a_0^2 z^2 (R/mv^2) M_n^2 \ln (2mv^2 c_n/R)$$

arises from interactions due to virtual photons whose polarization vectors are parallel to the momentum transfer $\hbar\mathbf{K}$ and approaches a constant value as $\beta \to 1$. The remainder

$$8\pi a_0^2 z^2 (R/mv^2) M_n^2 [-\ln (1-\beta^2) - \beta^2]$$

stems from virtual photons whose polarization vectors are perpendicular to $\hbar\mathbf{K}$ and represents the cause for the "relativistic rise." This contribution behaves as β^2 for small β.

4.2. The Fano Plot and Its Applications

As first pointed out by Fano (F54), the analytical form of the Bethe cross sections [Eqs. (4.18), (4.20), (4.26), and (4.28)] suggests a plot of $[(T/R)\sigma_n](4\pi a_0^2 z^2)^{-1}$ against $\ln (T/R)$ in the nonrelativistic region, and a plot of $[(mv^2/2R)\sigma_n](4\pi a_0^2 z^2)^{-1}$ against $\ln [\beta^2/(1-\beta^2)] - \beta^2$ in the relativistic region. In either case, the plot extended to sufficiently large velocities will become a straight line, whose slope corresponds to M_n^2 and whose intercept with the vertical axis relates to $M_n^2 \ln c_n$ or b_n. (An analysis of data in the relativistic region is greatly facilitited by use of tabulations such as MMH56.)

Figure 17 is an example of the Fano plot. In this particular instance, accurate theoretical values of the slope and the intercept are known. Thus, the plot provides a method of clear-cut comparison of experimental data with theory; the set of data represented by open circles is most consistent with theory. [The apparent continuation of the straight-line behavior of the data to the region $T \lesssim 200$ eV (where the first Born approximation is unrealistic) is unexpected and probably fortuitous.]

Actually the Fano plot presumes no theoretical values of the slope and the intercept, and therefore can be applied to any set of data on the integrated cross section σ_n. From such a plot one can draw a number of inferences about the parameters characterizing σ_n. First, if the plot shows a straight-line behavior over an interval of large T values, it suggests, but not necessarily establishes, the applicability of the Bethe theory in that interval. (It should be borne in mind, however, that judgment of a straight-line behavior of data points with some random errors always requires caution.) Second, values of the slope and the intercept then may be extracted from the plot. The slope value M_n^2 can be converted into the optical oscillator strength f_n and then can be compared with photoabsorption data. If the slope turns out to be zero within numerical uncertainties, then the optically forbidden character of the transition is suggested. Third, sometimes cross-section data are determined only relatively, that is, within a multiplicative factor that is independent of T. One may still plot such data in the same manner and then adjust the vertical scale so that the asymptotic slope corresponds to a value of f_n if it is known. In this way the originally relative data may be put on an absolute scale (as is done, for example, in VDJ70). All these advantages of the Fano plot have been amply demonstrated by a series of systematic studies on many atoms and molecules by the Amsterdam group (SDVK65, SBK66, S66, SMSD66, SVDM66, SDMBK66, MD67, ADV68, MDS69, VEV69, VD69a, VD69b, VD69c, EVD70). Further examples of the Fano plot are found in RP65–RP70, DV67, PWD69, and PWD70.

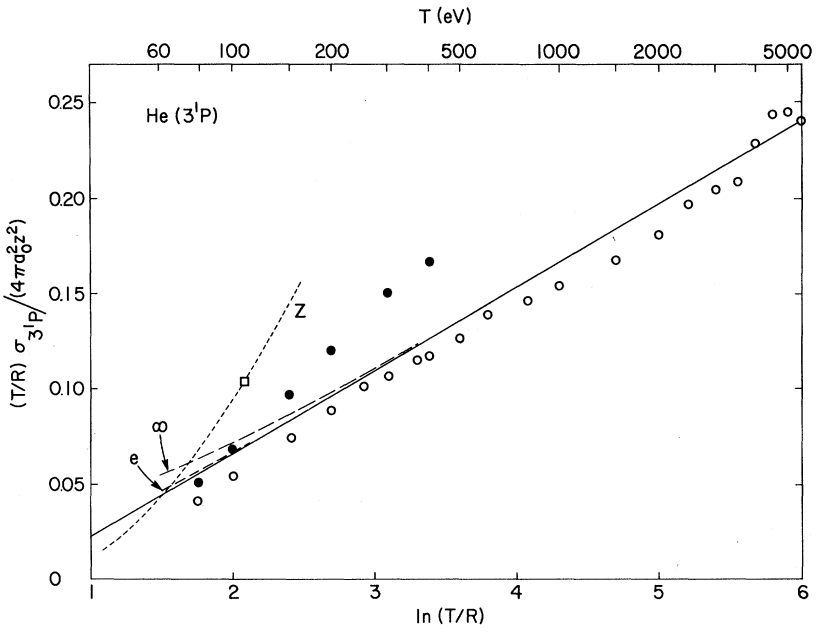

FIG. 17. The Fano plot for the excitation of the 3^1P state of He, taken from KI68. The solid straight line represents the Bethe asymptotic cross section [Eq. (4.15)] for any charged particle. The broken (- - -) curves represent the same with the γ_n term [Eq. (4.18)] for an electron or positron (labeled "e") and for a heavy charged particle such as proton (labeled "∞"). The dots show the electron-collision data of SML64, and the circles those of MDS69. The square shows the measurements of GH60 and the dashed curve (- - - -, labeled "Z") those of Z66. (See also VDJ70 for additional data not included in this figure.)

Whereas the Fano plot is applicable to any integrated cross section, it has been utilized most frequently and fruitfully for analyses of ionization cross sections. Therefore, it may be appropriate to make some detailed remarks concerning the meaning of the parameters characterizing the ionization cross sections.

For an *atom*, one may simply integrate $d\sigma/dE$ of Eq. (4.22) over the continuum energy E and obtain the ionization cross section

$$\sigma_i = \frac{4\pi a_0^2 z^2}{T/R}\left[M_i^2 \ln(4c_i T/R) + \frac{\gamma_i}{T/R} + O\left(\frac{R^2}{T^2}\right)\right], \quad (4.29)$$

where

$$M_i^2 = \int_{I_1}^{\infty} \left(\frac{R}{E}\right)\left(\frac{df}{dE}\right) dE \quad (4.30)$$

and

$$M_i^2 \ln c_i = \int_{I_1}^{\infty} \left(\frac{R}{E}\right)\left(\frac{df}{dE}\right) \ln c_E dE. \quad (4.31)$$

The integrations in Eqs. (4.30) and (4.31) have been extended to infinity, the kinematical limitation having been thereby disregarded. This procedure is justified as far as the quantities M_i^2 and $\ln c_i$ are concerned because kinematically impossible excitations with $E \gtrsim (M/m)T$ contribute very little to the integrals so long as T is sufficiently large. A treatment of the quantity γ_i, however, requires more detailed considerations, and is thus deferred until Sec. 4.3. The quantity M_i^2, which one may call the dipole-matrix-element squared for ionization, is an important index of the distribution df/dE of the optical oscillator strength (F54). Recent advances in measurements and theoretical understanding of df/dE (FC68) are enabling one to obtain trustworthy M_i^2 values for more and more atoms and perhaps even to start studying their systematics across the Periodic Table.

The possibility of multiple ionization, i.e., ejection of more than one electron from an atom as a result of a single encounter of a charged particle, requires a more precise definition of the term "ionization cross section." One may define the probability $\eta_\tau(E)$ that, as a result of energy transfer E by a single collision, τ electrons are ejected (i.e., a τ-fold ionization occurs). The quantity $\eta_\tau(E)$ is a definite property of the continuum states at E although a mathematical formulation to compute it from corresponding continuum wave functions may be highly complicated. Then, the cross section $\sigma_{i\tau}$ for the τ-fold ionization is an integral of $\eta_\tau(E)d\sigma/dE$ over E, where $d\sigma/dE$ is given by Eq. (4.22). Thus, the leading term for the asymptotic $\sigma_{i\tau}$ is expressed as

$$\sigma_{i\tau} = 4\pi a_0^2 z^2 (R/T)[M_{i\tau}^2 \ln(4c_{i\tau} T/R) + O(I_\tau/R)], \quad (4.32)$$

where

$$M_{i\tau}^2 = \int_{I_\tau}^{\infty} \eta_\tau(E)\left(\frac{R}{E}\right)\left(\frac{df}{dE}\right) dE, \quad (4.33)$$

$$M_{i\tau}^2 \ln c_{i\tau} = \int_{I_\tau}^{\infty} \eta_\tau(E)\left(\frac{R}{E}\right)\left(\frac{df}{dE}\right) \ln c_E dE, \quad (4.34)$$

and I_τ is the threshold energy for the τ-fold ionization. Applications of Eqs. (4.32)–(4.34) are found in SBK66, S66, VEV69, EVD70, and VW71.

The ionization cross section σ_i as given in Eqs.

(4.29)–(4.31) is the simple sum

$$\sigma_i = \sum_\tau \sigma_{i\tau} \tag{4.35}$$

and is sometimes called the "counting" ionization cross section. If an experiment measures the *number of ionization events* regardless of how many electrons are ejected in each of the events (as in the case in M53 and RP65–RP70), then the result of the experiment corresponds to σ_i. If another kind of experiment measures the *total current* produced by all different ionization events (as is the case in SDVK65), then the result corresponds to the "gross" ionization cross section

$$\sigma_{ig} = \sum_\tau \tau\sigma_{i\tau}. \tag{4.36}$$

Although σ_{ig} is expressed in the same analytical form as σ_i [Eq. (4.29)], the coefficients there are different; they include contributions from the τ-fold ionization with weight τ. For example, the slope M_{ig}^2 of the Fano plot for σ_{ig} is

$$M_{ig}^2 = \sum_\tau \tau M_{i\tau}^2, \tag{4.37}$$

which is in general greater than M_i^2 of Eq. (4.30). This point is utterly elementary but has caused occasional confusion in the literature (K65, KSD65).

For a *molecule*, even Eqs. (4.29)–(4.31) require modifications. As Platzman has forcibly shown (P60, P62, P63), an excitation to a state above the first ionization energy does not always give rise to an ionization, but sometimes leads to atomic rearrangements such as decomposition into neutral products. One may introduce the (quantum) yield for ionization $\eta(E)$ as the probability that the molecule ionizes when it has received an energy transfer E. [In the present discussion, the quantity $\eta(E)$ includes contributions from all multiple ionizations possible at E. In other words, it is to be understood that $\eta(E) = \sum_\tau \eta_\tau(E)$.] Then, the ionization cross section σ_i is an integral of $\eta(E)d\sigma/dE$ over E and is expressed in the same analytical form as Eq. (4.29) but with the coefficients redefined by

$$M_i^2 = \int_{I_1}^\infty \eta(E)\left(\frac{R}{E}\right)\left(\frac{df}{dE}\right)dE \tag{4.38}$$

and

$$M_i^2 \ln c_i = \int_{I_1}^\infty \eta(E)\left(\frac{R}{E}\right)\left(\frac{df}{dE}\right)\ln c_E dE. \tag{4.39}$$

As is often the case with polyatomic molecules, $\eta(E)$ [$\eta_1(E)$ in effect] may be substantially smaller than unity in a region of E near I_1, where $(R/E)(df/dE)$ has appreciable values. The introduction of $\eta(E)$ in Eq. (4.38) then is essential for correct evaluation of M_i^2. In contrast, $\eta(E)$ may play a somewhat less significant role in $\ln c_i$ because $\eta(E)$ is likely to approach unity for $E \gg I_1$ and $(R/E)(df/dE)\ln c_E$ weighs relatively higher portions of the continuum.

In many cases, M_i^2 has been evaluated by use of the photoionization cross section, which is equal to $\eta(E)df/dE$ apart from a universal multiplicative factor. This procedure provides a useful estimate which may be compared with data on σ_i if available.

The ionization yield $\eta(E)$ depends upon several phenomena; in particular it depends upon atomic rearrangements in a highly excited molecule, and therefore is expected to be influenced by an isotopic substitution. It follows then that σ_i may have an isotope effect. Furthermore, Platzman has predicted that, when $\eta(E) < 1$, substitution by a heavier isotope could increase $\eta(E)$, and hence σ_i. Experimental data on σ_i of some hydrocarbon molecules (MGV63, SVDM66), for example, support the prediction, while isotope effects on $\eta(E)$ appear more involved in detail (Per65, PN68, PN70).

The emission of light as a consequence of charged-particle impact may be treated similarly. The conditional probability $\phi_l(E)$ that, upon excitation to a state at E, a molecule (or its fragment) emits a photon of a specified kind l is customarily called quantum yield of luminescence, where l may designate the frequency and/or the polarization vector of the photon. The cross section σ_l for the luminescence l is given by an integral of $\phi_l(E)d\sigma/dE$. Thus, it has the same analytical form as σ_i of Eq. (4.29), but the coefficients therein are different. For example, the slope M_l^2 of the Fano plot for σ_l is

$$M_l^2 = \int_{J_l}^\infty \phi_l(E)\left(\frac{R}{E}\right)\left(\frac{df}{dE}\right)dE, \tag{4.40}$$

where J_l is the threshold energy for the luminescence l and often may be smaller than the first ionization threshold I_1, in which case the integration includes contributions from discrete excitations as well. Analyses of emission cross sections in terms of the Fano plot have been fruitfully applied to Lyman and Balmer lines resulting from dissociation of molecules containing hydrogen (VD69a, VD69b, VD69c), as well as to some atomic lines and molecular bands resulting from excitation of N_2 and CO (ADV68, DA70, AD70a, AD70b, AD71).

4.3. Total Cross Section for Inelastic Scattering and Stopping Power

The total cross section for inelastic scattering σ_{tot} is defined as the sum of σ_n [Eqs. (4.18), (4.20), (4.26), and (4.28)] over kinematically accessible excited states of an atom or molecule, including discrete as well as continuum states. The dependence of σ_{tot} upon T, again presumed to be sufficiently large, is obviously of the same analytical form as that of σ_n

or σ_i. In the nonrelativistic case, one may thus write

$$\sigma_{\rm tot}=\frac{4\pi a_0^2 z^2}{T/R}\left[M_{\rm tot}^2\ln\left(\frac{4c_{\rm tot}T}{R}\right)+\frac{\gamma_{\rm tot}}{T/R}+O\left(\frac{R^2}{T^2}\right)\right], \tag{4.41}$$

where $M_{\rm tot}^2$, $c_{\rm tot}$, and $\gamma_{\rm tot}$ are constants to be discussed below.

The use of appropriate sum rules (Sec. 3.3) provides a powerful method[6] for evaluating the coefficients in Eq. (4.41) (IKP67, KI71). In the following discussion, as in Sec. 3.3, the symbol

$$\sum_n$$

means the summation over all excited states including integration over continua. First,

$$M_{\rm tot}^2=\sum_n M_n^2 \tag{4.42}$$

is nothing more than $S(-1, 0)$ given by Eq. (3.18). Second, manipulations based on Eqs. (3.17), (4.12), (4.14) and (4.21) give (IKP67)

$$M_{\rm tot}^2\ln c_{\rm tot}=\sum_n M_n^2\ln c_n+\sum_n b_n=-2L(-1)+\mathcal{G}_1-\mathcal{G}_2, \tag{4.43}$$

where $L(-1)$ is an optical quantity defined by Eq. (3.42), and the quantities $\mathcal{G}_1$ and $\mathcal{G}_2$ are integrals containing the incoherent-scattering function $S_{\rm inc}(K)$, an initial-state property (Sec. 3.3). They are given by

$$\mathcal{G}_1=\int_1^\infty ZS_{\rm inc}(K)\,(Ka_0)^{-4}d(Ka_0)^2, \tag{4.44}$$

$$\mathcal{G}_2=\int_0^1 [M_{\rm tot}^2-ZS_{\rm inc}(K)/(Ka_0)^2](Ka_0)^{-2}d(Ka_0)^2. \tag{4.45}$$

According to Eq. (4.43), $\ln c_{\rm tot}$ can be computed from two items of information, namely, the optical oscillator-strength distribution and the wave function of the initial state (most commonly the ground state).

The third coefficient $\gamma_{\rm tot}$ is slightly more involved; it is not simply the sum of individual γ_n

$$\sum_n\gamma_n=-\tfrac{1}{2}(m/M)\,S(0, 0)-\tfrac{1}{4}S^{(1)}(1) \tag{4.46}$$

[as derived from Eqs. (3.19), (3.37), and (4.19)], but includes additional contributions. In the derivation of Eqs. (4.42) and (4.43), the summation (actually integration) over final states has been extended to infinity. More rigorously, the summation should be restricted to $E\leq E_{\rm max}(T)$, where $E_{\rm max}(T)$ is an appropriate upper limit of energy transfer at given T. The consideration of this kinematical limitation leads to contributions that are of the same order of magnitude as the sum of γ_n terms, Eq. (4.46). The upper limit may be set at $R(\tilde{K}a_0)^2_{\rm max}$, where $(\tilde{K}a_0)^2_{\rm max}$ is defined by Eq. (2.19) (see also Figs. 1 and 2). Thus for heavy particles ($M\gg m$) we have

$$E_{\rm max}(T)=4T, \tag{4.47}$$

while for $M=m$

$$E_{\rm max}(T)=T. \tag{4.48}$$

The contributions that have been included in the sum-rule evaluation of $M_{\rm tot}^2\ln c_{\rm tot}$ [Eq. (4.43)] and that now should be removed therefrom, are estimated by means of Eq. (4.25) to be

$$\int_{E_{\rm max}(T)}^\infty \frac{R}{E}\frac{df}{dE}\ln c_E dE=\frac{ZR}{E_{\rm max}(T)}=\frac{R}{T}\frac{ZT}{E_{\rm max}(T)}.$$

Therefore, one obtains

$$\gamma_{\rm tot}=\sum_n\gamma_n-ZT/E_{\rm max}(T), \tag{4.49}$$

and hence

$$\begin{aligned}\gamma_{\rm tot}&=-\tfrac{1}{4}Z-\tfrac{1}{4}S^{(1)}(1) &&\text{for } M\gg m\\ &=-\tfrac{3}{2}Z-\tfrac{1}{4}S^{(1)}(1) &&\text{for } M=m.\end{aligned} \tag{4.50}$$

A more rigorous derivation of this result is given in KI71. If one neglects electron correlations in an atom or molecule, one obtains $S^{(1)}(1)\approx Z$ [Eq. (3.40)] so that

$$\begin{aligned}\gamma_{\rm tot}&\approx-Z/2 &&\text{for } M\gg m\\ &\approx-7Z/4 &&\text{for } M=m.\end{aligned} \tag{4.51}$$

It may be added that the above result for $M=m$ applies literally to *positron collisions* but requires a modification for *electron collisions*. The indistinguishability of an incoming electron from atomic electrons actually influences the $\gamma_{\rm tot}$ term in Eq. (4.41). An approximate treatment (KI71) of this "exchange" effect by the use of the Mott formula [Eq. (4.90)] gives

$$\begin{aligned}\gamma_{\rm tot}&\approx-\tfrac{3}{2}Z-\tfrac{1}{4}S^{(1)}(1)+Z\ln(B/T)\\ &\approx[-\tfrac{7}{4}+\ln(B/T)]Z,\end{aligned} \tag{4.52}$$

where B is an average binding energy of atomic electrons and is assumed to be much smaller than T. The result (4.52) should be distinguished from Eq. (4.51) in two respects: it is based on an additional argument beyond the first Born approximation and is weakly dependent upon T.

The considerations leading to Eqs. (4.50)–(4.52) also apply to the ionization cross section σ_i. Thus,

[6] A similar method is used in the discussion of the cross section for the excitation of a definite molecular term, i.e., the cross section including transitions to all the vibrational and rotational states belonging to that electronic manifold (P69, PG69).

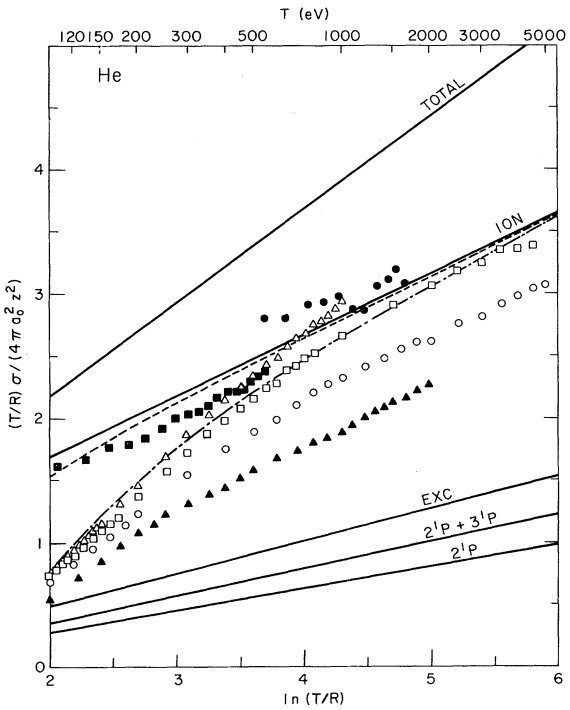

FIG. 18. The Fano plot for various inelastic-scattering cross sections for He, taken from IK69 and K171. Straight lines, in order from top to bottom, represent the Bethe asymptotic cross sections for total inelastic scattering (TOTAL), for ionization (ION), for excitations to all discrete levels (EXC), for excitations to the 2^1P and 3^1P levels, and for 2^1P excitation only. The dashed curve represents the ionization cross section for heavy-particle impact including the γ_i term of Eq. (4.53); the dot-dash curve represents the same for electron impact, including the γ_i term of Eq. (4.54), which accounts for the electron-exchange effect by means of the Mott formula. These two curves are to be compared with the measurements shown as data points. The open squares are the electron-impact data of Smith (S30), the open circles are those of Schram *et al.* (SDVK65, SBK66, SMSD66), the closed triangles are those of Gaudin and Hagemann (GH67), and the open triangles are those of Rapp and Englander-Golden (RE65). The closed squares are the proton-impact data of Hooper *et al.* (HHMM62) and the closed circles are those of Pivovar and Levchenko (PL67).

γ_i in Eq. (4.29) is given by

$$\gamma_i=\int_{I_1}^{\infty}\left(\frac{d\gamma}{dE}\right)dE-ZT/E_{\max}(T)$$

$$=\int_{I_1}^{\infty}\left(\frac{d\gamma}{dE}\right)dE-\tfrac{1}{4}Z \qquad \text{for } M\gg m$$

$$=\int_{I_1}^{\infty}\left(\frac{d\gamma}{dE}\right)dE-Z \qquad \text{for positrons.} \quad (4.53)$$

For electrons, γ_i including the exchange correction is given by

$$\gamma_i\approx\int_{I_1}^{\infty}\left(\frac{d\gamma}{dE}\right)dE-Z+Z\ln\left(\frac{B}{T}\right). \quad (4.54)$$

For relativistic velocities ($T=\frac{1}{2}mv^2\gtrsim 10^4$ eV), the asymptotic total cross section is given by

$$\sigma_{\rm tot}=\frac{8\pi a_0^2 z^2}{mv^2/R}\left\{M_{\rm tot}^2\left[\ln\left(\frac{\beta^2}{1-\beta^2}\right)-\beta^2\right]+C_{\rm tot}\right\}, \quad (4.55)$$

where

$$C_{\rm tot}=M_{\rm tot}[\ln c_{\rm tot}+\ln(2mc^2/R)]$$

$$=M_{\rm tot}^2[\ln c_{\rm tot}+11.2268]. \quad (4.56)$$

The same two constants $M_{\rm tot}^2$ and $\ln c_{\rm tot}$ still characterize $\sigma_{\rm tot}$. The contributions corresponding to the term with $\gamma_{\rm tot}$ in Eq. (4.41) are negligible in the relativistic domain and therefore are omitted in Eq. (4.55).

Equations (4.41) and (4.55) have been applied to several cases (IKP67, IK68, KI70, KI71, BK71). The principal virtue of the knowledge of $\sigma_{\rm tot}$ is the compatibility it requires among the individual inelastic-scattering cross sections σ_n. For example, if $\sigma_{\rm exc}$ is the sum of all discrete-excitation cross sections, the (counting) ionization cross section σ_i is expressed as

$$\sigma_i=\sigma_{\rm tot}-\sigma_{\rm exc}. \quad (4.57)$$

This subtraction method of computing σ_i has been applied to He (Fig. 18) and Li^+, for which $\sigma_{\rm tot}$ and $\sigma_{\rm exc}$ are evaluated to good accuracy (IK69, KI70, KI71). It should be noted that direct computation of σ_i always presumes knowledge of the continuum generalized oscillator strength $df(K, E)/dE$, which in turn requires continuum wave functions that are difficult to evaluate precisely (P56, VG61, S65, Pea65, R68, EM69, BK69a, BK69b). Sometimes, σ_i may be known fairly well from experiment. Then a knowledge of $\sigma_{\rm tot}$ immediately provides $\sigma_{\rm exc}$ by use of Eq. (4.57).

Finally, the evaluation of $\sigma_{\rm tot}$ for molecules also is useful. For example, the total cross section for dissociation of H_2^+ by electron impact has been computed via $\sigma_{\rm tot}$ (P67). The result agrees only roughly with earlier measurements (DV67, DHRS67), but excellently with a recent remeasurement (PD71).

The mean energy loss per unit path length of a particle transversing matter is called the stopping power, and its evaluation was the primary purpose of Bohr (B13, B15) and of Bethe (B30). This subject has been fully treated in excellent reviews (B48), BA53, F63, B71), and the following brief sketch merely attempts to show the similarity between the theoretical formulation, of the stopping power, and of the total inelastic-scattering cross section.

When the matter may be regarded as a homogeneous assembly of N_a individual atoms or molecules of a single species per unit volume, the stopping power is $N_a\sum_n E_n\sigma_n$, where the summation extends over kinematically accessible excited states n. The essential

part is the stopping cross section

$$\sigma_{\rm st}=\sum_n (E_n/R)\sigma_n. \tag{4.58}$$

For sufficiently large (but still nonrelativistic) T, the leading term of Eqs. (4.15) and (4.20) may be used so that, recalling Eq. (2.10), one writes

$$\sigma_{\rm st}=4\pi a_0^2 z^2 (R/T)\Big[\sum_n f_n \ln (4c_nT/R) + \sum_n (E_n/R) b_n + O(R/T)\Big]. \tag{4.59}$$

By use of Eqs. (4.12), (4.14), and (4.21), one puts the content of the square bracket in the form

$$\sum_n f_n \ln (4c_nT/R)+\sum_n (E_n/R)b_n=\sum_n f_n \ln (4T/R) - 2\sum_n f_n \ln\left(\frac{E_n}{R}\right) - \sum_n \int_0^1 [f_n - f_n(K)](Ka_0)^{-2} d(Ka_0)^2 + \sum_n \int_0^\infty f_n(K)(Ka_0)^{-2} d(Ka_0)^2. \tag{4.60}$$

An exact evaluation of Eq. (4.60) requires knowledge of the totality of $f_n(K)$, i.e., knowledge of the Bethe surface. The asymptotic behavior for large T, however, can be determined in the following way. The summation in the first term as well as that in the second term on the right-hand side of Eq. (4.60) may be extended to infinity because the optical oscillator strength declines rapidly for higher portions of continua; more precisely, df/dE behaves as $E^{-3.5}$ for large E (RF67). One thus obtains asymptotic estimates, $Z \ln (4T/R)$ for the first term and $-2L(0)$ [Eq. (3.42)] for the second term. The summation in the third term, after being placed under the integral sign, may be extended to infinity again. Then according to the Bethe sum rule [Eq. (3.19)], the third term vanishes. To estimate the last term, one recalls that, for large $(Ka_0)^2$, the function $f_n(K)$ is nonvanishing only in the neighborhood of the Bethe ridge $E/R \approx (Ka_0)^2$ (Sec. 3.2, Fig. 10). Therefore, one may exchange the order of the summation and the integration if one simultaneously sets the upper limit of the $(Ka_0)^2$ integration at $(\tilde{K}a_0)^2_{\rm max}$ of Eq. (2.19). Then we have

$$\sum_n \int_1^\infty f_n(K)(Ka_0)^{-2} d(Ka_0)^2 = \int_1^{(\tilde{K}a_0)^2_{\rm max}} \sum_n f_n(K)(Ka_0)^{-2} d(Ka_0)^2 = Z \ln (\tilde{K}a_0)^2_{\rm max}.$$

The meaning of this procedure may be seen from Figs. 1 and 2. The point B, where $E_n/R=(Ka_0)^2=(\tilde{K}a_0)^2_{\rm max}$, is defined as the intersection of the Bethe ridge with the curve $(Ka_0)^2=(Ka_0)^2_{\rm min}$.

Collecting all the terms, one arrives at

$$\sigma_{\rm st}=4\pi a_0^2 z^2 (R/T)[Z \ln (4T/R) - 2L(0) + Z \ln (\tilde{K}a_0)^2_{\rm max} + O(R/T)]. \tag{4.61}$$

It is customary to introduce the "mean excitation energy" I_0 defined by

$$\ln (I_0/R) = Z^{-1}L(0) = Z^{-1}\sum_n f_n \ln (E_n/R) \tag{4.62}$$

and to write the result as

$$\sigma_{\rm st}=\frac{8\pi a_0^2 z^2}{T/R}\left[Z \ln\left(\frac{4T}{I_0}\right)+O\left(\frac{R}{T}\right)\right] \quad \text{for } M \gg m$$

$$=\frac{8\pi a_0^2 z^2}{T/R}\left[Z \ln\left(\frac{2T}{I_0}\right)+O\left(\frac{R}{T}\right)\right] \quad \text{for } M=m. \tag{4.63}$$

[For electrons, the indistinguishability between a primary electron and a secondary electron in ionizing collisions again makes a modification necessary. Following Bethe (B32), one may define the faster of the two as the primary electron. Then, $\ln (2T/I_0)$ should be replaced by $\ln (T/I_0)+\frac{1}{2}(1-\ln 2)$ (p. 521 of B32).]

The structure of Eq. (4.63) is similar to that of Eq. (4.41) for $\sigma_{\rm tot}$, but the following differences are notable. The factor in front of the bracket of Eq. (4.63) is twice the corresponding factor in Eq. (4.41). The coefficient Z in Eq. (4.63) is a property much simpler than the coefficient $M_{\rm tot}^2$ in Eq. (4.41). Equation (4.61) contains $L(0)$, in contrast to $L(-1)$, I_1, and I_2 in Eq. (4.43). The remainder of the asymptotic expression, represented by $O(R/T)$ in the bracket of Eq. (4.63), is customarily called the inner-shell correction, since it stems primarily from contributions of inner-shell excitations (F63). While the asymptotic expansion of $\sigma_{\rm st}$ has been extended to the next-higher order in $1/T$ (FT64), the inner-shell correction usually has been evaluated numerically from explicit data of $f_n(K)$ based, for example, on the hydrogenlike model (B50, W52, W56, KM66a, B71). Since more realistic data on $f_n(K)$ are becoming available (Ma69, ACS70), one hopes to see in the near future improved calculations of the inner-shell correction.

For relativistic particles ($T \gtrsim 10^4$ eV), Eq. (4.63) must be modified. The result is (B33, F63, BA53)

$$\sigma_{\rm st}=\frac{16\pi a_0^2 z^2 Z}{mv^2/R}\left\{\ln\left[\frac{2mv^2}{I_0(1-\beta^2)}\right]-\beta^2\right\} \tag{4.64}$$

for a heavy particle ($M \gg m$), and

$$\sigma_{\rm st}=8\pi a_0^2 z^2 Z (R/mv^2)\{\ln[(mv^2T_e/I_0^2)(1-\beta^2)^{-1}] - [2(1-\beta^2)^{1/2}+\beta^2]\ln 2 + 1-\beta^2+\tfrac{1}{8}[1-(1-\beta^2)^{1/2}]^2\}, \tag{4.65}$$

for an electron,

$$T_e = mc^2[(1-\beta^2)^{-1/2}-1] \tag{4.66}$$

being the electron kinetic energy. In either case, the mean excitation energy I_0 is the only nontrivial property of the atom or molecule appearing in these expressions. At extremely high energies, further modifications are necessary because of the density effect and radiative corrections (F63, CF70).

The final remark of this section deals with the cross section $d\sigma_{\rm tot}(\theta)/d\omega$ for the total inelastic scattering into a given solid-angle element $d\omega$ near θ regardless of the final state of the atom or molecule. This cross section is defined by

$$d\sigma_{\rm tot}(\theta)/d\omega = \sum_n d\sigma_n/d\omega, \tag{4.67}$$

where the summation runs over all the final states n (discrete and continuum) that are kinematically accessible. The use of Eqs. (2.6) and (2.9) enables one to write

$$\frac{d\sigma_{\rm tot}(\theta)}{d\omega} = 4z^2a_0^2\left(\frac{M}{m}\right)^2\sum_n\left(\frac{k'}{k}\right)(Ka_0)^{-2}\left(\frac{R}{E_n}\right)f_n(K). \tag{4.68}$$

The summation here is in general complicated because the three factors k'/k, $(Ka_0)^{-2}$, and $(R/E_n)f_n(K)$ all depend upon the final state n. A simplification is possible, however, if one limits the discussion to an interval of θ. When $R/T \ll \theta \ll 1$, for example, Eq. (2.16) may be approximated by

$$(Ka_0)^2 \cong (T/R)(M/m)^2\theta^2, \tag{4.69}$$

an expression that is independent of n. On Figs. 1 and 2 one sees indeed that in the "interior" region within $ABCD$ or ABD the curves for $(Ka_0)^2$ exhibit a nearly horizontal behavior corresponding to Eq. (4.69). Notice at the same time that the curves for $(Ka_0)^2_{\rm min}$ are never horizontal, i.e., that Eq. (4.69) breaks down near zero scattering angle. Under the same condition, k'/k may be set effectively equal to unity. One thus obtains the Morse formula (Mo32)

$$d\sigma_{\rm tot}(\theta)/d\omega = 4z^2a_0^2(M/m)^2(Ka_0)^{-2}ZS_{\rm inc}(K), \tag{4.70}$$

where K is given by Eq. (4.69). Equation (4.70) also relies upon the sum rule (3.17) and therefore assumes that higher continuum states with $E_n > (M/m)(T/R)$ do not contribute appreciably to the summation involved. Analogs of Eq. (4.70) appropriate for greater scattering angles also have been discussed in the literature (TB69).

Although Eq. (4.70) is often useful, the range of its validity must be borne in mind. For instance, an attempt (such as in MS41) to derive $\sigma_{\rm tot}$ from Eq. (4.70) and its analogs invariably involves some ambiguity because the correspondence between θ and K in general depends upon n.

4.4. Relations to Other Theories

The purpose of this section is to indicate points of logical contact between the Bethe theory and certain other treatments of fast collisions. The following discussions will be limited to the most significant aspects considered from the standpoint of the Bethe theory.

When the de Broglie wavelength associated with the relative motion of a colliding system is sufficiently small compared to the size of a spatial region in which interactions with the atom or molecule take place, one is justified in treating the relative motion in a classical-mechanical sense—i.e., in describing it in terms of a well defined trajectory. Such a situation actually obtains when the incident particle is heavy ($M \gg m$) and at least moderately fast. In this case, collisions are classified by means of the impact parameter b, i.e., the distance between the initial line of motion and the center of the atom or molecule. Thus, one may first evaluate the probability $P_n(b, v)$ that the atom or molecule becomes excited to the state n as a result of a collision with impact parameter b and relative velocity v. Then the integrated cross section σ_n will be given by

$$\sigma_n = 2\pi\int_0^\infty P_n(b, v)\, b\, db. \tag{4.71}$$

Analyses based on this point of view (F24, W37) are known as impact-parameter theories, and their relation to the Born approximation has frequently been discussed in the literature (F31, M31, Bl33, S62, M66, p. 321 of BJ68). A major result is that, if one treats $P_n(b, v)$ to the lowest order in the interactions between the colliding partners, the resulting σ_n given by Eq. (4.71) is identical to that of the Bethe theory, Eq. (4.1). This fact, which might sound almost trivial, has an important implication in regard to the applicability of Eq. (4.1) and of many results derived therefrom (H33, BJ68). While the first Born approximation is justified if the incident velocity v is much larger than that of atomic electrons [conditions (i)], the impact-parameter theories are justified if the de Broglie wavelength is sufficiently small (i.e., if the incident momentum is sufficiently large) [condition (ii)]. For the K-shell excitation of an atom with nuclear charge Z_Ne, for example, condition (i) is

$$v \gg Z_Ne^2/\hbar \quad \text{or} \quad T = \tfrac{1}{2}mv^2 \gg RZ_N^2, \tag{4.72}$$

and condition (ii) is

$$Mv \gg Z_Nme^2/\hbar \quad \text{or} \quad T = \tfrac{1}{2}mv^2 \gg (m/M)^2RZ_N^2. \tag{4.73}$$

Clearly for $M \gg m$, the latter condition is far less restrictive than the former.

The above justification of Eq. (4.1) under the wide condition (4.73) has been the logical basis of a number of calculations on the inner-shell excitation by protons and other heavy particles with kinetic energies

above a few MeV (KCM69, CM69, CM70). In particular, the evaluation of the inner-shell correction to stopping power by means of Eq. (4.1) is considered to be meaningful also in this context (W51, W52, W56, B71). Actually, Eq. (4.1) is sometimes used even for discussion of the cross section for the inner-shell excitation near its threshold energy (H33).

It may also be added that Bloch (Bl33) used an impact-parameter formulation of the stopping power to show a logical connection between the Bethe theory and the Bohr theory.

The classification of collisions according to the impact parameter b is complementary to the classification according to the momentum transfer $\hbar K$; in other words, the majority of collisions satisfy

$$Kb \approx 1. \tag{4.74}$$

Although this situation is intuitively plausible, a precise statement of the relationship between K and b is not quite simple. (For example, an apparent difficulty in this context is that K is an observable quantity, while b is not.) Analyses of the relationship, carried out in several different ways (BJ68, M66, F70), show that b is conjugate, in the sense of the Fourier transform, to the component $\mathbf{K}_\perp$ that is perpendicular to the incident direction and is defined by

$$\mathbf{K} = \mathbf{K}_\perp + \mathbf{K}_\parallel \tag{4.75}$$

with

$$K_\parallel = E_n/(\hbar v). \tag{4.76}$$

For those collisions upon which the incident particle imparts *a sufficiently large energy* ($E \gg I_1$) to one of the atomic electrons, the binding of the atomic electrons to the nucleus plays a secondary role so that the energy transfer and the momentum transfer are correlated nearly as if the electrons were free (Sec. 3.2). Emphasis on this fact leads to a class of approximations that may somewhat loosely be called impulse approximations. (The term "impulse approximation" is used in the literature (GW64) sometimes in a far more specific sense.) In this approach, one initially regards a collision as merely causing a sudden transfer of momentum to the atomic electrons. Consequently, one assumes that, during the collision process, the electrons hardly interact with the nucleus or among themselves. Then, one may take account of the effect of the binding in succeeding steps of the formulation.

This point of view was utilized in earlier studies on the ionization cross section by Thomson (T12) and on the stopping power by Bohr (B13). These studies were remarkably successful in part because of the fortunate and intriguing fact that the same differential cross section for scattering by the Coulomb field (the Rutherford cross section) is *exactly valid at any velocity* both in quantum mechanics and in classical mechanics. Moreover, the first Born approximation also gives the identical result (W45). (This situation is especially remarkable when one recalls, for example, the scattering of a neutron by a nucleus, for which the predominant forces are short ranged so that quantum-mechanical results are entirely different from classical-mechanical results.)

The approach of Thomson and Bohr is occasionally used at present in an extended form, which is referred to as the binary-encounter theory (reviewed in BP68, and V69). For sufficiently fast collisions, this theory may be considered as an approximation to the Bethe theory. In order to clarify this point, one may rewrite Eqs. (2.34)–(2.36) in a different form.

When the Hamiltonian H of the atom or molecule is given by Eq. (3.24), one obtains

$$[H, \exp(i\mathbf{K}\cdot\mathbf{r}_k)] = \exp(i\mathbf{K}\cdot\mathbf{r}_k) \times [(\hbar K)^2/2m + \hbar\mathbf{K}\cdot\mathbf{p}_k/m]. \tag{4.77}$$

Therefore, one can write

$$\begin{aligned}\exp[i\mathbf{K}\cdot\mathbf{r}_k(t)] &= \exp(iHt/\hbar)\exp(i\mathbf{K}\cdot\mathbf{r}_k) \times \exp(-iHt/\hbar) \\ &= \exp(i\mathbf{K}\cdot\mathbf{r}_k)\exp\{(it/\hbar)[H + (\hbar K^2)/2m \\ &\quad + \hbar\mathbf{K}\cdot\mathbf{p}_k/m]\}\exp(-iHt/\hbar).\end{aligned} \tag{4.78}$$

By use of the operator calculus (F51), one can further rewrite the last two factors as

$$\exp\{(it/\hbar)[H + (\hbar K)^2/2m + \hbar\mathbf{K}\cdot\mathbf{p}_k/m)\} \times \exp(-iHt/\hbar) = \exp\left\{(i/\hbar) \times \int_0^t [(\hbar K)^2/2m + \hbar\mathbf{K}\cdot\mathbf{p}_k(t')/m]\,dt'\right\}, \tag{4.79}$$

where the Heisenberg momentum operator $\mathbf{p}_k(t)$ at time t for the kth electron is given by

$$\mathbf{p}_k(t) = \exp(iHt/\hbar)\,\mathbf{p}_k \exp(-iHt/\hbar) \tag{4.80a}$$

$$= \mathbf{p}_k + (it/\hbar)[H, \mathbf{p}_k] + \tfrac{1}{2}(it/\hbar)^2[H, [H, \mathbf{p}_k]] + \cdots. \tag{4.80b}$$

The use of Eqs. (4.78) and (4.79) in Eqs. (2.34) and (2.35) leads to

$$\frac{df(K, E)}{dE} = \frac{E/R}{2\pi\hbar(Ka_0)^2}\int_{-\infty}^{\infty} dt \exp\left(-\frac{iEt}{\hbar}\right) \times \left\{\sum_j \sum_k \left\langle \exp[i\mathbf{K}\cdot(\mathbf{r}_j - \mathbf{r}_k)] \times \exp\left[\frac{i}{\hbar}\int_0^t dt'\left(\frac{(\hbar K)^2}{2m} + \frac{\hbar\mathbf{K}\cdot\mathbf{p}_k(t')}{m}\right)\right]\right\rangle - \left|\sum_j \langle \exp(i\mathbf{K}\cdot\mathbf{r}_j)\rangle\right|^2\right\}. \tag{4.81}$$

Though Eq. (4.81) is still exact, one now restricts

the discussion to the case where E is large and introduces an impulse approximation. Notice that the right-hand side of Eq. (4.81) requires taking the Fourier component of the quantity in the brace. For large E, the only significant term in the brace is the one that varies most slowly with t. Thus, one may put $\mathbf{p}_k$ instead of $\mathbf{p}_k(t')$ in the t' integration. In other words, one neglects all but the first term in Eq. (4.80b). Then, the integrations with respect to t and t' may be performed to give

$$\frac{df(K,E)}{dE}=\frac{E/R}{(Ka_0)^2}\sum_j\sum_k\left\langle\exp\left[i\mathbf{K}\cdot(\mathbf{r}_j-\mathbf{r}_k)\right]\times\delta\left(\frac{(\hbar K)^2}{2m}+\frac{\hbar\mathbf{K}\cdot\mathbf{p}_k}{m}-E\right)\right\rangle. \quad (4.82)$$

[The second term in the brace on the right-hand side of Eq. (4.81) makes no contribution for any finite E.] The argument of the delta function may be rewritten as

$$\frac{(\hbar K)^2}{2m}+\frac{\hbar\mathbf{K}\cdot\mathbf{p}_k}{m}-E=\frac{(\hbar\mathbf{K}+\mathbf{p}_k)^2}{2m}-\frac{\mathbf{p}_k^2}{2m}-E$$

and thus permits an elementary interpretation: The gain of the kinetic energy of the kth electron, which has momentum $\mathbf{p}_k$ before the collision and momentum $\mathbf{p}_k+\hbar\mathbf{K}$ after the collision, is equal to the energy E transferred from the incident particle. That is to say, the electron behaves as if it were free, precisely in accordance with the neglect of the forces acting upon it within the atom, as represented by the term

$$[H,\mathbf{p}_k]=i\hbar\nabla_k U$$

in Eq. (4.80b). The delta function in Eq. (4.82) also implies that $df(K,E)/dE$ is appreciable only for large $(\hbar K)^2/(2m)$, so long as E is large. Then,

$$\exp\left[i\mathbf{K}\cdot(\mathbf{r}_j-\mathbf{r}_k)\right]$$

is a rapidly oscillating function of $\mathbf{r}_j-\mathbf{r}_k$ and makes no significant contribution unless $j=k$. (That is to say, electron correlations are unimportant for collisions with large momentum transfers.) Therefore, one may safely neglect the term with $j\neq k$ to obtain

$$\frac{df(K,E)}{dE}=\frac{E/R}{(Ka_0)^2}\sum_j\left\langle\delta\left(\frac{(\hbar K)^2}{2m}+\frac{\hbar\mathbf{K}\cdot\mathbf{p}_i}{m}-E\right)\right\rangle, \quad (4.83)$$

a standard expression of the binary-encounter theory (V69). The same formula also appears in the nonrelativistic theory of the Compton scattering of photons by weakly bound atomic electrons (EP70).

In order to obtain an expression for $d\sigma/dE$ [Eq. (4.22)][2] valid at large E, one may insert Eq. (4.83) into Eq. (4.1) and write

$$\frac{d\sigma}{dE}=\frac{4\pi a_0^2z^2}{T/R}\int\frac{R}{E}\frac{df(K,E)}{dE}\frac{d(Ka_0)^2}{(Ka_0)^2}$$
$$=4\pi a_0^2z^2(R^2/T)R\times\sum_j\int\left\langle\delta\left[Q-E+\left(\frac{2Q}{m}\right)^{1/2}p_{zj}\right]\right\rangle Q^{-2}dQ, \quad (4.84)$$

where $Q=(\hbar K)^2/(2m)=R(Ka_0)^2$ and $p_{zj}=(\mathbf{K}\cdot\mathbf{p}_j)/K$. Further, one takes here the interval of the Q integration as including the point $Q=E$ (i.e., the Bethe ridge discussed in Sec. 3.2). Notice also that the delta function makes the lower limit of the Q integration irrelevant to the calculation. It follows from Eq. (4.84) that

$$d\sigma/dE=4\pi a_0^2z^2(R^2/T)\sum_j\langle Q^{-2}(\xi_j)\,dQ(\xi_j)/d\xi_j\rangle\,|_{\xi_j=0}, \quad (4.85)$$

where the function $Q(\xi_j)$ is defined implicitly by

$$\xi_j=Q(\xi_j)-E+[2Q(\xi_j)/m]^{1/2}p_{zj}. \quad (4.86)$$

Assuming the momentum p_{zj} of the atomic electron as sufficiently small compared to the momentum transfer $\hbar K$, one expands through elementary calculation the right-hand side of Eq. (4.85) into a power series in p_{zj} to obtain

$$\frac{d\sigma}{dE}=\frac{4\pi a_0^2z^2}{T/R}R\sum_j\left\langle\frac{1}{E^2}+\frac{3}{E^{2/5}}\frac{p_{zj}}{(2m)^{1/2}}+\frac{4}{E^3}\frac{p_{zj}^2}{2m}+\cdots\right\rangle.$$

The second term always vanishes because $\langle p_{zj}\rangle=0$. Thus one obtains

$$\frac{d\sigma}{dE}=\frac{4\pi a_0^2z^2}{T/R}ZR\left(\frac{1}{E^2}+\frac{4B}{3E^3}+\cdots\right), \quad (4.87)$$

where B is defined as

$$B=Z^{-1}\sum_j\mathbf{p}_j^2/(2m), \quad (4.88)$$

and, by virtue of the virial theorem, is equal to the average binding energy of the atomic electrons.

Comparison of Eq. (4.87) with the general result (4.22) of the Bethe theory leads to a few significant observations. First, the approximate result (4.87) lacks the $T^{-1}\ln T$ term, which is decisive for large T. This is understandable from the argument leading to Eq. (4.87) which assumes large E and, in turn, large Q, while the $T^{-1}\ln T$ term in Eq. (4.22) stems from collisions with small Q. Second, Eq. (4.87) may be put in the form

$$(R/E)(df/dE)\ln c_E=ZR[E^{-2}+4BE^{-3}/3+\cdots]. \quad (4.89)$$

This proves Eq. (4.25), an important fact utilized a

few times in Sec. 4.3. [The coefficient of the second term in Eq. (4.89), however, is subject to qualifications, inasmuch as it has been derived through approximations such as the neglect of terms with $j \neq k$ in Eq. (4.82).] Explicit calculations for atomic hydrogen (I66, Om69a) verify Eq. (4.89).

The binary-encounter approach is useful for an approximate treatment of the electron-exchange effect in collisions of fast *electrons* with an atom or molecule. This effect arises because an inelastically scattered electron is indistinguishable from an electron ejected as a result of an ionizing collision. While a fully detailed theory of this effect must include intricacies of the many-body problem (Sec. 5.2), an approximate treatment is made possible by the simple recognition that the indistinguishability must be most important for those collisions in which the incident electron transfers a large amount of energy to the atom or molecule. For these collisions, the major fraction of the energy transferred then appears as the kinetic energy of the ejected electron, and the binding of atomic electrons plays a secondary role. One may thus start with the cross section for a collision of two free electrons and consider the binding at a succeeding step. In the nonrelativistic case, the Mott formula (M30, see also pp. 525 and 575 of LL65) gives the differential cross section expressed in terms of the kinetic energy w of the slower electron after the collision; that is, we have

$$\frac{d\sigma^{\text{Mott}}}{dw} = \frac{4\pi a_0^2 R}{T/R}\left[\frac{1}{w^2} - \frac{1}{w(T-w)} + \frac{1}{(T-w)^2}\right], \quad (4.90)$$

where $T=\frac{1}{2}mv^2$ is the kinetic energy of the incident electron. (Incidentally, the Mott formula is exactly valid for any T and w, so long as the two electrons involved are free.) The first term in the bracket is the direct term corresponding to the leading term of Eq. (4.87) and merely represents the Rutherford cross section. The exchange effect is described by the second and third terms.

This idea of treating the exchange effect was first applied to the stopping-power theory by Bethe (p. 521 of B33, see also p. 575 of LL65). Later it was adapted to the evaluation of the ionization cross section by Platzman and Miller (Fig. 7 of F63, M56; see also KI71). The same approach is readily applicable to the relativistic case ($T \geq 10^4$ eV), for which one should replace the Mott formula by the Møller formula (M32, see also p. 817 of MM65); for example, Eq. (4.65) was derived in this manner. The exchange effect will be discussed further in Sec. 5.2.

An additional remark concerns an extended application of the generalized oscillator strength to inelastic collisions between atomic systems. For example, suppose that an atom A and another atom B, both in the ground state, collide with each other at relative velocity v much greater than the velocities of the atomic electrons involved, and that after the collision A and B become excited to electronic states n_A and n_B, respectively. The cross section $\sigma(n_A, n_B)$ for this process is given, within the first Born approximation, as

$$\sigma(n_A, n_B) = 4\pi a_0^2 (R/T) \int |\epsilon_A(n_A; K)|^2 \times |\epsilon_B(n_B; -K)|^2 (Ka_0)^{-4} d(Ka_0)^2, \quad (4.91)$$

where $T=\frac{1}{2}mv^2$, m is the electron mass, and $\epsilon_A(n_A; K)$ and $\epsilon_B(n_B; K)$ are matrix elements defined by Eq. (2.5) in reference to A and B, respectively (BG54, BG55). Here again, the limits of the $(Ka_0)^2$ integration are dictated by kinematics. [The quantity $(Ka_0)^2$ is still given by Eq. (2.16) with E_n replaced with the sum of electronic excitation energies in A and B.] Since the matrix elements $\epsilon_A(n_A; K)$ and $\epsilon_B(n_B; K)$ are simply related to the corresponding generalized oscillator strengths [Eq. (2.9)], $\sigma(n_A, n_B)$ can be evaluated if these are known either theoretically or experimentally. The integrand in Eq. (4.91), in contrast to that in Eq. (4.1), is nonsingular at $(Ka_0)^2=0$. Therefore, in the limit of large T, the integral tends to a constant and $\sigma(n_A, n_B)$ varies as $1/T$.

This kind of approach may be extended to cases in which the colliding partners are molecules and also to cases in which their final electronic states belong to ionization continua. A modification is necessary if either one of the partners, say B, remains in the ground state after the collision. Then, the matrix element $\epsilon_B(n_B; K)$ must be taken as an elastic-scattering form factor. A considerable number of applications of this approach are found in the recent literature (G67, PGW67, GP68, BDK69, BDK70).

5. CONCLUDING REMARKS

5.1. Areas for Further Studies Within the Bethe Theory

Having summarized the current understanding, I now wish to indicate some problems that may be attacked fruitfully in the not too distant future. The discussion in this section will be limited to theoretical problems within the framework of the first Born approximation.

It is obviously desirable to carry through reliable calculations of the generalized oscillator strengths for different transitions in as many atoms and molecules as possible. In this respect, the following alternative lines of approach seem to deserve attention at present.

First, it is important to understand the gross but realistic features of the Bethe surfaces of *atoms* and to search for the systematics across the Periodic Table. The merit of the calculations within one-electron models (Ma69, ACS70, A71, Ma71, Mc71) is seen precisely in this context. Further extension of similar calculations to many atoms is entirely feasible and will serve

at least two immediate ends. On the one hand, the resulting data themselves will be useful for many applications for which only estimates of cross sections are required. On the other hand, the same data may reveal specific aspects that are especially appropriate for detailed experimental investigations. The occurrence of the minima of the generalized oscillator strength (as discussed in Sec. 3.4) is a case in point.

Second, evaluation of the generalized oscillator strength from improved wave functions including electron correlation is desirable for several atoms. Even for He, existing calculations on transitions into continua are based on atomic models of modest accuracy. The generalized oscillator strengths for transitions into doubly excited states (apart from the optical limits) are only beginning to be computed (BK70). Most of the published reports on double excitation and double ionization of He (BJ66, W70, A69 and references therein) present only the corresponding integrated cross sections, but clearly attest the important role of electron correlations in the atom. Progress in the photoionization calculations on rare-gas atoms (S70, A71) seems to open up the possibility of reliable calculations of the generalized oscillator strength for ionization with explicit consideration of electron correlation. Work in this direction will provide a test of continuum wave functions and, in turn, of the methods by which they are constructed, when sufficient dependable experimental data are available for comparison.

Third, it appears worthwhile to explore theoretical formulations that are different from the traditional scheme of computing first a pair of wave functions and then the matrix element $\epsilon_n(K)$ [Eq. (2.5)] to obtain the generalized oscillator strength. For example, an appropriate approximation to the correlation function $\phi(K, T)$ [Eq. (2.35)] will be an alternative that may prove useful for certain purposes. Such an approach may be regarded also as an approximate evaluation of the Green's function, which is discussed often in the context of many-body problems in solid-state physics (N64). An initial exploration along these lines is found in Sc70.

Fourth, the generalized oscillator strength of *molecules* has been calculated for only a few cases. Calculation of lower discrete excitations of H_2 by use of correlated wave functions may prove valuable as a guide for thorough understanding of intricacies of the molecular generalized oscillator strength. At the same time, studies on other basic diatomic molecules such as N_2, O_2, NO, and CO, even within a modest model (say, a single-configuration description), will be valuable for comparison with a large amount of experimental data already available. A particular point of interest will be the sensitivity of the electronic matrix element $\epsilon_n(K; \rho, \Theta, \Phi)$ [Eq. (3.47)] to the internuclear distance ρ and how this sensitivity affects the role of Franck–Condon factors.

Fifth, precise evaluation of the relativistic form factor [appearing in Eq. (2.23)], even for atoms, belongs to the future program. Although the approximate relations (2.29) and (2.30) are adequate for most excitations, rigorous relativistic form factors are desirable for detailed treatment of inner-shell excitations in very heavy atoms. Existing calculations on the relativistic form factor are all based on hydrogenic models (M68). Recent progress in the relativistic Hartree–Fock theory (as reviewed in G70) is encouraging in this respect, although no readily usable results on excited-state wave functions appear available at present.

Finally, it is important to discuss a finer classification of the generalized oscillator strength. The definition of $df(K, E)/dE$ [Eq. (2.21)] includes the sum over all degenerate final states of the atom or molecule. Consider, for example, ionizing collisions in which a given amount of energy E and a given amount of momentum $\hbar\mathbf{K}$ are transferred to an *atom*. Even in this simple case, electrons will be ejected in general into nonunique directions (depending upon the sharing of $\hbar\mathbf{K}$ among atomic electrons) and with nonunique energies (depending upon the electronic states of the ion left behind). The resulting distribution of the ejected electrons with respect to the direction and to the kinetic energy may be considered as a finer classification of $df(K, E)/dE$. So far this distribution has been treated theoretically in a few instances only (O65, O67, GI68, CM69, CM70, CK71), while pertinent experimental data are rapidly becoming available (Sec. 5.3).

For molecules, the energy distribution is more involved because of the internal degree of freedom of the ion left after electron ejection. Furthermore, a molecule excited into the continuum ($E > I_1$) may take decay channels alternative to ionization such as dissociation into neutral fragments and internal conversion. In general, excitation to states at given E may lead to emission of corpuscles (electrons, photons, and dissociation fragments), and the distribution of these corpuscles in terms of direction and energy is important as a potential source of information about the dynamics of molecular excited states.

Among a variety of such distributions, the angular distribution of fluorescence from atoms is perhaps the best understood, and the knowledge of it is utilized in measurements of the excitation cross section by optical methods (MS68). Other instances discussed so far concern atomic fluorescence resulting from molecular dissociation (VZ68) and dissociative ionization (DK63, GP69, VK70). Further theoretical studies on these and similar problems appear desirable.

5.2. Departures from the Bethe Theory at Low Velocities

As the incident velocity decreases and approaches the velocity of atomic electrons, it becomes less and

less justified to treat an inelastic collision as a small perturbation. It is indeed well known that true cross sections at such low velocities depart from the prediction of the first Born approximation. But the precise way in which departures from the first Born approximation occur remains only poorly understood at present. Following are the writer's tentative points of view based on fragmentary evidence concerning this question. The discussion here will concern still moderately fast collisions, for which the departures first become apparent as the velocity falls below the Bethe asymptotic domain.

Traditionally the departures have been discussed most often in connection with the velocity dependence of the integrated cross section σ_n for discrete excitation of a specified kind n or of the ionization cross section σ_i (MM65, MS68). For sufficiently high velocities, the Fano plot (Sec. 4.2) of experimental σ_n or σ_i should asymptotically approach a straight line. The inclusion of the γ term [Eqs. (4.18), (4.20), (4.29)] causes a deviation from the straight line at lower velocities. The nature of this deviation is well understood [Eqs. (4.19), (4.53), (4.54)]. Any further deviation at even lower velocities may be attributed to a breakdown of the first Born approximation.

Although the analysis sketched above is conceptually straightforward, its application is often difficult, simply because experimental data on σ_n or σ_i are not always reliable (KD66, MS68). The σ_i of He, one of the most frequently studied cases, exemplifies the difficulty. All the symbols in Fig. 18 represent experimental data, which should be compared for sufficiently large T/R with the accurate theoretical straight line labeled "ION". The serious discrepancies between the asymptote and the data sets represented by open circles and filled triangles are alarming especially when one notices that these sets are the most recently reported among all the quoted data. Improved measurements of integrated cross sections are thus highly desirable.

Another important point is that the Bethe asymptote is theoretically well known only in exceptional instances such as He. It is essential that trustworthy calculations within the first Born approximation be carried out before one may confidently ascertain any departures from it.

In view of the above qualifications, it is difficult at present to make a quantitative statement on the magnitude of the departures for given T. For discrete transitions with excitation energy E_n, it is commonly believed that the ratio E_n/T is a measure of the validity of the first Born approximation. However, data for He on σ_n for the 2^1P, 3^1P, 2^1S, 3^1S, and 3^1D excitations, all with comparable E_n, apparently suggest that the nature of each transition plays an important role in this context; at intermediate electron kinetic energies ($T\approx$200–400 eV), the departures for the optically forbidden transitions are clearly appreciable, while those for the optically allowed transitions are hardly significant (KI68, KI69b).

For the ionization cross section, one might be inclined to consider naively the ratio I_1/T as a parameter pertinent to the departures. Actually, one should keep in mind at least two qualifications. First, the ionization energy I_1 by definition merely represents the minimum energy transfer—not a "typical" energy transfer $\bar{E}$ involved in all ionizing collisions. The latter may be in effect an average of E over all the relevant region of the Bethe surface, and will be in general substantially greater than I_1, because the excitation spectrum $(R/E)df(K, E)/dE$ is appreciable in higher portions of the continuum. Since $\bar{E}$ is a global property of the spectrum, one expects $\bar{E}$ to differ from one atomic system to another in a way not necessarily parallel to the difference for I_1. Second, an appropriate value of $\bar{E}$ depends upon the electron shell. Thus, departures of the ionization cross section from the Born-approximation result must be considered for each individual shell or even subshell.

The differential cross section $d\sigma_n/d\omega$, or equivalently the apparent generalized oscillator strength $\mathrm{f}_n(K, T)$ [Eq. (3.1)], provides in general more conclusive evidence regarding the departures at lower velocities. Again, the $2^1P\leftarrow1^1S$ excitation in He seems to be the best studied in this respect (CMK70, TRKTC70). The extensive data of TRKTC70 for electrons with intermediate kinetic energies ($\lesssim$82 eV), however, cannot be summarized briefly.

A very recent development in this connection must be mentioned. Skerbele and Lassettre (SL70b) measured with electrons of kinetic energies 300, 400, and 500 eV $d\sigma_n/d\omega$ for two optically forbidden transitions $a\,{}^1\Pi_g\leftarrow X\,{}^1\Sigma_g^+$ and $a''\,{}^1\Sigma_g^+\leftarrow X\,{}^1\Sigma_g^+$ in N_2. The apparent generalized oscillator strength for the former transition turned out to be the same for the three kinetic energies; this constancy is a necessary (though not sufficient) condition for the validity of the first Born approximation. In contrast, the apparent generalized oscillator strength for the latter transition markedly depended upon the kinetic energy. There is little difference in the excitation energy E_n; it is about 9.2 eV for the former transition and about 12.3 eV for the latter transition. Guided in part by that experimental result, Lassettre (L70) theoretically showed that the deviation from the first Born approximation at a given T can be more appreciable for a transition between states with the same spectroscopic designation than for a transition between states with different designations. This same theoretical result also seems to account for the observation that the apparent generalized oscillator strength $\mathrm{f}_{2^1S}(K, T)$ of He measured for $T\approx$200–500 eV depends upon T but that $\mathrm{f}_{2^1P}(K, T)$ is practically independent of T in the same interval.

An obvious extension of the first Born approximation is the study of higher-order terms in the Born

series of the scattering amplitude[5] (KMS60, MP65, HM68a, HM68b, H69a). Unfortunately, explicit evaluation of the second Born amplitude is already so complicated mathematically that no rigorous result has been given even for discrete excitations in atomic hydrogen. The higher-order Born approximation physically amounts to inclusion of virtual intermediate states of the atom or molecule during a collision, and the main difficulty of the calculation stems from the infinitely many possibilities of these intermediate states. Under certain circumstances, however, one may be able to argue that only a few intermediate states are decisive and to estimate their effects approximately.

In this connection, it is important to recognize a distinction between an optically allowed transition and an optically forbidden transition. To be specific, consider a transition $n \leftarrow 0$. The second-order Born amplitude for $n \leftarrow 0$ is a sum of terms, each of which corresponds to a virtual process $n \leftarrow n' \leftarrow 0$, n' being an intermediate state. First, suppose that the transition $n \leftarrow 0$ is allowed. For example, take the $2^1P \leftarrow 1^1S$ transition in He. It is easy to see that, for any choice of n', at least one of the two virtual transitions (i.e., $n \leftarrow n'$ or $n' \leftarrow 0$) is optically forbidden. Assuming that the virtual transitions are largely associated with small momentum transfers, one expects that the indirect process may be inefficient compared to the strong direct process $n \leftarrow 0$ described by the first-order Born amplitude. [An alternative statement of the above assumption is that the asymptotic behavior of the coupling potentials $V_{nn'}(\mathbf{r})$ and $V_{n'0}(\mathbf{r})$, as discussed in Footnote 3, is decisive. The plausibility of this assumption must be considered in individual cases.] The situation is different when the transition $n \leftarrow 0$ is optically forbidden. It is sometimes possible to have intermediate states n' for which both virtual transitions ($n \leftarrow n'$ and $n \leftarrow 0$) are allowed. In this case, the indirect process may be nearly as efficient as the weak direct process $n \leftarrow 0$. For example, notable departures of the integrated cross section for the $4^1D \leftarrow 1^1S$ excitation in He from the Born-approximation result are attributed in part to the intermediate 2^1P state; indeed, the two virtual transitions here ($4^1D \leftarrow 2^1P$ and $2^1P \leftarrow 1^1S$) have oscillator strengths of appreciable magnitude (VP68).

From the above point of view, several significant findings of recent years appear quite understandable. The theoretical result of Lassettre (L70), quoted earlier, is an example. Lin and coworkers (CL69, SSLF70, and references therein) have arrived at virtually the same point of view after a series of experimental and theoretical studies on electron-impact excitation of many atoms. For electron collisions on He, close-coupling calculations including various sets of atomic eigenstates (CL69) seem to demonstrate an important role of the indirect processes for forbidden transitions at electron kinetic energies below 100 eV. As for proton collisions, experimental data on the $4^1D \leftarrow 1^1S$ excitation of He at kinetic energies around 1 MeV disagree seriously with the Born-approximation result, as noted by Thomas (T67). Motivated in part to elucidate this discrepancy, van den Bos (VdB69b) applied to proton collisions on He an impact-parameter treatment including the close coupling of several atomic eigenstates. His result for the $3^1D \leftarrow 1^1S$ excitation shows an appreciable deviation from the first Born approximation even at proton kinetic energies of 1–10 MeV, but his result for the $2^1P \leftarrow 1^1S$ excitation is virtually indistinguishable from the Born-approximation result in the same energy range. (The calculation of VdB69b does not include the 4^1D state, however.)

Other evidence of departures of a similar nature concerns the stopping power and the range of charged particles, both of which are now being measured with high precision (B71). Measurements with $\Sigma^{\pm}$ hyperons (BDH63) and with pions (BOSS65, HL69) indicate that the stopping power, in nuclear emulsions, of a negative particle is smaller than that of a positive particle with the same mass and the same velocity, the relative difference amounting to several percent for $\beta \lesssim 0.2$. This observation clearly represents a deviation from the first Born approximation, according to which all cross sections—and consequently the stopping power [Eq. (4.64)]—have a quadratic dependence on the particle charge ze. Roughly speaking, one may interpret the stopping-power difference in terms of a charge polarization of the target during a collision; a negative incident particle tends to repel atomic electrons away from itself, thereby rendering energy transfer less efficient, while a positive incident particle tends to attract atomic electrons toward itself thereby rendering energy transfer more efficient. The second Born approximation certainly includes this effect, and will give rise to a z^3 term in the stopping power, in addition to the usual z^2 term. A recent analysis (AEB71) based on an impact-parameter formulation may be considered as an initial attempt at quantitative understanding of this z^3 term. The charge-dependent deviation from the Bethe formula has been studied also through comparison between the stopping power of a doubly charged particle and that of a singly charged particle at the same velocity (ASS69).

A remarkable effect recently discussed by Salin (S69) and by Macek (M70) exemplifies the wealth of physics involved in the angular distribution of the ejected electrons and at the same time illustrates a failure of the first Born approximation. For example, consider an ionizing collision of a fast proton with a helium atom. Sometimes an electron will emerge with a velocity comparable to the proton velocity, which presumably does not change much during the collision. For a considerable period of time, such an electron is subject to the field of the moving proton, as well as to the field of the residual He^+ ion. (The first Born

approximation includes only effects of the latter field.) Calculations have shown (S69, M70) that the distortion of the electron wave function due to the moving proton significantly affects the angular distribution of ejected electrons near the forward direction. A convincing experimental verification of this effect has been reported recently (CR70).

Another effect not included in the first Born approximation for electron impact is the exchange of the incident electron with one of the atomic electrons. As has been discussed in Sec. 4.4, this effect is reasonably well understood for those collisions in which the energy transfer is much greater than the binding energy of atomic electrons. Various theories have been designed to treat the effect for a more general situation, but none of them appears to be very well established. Indeed, applications of these theories to concrete examples (JM65, TCK68) give widely different results, particularly with respect to differential cross sections.

Transitions involving a change in the spin multiplicity in a light atom or molecule are especially interesting in connection with the electron-exchange effect, because the first-order Born approximation gives (near) zero cross sections for these transitions. For example, the $2^3S \leftarrow 1^1S$ excitation of He by electron impact is possible only through an electron exchange although other remote possibilities have been considered as well (M67). Experimentally, the angular distribution of scattered electrons resulting from this excitation is peaked forward at incident kinetic energies as high as 200 eV (VSM68). In contrast, most theories predict a distribution peaked at a fairly large angle (MK68, JV70) although a recent calculation qualitatively reproduces the forward peaking (SLi70). For other singlet–triplet transitions ($2^3P \leftarrow 1^1S$ in He, $b\,^3\Sigma_u^+ \leftarrow X\,^1\Sigma_g^+$ in H_2), the angular distributions are peaked at finite angles (SLi70, TCRBK68). As for the velocity dependence of the integrated cross section, presently available evidence indicates that the integrated cross section for this kind of transition varies as T^{-3} for large T, so that σ_{tot} of Eq. (4.41) needs no modification to the order explicitly given.

An additional remark concerns collisions with an ion. Deviations from the first Born approximation are expected to be more apparent in this case than in the case of collisions with a neutral atom or molecule. Suppose an incident particle of charge ze collides with an atomic ion having Z electrons and a nucleus of charge $Z_N e$. One may split the interaction V of Eq. (2.2) into two parts as

$$V = V_C + V', \tag{5.1}$$

where

$$V_C = z(Z_N - Z)e^2/r \tag{5.2}$$

represents the net Coulomb interaction between the incident particle and the ion, and

$$V' = -\sum_{j=1}^{Z} \frac{ze^2}{|\mathbf{r}-\mathbf{r}_j|} + \frac{zZe^2}{r} \tag{5.3}$$

represents the interaction directly causing the inelastic scattering. Here one may regard V_C as a part of the unperturbed Hamiltonian for the system consisting of the incident particle and the ion and treat V' as a perturbation. Then, one obtains an expression for $d\sigma_n$ similar to Eq. (2.1) but with the matrix element replaced by

$$\int [\psi_{\mathbf{k}'}{}^+(\mathbf{r})]^* u_n^*(\mathbf{r}_1, \cdots, \mathbf{r}_Z) \times V' \psi_{\mathbf{k}}{}^-(\mathbf{r}) u_0(\mathbf{r}_1, \cdots, \mathbf{r}_Z) d\mathbf{r}_1 \cdots d\mathbf{r}_Z\, d\mathbf{r},$$

where $\psi_{\mathbf{k}'}{}^+(\mathbf{r})$ and $\psi_{\mathbf{k}}{}^-(\mathbf{r})$ are the Coulomb wave functions defined on p. 522 of LL65. This procedure is known as the Coulomb–Born approximation and has been applied to a number of cases (as reviewed in MS68 and MBG69).

For sufficiently high incident velocity, the Coulomb–Born approximation reduces to the first Born approximation; but the precise way in which the Bethe asymptotic cross section [Eq. (4.15) or (4.20)] is affected by the net Coulomb field V_C has been analyzed only incompletely. From the analyses of MG51 and Ga66, for example, one sees that the leading ($T^{-1} \ln T$) term in the asymptotic cross section σ_n is still given in the same form as in Eq. (4.15), but possible modifications of other terms remain obscure. (The standard evaluation of the Coulomb–Born approximation starts with the partial-wave expansion of the Coulomb wave functions. For high velocities, the resulting series converges slowly at best and therefore does not seem to be advantageous for the examination of an analytic form in the asymptotic region.)

Comparison of the first-Born-approximation results with experiment for H^- (IK68), Li^+ (KI70), and He^+ (KI71) seems to suggest that the effect of the net Coulomb field V_C on the asymptotic cross sections is not outstanding as compared to all other causes for the departures from the first Born approximation so long as $|Z - Z_N| = 1$. Also, a recent Coulomb–Born calculation (BS69) on the electron-impact ionization of H^- gives an asymptotic behavior in close agreement with the Bethe asymptote (IK68). When $|Z - Z_N|$ is large compared to unity, however, the result of the Coulomb–Born approximation is very different from the result of the first Born approximation (as seen in the cases quoted in MS68).

Numerous theories have been proposed for the description of lower-velocity collisions for which the first Born approximation is inapplicable. Most of these theories are reviewed in standard references (WO62, GW64, MM65, MS68). Among the theories that appear most relevant to the theme of this section are the eikonal approximation (GW64), the Glauber approximation (TBGF70), and a class of theories called

the impulse approximation (GW64, S68, C69). Chiefly because of computational difficulties, these approximations have been applied to only a few concrete examples.

The concluding remark of this section represents a point of view that may be important for further developments. It seems to be common to many problems in physics that, when a simple schematization breaks down, it does so in a variety of ways, and not just in one way or another. When the true cross section departs from the asymptotic behavior as the velocity decreases, there are many causes that are mutually related. These causes are commonly referred to as the distortion of the incident wave, the charge polarization of the target, effects of compound states, exchange effects (for electron collisions), and so on. In order to understand low-velocity collisions, one must attempt to devise a balanced treatment of all these effects. An unbalanced theory, which overemphasizes one of these effects, is bound to be at most tentative, and may often be seriously misleading.

5.3. Desirable Experiments

As may be apparent from the discussions in the two preceding sections, a great deal of what is learned about fast collisions will continue to come from experiment rather than from theory. In this respect, the following areas are suggested for experimental study in the near future.

First, both for discrete excitations and for ionizations, reliable absolute measurements of integrated cross sections at high velocities still remain of basic importance. The measurements should be precise within several percent or better, in order to be significant for elucidation of the asymptotic behavior and of the departures therefrom. It is also desirable to extend the variety of atoms and molecules beyond those which form static-gas targets in traditional measurements. For example, cross-section data on open-shell atoms, metastable atoms, ions, and radicals are very scanty at present. Recent developments of crossed-beam techniques are encouraging in this respect (D69).

A related topic is measurement of the electron attenuation in gases. To make the resulting data accurate, one must use well-collimated electron beams and low-pressure gases. The result will give the total scattering cross section of an atom or molecule, including the contributions from elastic and inelastic collisions. This information will be useful in several respects. For example, it is an important item of the input data in a dispersion-theoretical analysis of all the cross sections (BM69, BM70). Further, if the elastic-scattering cross section is known either experimentally or theoretically, the total inelastic-scattering cross section σ_{tot} may be obtained by subtraction. Data on σ_{tot} are sometimes useful simply as upper limits on any individual inelastic-scattering cross section, for example, the (counting) ionization cross section. Besides, σ_{tot} at sufficiently high velocities may be compared fruitfully with theoretical results derived by sum rules (Sec. 4.3). Finally, data on total scattering are sometimes required in the design of other experiments—e.g., on angular distribution of scattered electrons. Since the early pioneering studies (B25, N30), however, the electron-attenuation measurement appears to have been unduly neglected, except at very low velocities (GB65, GB66, GBS66, SN70).

Second, electron energy-loss measurements need to be extended to more varied targets, most notably to atoms and molecules that do not usually form permanent gases. An initial exploration of electron collisions with atomic beams has already proved feasible and valuable (HR68a, HR68b, HR69a, HR69b).

Third, electrons ejected from various atoms and molecules as a result of ionizing collisions deserve detailed investigations. Actually a considerable number of reports already seem to promise riches of knowledge to be obtained from analyses of the ejected electrons (RSB66, DM68, RS68, ER68, ESTW69, KSLCM70, CMPK70, CMKr70, MDPM70, T71, OPB71, VCM71). The distribution of these electrons with respect to the kinetic energy and the angle of ejection is important in several different ways. First, of all, data on the distribution over wide ranges of the variables involved are needed in radiation physics, atmospheric physics, and other areas of application, in which the ejected electrons play a key role in many phenomena. Next, the most energetic electrons emerge nearly as if they were initially free and stationary, and the deviations from the free-electron behavior reveal information about the electron binding in the atom or molecule (RG69, MDPM70, CK71). Further, if one analyzes the electron kinetic energy with sufficiently high resolution, one may learn much about the intricacies of ionization processes such as autoionizing states of Auger effects following inner-shell excitations (RS68, ER68, KSLCM70, CMPK70, CMKr70, ONT70, SKYW70, YS71). Finally, analyses of the ejected electrons (ESTW69) and of ions (VdW70), in coincidence with the determination of the energy loss of the incident particle, provide even more detailed knowledge. Studies of the light emission in coincidence with the energy-loss determination will also be valuable. The merit of the coincidence measurements is that the resulting data will pertain to final states of an atom or molecule at a definite excitation energy and therefore will permit conceptually simple interpretations.

Fourth, experimental data on collisions of positrons with atoms and molecules may give a valuable guide to theory in regard to the departures from the first Born approximation. Whereas this approximation predicts an identical cross section for electrons and positrons at the same velocity, the departures at the lower velocities arise from quite different causes for electrons and positrons. For example, instead of the exchange

effect for electron collisions, positron collisions involve the effects of virtual and real positronium formation. The technology of positron-collision experiments seems to be on the verge of promising developments (GCMH69).

This article has chiefly aimed at presenting a framework of thinking. It is hoped that coming years will see the advent of such experiments as suggested above so that one may put the framework to full use and learn the detailed dynamics of atoms and molecules as manifested in their Bethe surfaces.

ACKNOWLEDGMENTS

It is a great pleasure for me to thank a number of friends, too many to be listed, who have provided me with information of vital importance in the writing of this article. Especially I cannot help expressing my indebtedness to Professor U. Fano and Professor R. L. Platzman for their most valuable advice, and to Dr. Y.-K. Kim for his most devoted collaboration, all during the past several years in which I have formed the points of view presented in this article. I also am grateful for the hospitality of the colleagues at the Joint Institute for Laboratory Astrophysics, where I carried out a major part of the writing.

REFERENCES

A52 S. Altshuler, Phys. Rev. **87,** 992 (1952).
A53 S. Altshuler, Phys. Rev. **89,** 1093 (1953).
A69 T. Åberg, Ann. Acad. Sci. Fenn. Ser. *A* **6,** 308 (1969).
A71 M. Ya. Amusia, "Many-Electron Correlations in Atomic Electron Shells and Possible Ways of Their Experimental Detection" in *Proceedings of Second International Conference on Atomic Physics,* (Plenum, London, 1971).
ACS70 M. Ya. Amus'ya, N. A. Cherepkov, and S. I. Sheftel', Zh. Eksp. Teor. Fiz. **58,** 618 (1970) [Sov. Phys. JETP **31,** 332 (1970)].
AD70a J. F. M. Aarts and F. J. de Heer, J. Chem. Phys. **52,** 5354 (1970).
AD70b J. F. M. Aarts and F. J. de Heer, Physica **49,** 425 (1970).
AD71 J. F. M. Aarts and F. J. de Heer, Physica **52,** 45 (1971).
ADV68 J. F. M. Aarts, F. J. de Heer, and D. A. Vroom, Physica **40,** 197 (1968).
AGLS68 V. V. Afrosimov, Yu. S. Gordeev, V. M. Lavrov, and S. G. Shchemelinin, Zh. Eksp. Teor. Fiz. **55,** 1569 (1968) [Sov. Phys. JETP **28,** 821 (1969)].
ARB71 J. C. Ashley, R. H. Ritchie, and W. Brandt, Phys. Rev. (to be published).
ASS69 H. H. Andersen, H. Simonsen, and H. Sørensen, Nucl. Phys. **A125,** 171 (1969).
B13 N. Bohr, Phil. Mag. **25,** 10 (1913).
B15 N. Bohr, Phil. Mag. **30,** 581 (1915).
B25 R. B. Brode, Phys. Rev. **25,** 636 (1925).
B30 H. Bethe, Ann. Physik **5,** 325 (1930).
B32 H. Bethe, Z. Physik **76,** 293 (1932).
B33 H. Bethe, in *Handbuch der Physik,* edited by H. Geiger and K. Scheel (Springer, Berlin, 1933), Vol. 24/1, p. 273.
B34 F. Bloch, Phys. Rev. **46,** 674 (1934).
B48 H. Bohr, Kgl. Danske Videnskab. Selskab, Mat.-Fys. Medd. **18,** No. 8 (1948).
B50 L. M. Brown, Phys. Rev. **79,** 297 (1950).
B62 R. A. Bonham, J. Phys. Soc. Japan **17,** Suppl. B-II, 10 (1962).
B69 R. S. Berry, Ann. Rev. Phys. Chem. **20,** 357 (1969).
B71 H. Bichsel, in *American Institute of Physics Handbook,* edited by D. E. Gray (McGraw Hill, New York, 1971), 3rd ed., Sec. 8C.
BA53 H. A. Bethe and J. Ashkin, in *Experimental Nuclear Physics,* edited by E. Segrè (Wiley, New York, 1953), Vol. 1, p. 166.
BB65 L. C. Biedenharn and P. J. Brussaard, *Coulomb Excitation* (Oxford U. P., London, 1965).
BDH63 W. H. Barkas, J. N. Dyer, and H. H. Heckman, Phys. Rev. Letters **11,** 26 (1963).
BDK69 K. L. Bell, V. Dose, and A. E. Kingston, J. Phys. B **2,** 831 (1969).
BDK70 K. L. Bell, V. Dose, and A. E. Kingston, J. Phys. B **3,** 129 (1970).
BFM50 D. R. Bates, A. Fundaminsky, and H. S. W. Massey, Trans. Roy. Soc. (London) **A243,** 93 (1950).
BG54 D. R. Bates and G. W. Griffing, Proc. Phys. Soc. (London) **A67,** 663 (1954).
BG55 D. R. Bates and G. W. Griffing, Proc. Phys. Soc. (London) **A68,** 90 (1955).
BG70 G. R. Blumenthal and R. J. Gould, Rev. Mod. Phys. **42,** 237 (1970).
BGR61 H. Boersch, J. Geiger, and H.-J. Reich, Z. Physik **161,** 296 (1961).
BGS67 H. Boersch, J. Geiger, and B. Schröder, Abhandl. Deut. Akad. Wiss. Berlin, Kl. Math., Physik Tech. **1967,** No. 1, 15
BGT69 H. Boersch, J. Geiger, and M. Topschowsky, Z. Naturforsch. **26a,** 198.
BJ66 F. W. Byron, Jr., and C. J. Joachain, Phys. Rev. Letters **16,** 1139 (1966).
BJ68 H. A. Bethe and R. W. Jackiw, Intermediate Quantum Mechanics (Benjamin, New York, 1968), 2nd ed.
BK67 A. O. Barut and H. Kleinert, Phys. Rev. **160,** 1149 (1967).
BK69a K. L. Bell and A. E. Kingston, J. Phys. B **2,** 653 (1969).
BK69b K. L. Bell and A. E. Kingston, J. Phys. B **2,** 1125 (1969)
BK70 K. L. Bell and A. E. Kingston, J. Phys. B **3,** 1300 (1970).
BK71 J. S. Briggs and Y.-K. Kim, Phys. Rev. A **3,** 1342 (1971).
BKK68a K. L. Bell, D. J. Kennedy, and A. E. Kington, J. Phys. B **1,** 204 (1968).
BKK68b K. L. Bell, D. J. Kennedy, and A. E. Kingston, J. Phys. B **1,** 1028 (1968).
BKK69 K. L. Bell, D. J. Kennedy, and A. E. Kingston, J. Phys. B **2,** 26 (1969).
B133 F. Bloch, Ann. Physik **16,** 285 (1933).
BM69 B. H. Bransden and M. R. C. McDowell, J. Phys. B **2,** 1187 (1969).
BM70 R. H. Bransden and M. R. C. McDowell, J. Phys. B **3,** 29 (1970).
BOSS65 W. H. Barkas, W. Z. Osborne, W. G. Simon, and F. M. Smith, Proceedings of the Fifth International Conference on Nuclear Photography, 15–18 September 1964 (CERN Report 65-4, Vol. II., 1965).
BP68 A. Burgess and I. C. Percival, in Advan. At. Mol. Phys. **4,** 109 (1968).
Br69 J. P. Bromberg, J. Chem. Phys. **50,** 3906 (1969).
BS57 H. A. Bethe and E. E. Salpeter, *Quantum Mechanics of One- and Two-Electron Atoms* (Springer, Berlin/Academic, New York, 1957).
BS69 O. Bely and S. B. Schwartz, J. Phys. B **2,** 159 (1969).
C62 J. W. Cooper, Phys. Rev. **128,** 681 (1962).
C69 J. P. Coleman, in *Case Studies in Atomic Collision Physics I,* edited by E. W. McDaniel and M. R. C. McDowell (North-Holland, Amsterdam, 1969), p. 101.
CF70 A. Crispin and G. N. Fowler, Rev. Mod. Phys. **42,** 290 (1970).

CK71 J. W. Cooper and H. Kolbenstvedt, Phys. Rev. A **3,** (to be published).

CL69 S. Chung and C. C. Lin, in *Sixth International Conference on the Physics of Electronic and Atomic Collisions: Abstracts of Papers* (M.I.T., Cambridge, Mass., 1969), p. 363.

CM69 B.-H. Choi and E. Merzbacher, Phys. Rev. **177,** 233 (1969).

CM70 B.-H. Choi and E. Merzbacher, Phys. Rev. A **1,** 299 (1970).

CMK70 G. E. Chamberlain, S. R. Mielczarek, and C. E. Kuyatt, Phys. Rev. A **2,** 1905 (1970).

CMKr70 T. A. Carlson, W. E. Moddeman, and M. O. Krause, Phys. Rev. A **1,** 1406 (1970); **3,** 834 (1971).

CMPK70 T. A. Carlson, W. E. Moddeman, B. P. Pullen, and M. O. Krause, Chem. Phys. Letters **5,** 390 (1970).

Cr70 D. S. F. Crothers, J. Phys. B **3,** 1211 (1970).

CR70 G. B. Crooks and M. E. Rudd, Phys. Rev. Letters **25,** 1599 (1970).

CS66 F. J. Comes and H. G. Sälzer, Phys. Rev. **152,** 29 (1966).

Cu69 H. Curien, in *International Tables for X-Ray Crystallography*, edited by C. H. MacGillavry and G. D. Rieck (Kynoch, Birmingham, England, 1969), 2nd ed., Vol. 3, p. 247.

D60 A. Dalgarno, Proc. Phys. Soc. (London) **76,** 422 (1960).

D69 K. T. Dolder, in *Case Studies in Atomic Collision Physics I*, edited by E. W. McDaniel and M. R. C. McDowell (North-Holland, Amsterdam, 1969), p. 251.

DA70 F. J. de Heer and J. F. M. Aarts, Physica **48,** 620 (1970).

DHRS67 D. F. Dance, M. F. A. Harrison, R. D. Rundel, and A. C. H. Smith, Proc. Phys. Soc. (London) **92,** 577 (1967).

DK63 G. H. Dunn and J. L. Kieffer, Phys. Rev. **132,** 2109 (1963).

DM68 C. E. Dick and J. W. Motz, Phys. Rev. **171,** 75 (1968).

DV67 G. H. Dunn and B. Van Zyl, Phys. Rev. **154,** 40 (1967).

DW66 T. deForest, Jr., and J. D. Walecka, Advan. Phys. **15,** 1; 491 (1966).

DZ61 S. D. Drell and F. Zachariasen, *Electromagnetic Structure of Nucleons* (Oxford U. P., London, 1961).

E55 G. Elwert, Z. Naturforsch. **10a,** 361 (1955).

EM69 D. G. Economides and M. R. C. McDowell, J. Phys. B **2,** 1323 (1969).

EP70 P. Eisenberger and P. M. Platzman, Phys. Rev. A **2,** 415 (1970).

ER68 A. K. Edwards and M. E. Rudd, Phys. Rev. **170,** 140 (1968).

ESTW69 H. Ehrhardt, M. Schulz, T. Tekaat, and K. Willmann, Phys. Rev. Letters **22,** 89 (1969).

EVD70 T. M. El-Sherbini, M. J. van der Wiel, and F. J. de Heer, Physica **48,** 157 (1970).

F24 E. Fermi, Z. Physik **29,** 315 (1924).

F31 J. W. Frame, Proc. Cambridge Phil. Soc. **27,** 511 (1931).

F40 E. Fermi, Phys. Rev. **57,** 485 (1940).

F51 R. P. Feynman, Phys. Rev. **84,** 108 (1951).

F54 U. Fano, Phys. Rev. **95,** 1198 (1954).

F56a U. Fano, Phys. Rev. **102,** 385 (1956).

F56b U. Fano, Phys. Rev. **103,** 1202 (1956).

F61 U. Fano, Phys. Rev. **124,** 1866 (1961).

F63 U. Fano, Ann. Rev. Nucl. Sci. **13,** 1 (1963).

F69 U. Fano, Phys. Rev. **178,** 131; **184,** 250 (1969).

F70 U. Fano, in *Changed Particle Tracks in Solids and Liquids*, edited by G. E. Adams, D. K. Bewley, and J. W. Boag (The Institute of Physics and The Physical Society, London, 1970), p. 1 (Proceedings of the Second L. H. Gray Conference, Cambridge, England, April 1969).

FC68 U. Fano and J. W. Cooper, Rev. Mod. Phys. **40,** 441 (1968); **41,** 724 (1969).

FH14 J. Franck and G. Hertz, Verhandl. Phys. Ges. **16,** 457 (1914).

FT64 U. Fano and J. E. Turner, in *Studies in Penetration of Charged Particles in Matter* (National Academy of Sciences—National Research Council, Washington, D.C., 1964), p. 49 (Nuclear Science Series, Report 39, Committee on Nuclear Science. Publication 1133).

G63 J. Geiger, Z. Physik **175,** 530 (1963).

G64a J. Geiger, Z. Physik **177,** 138 (1964).

G64b J. Geiger, Z. Physik **181,** 413 (1964).

G66 R. H. Garstang, J. Chem. Phys. **44,** 1308 (1966).

G67 T. A. Green, Phys. Rev. **157,** 103 (1967).

G68 R. H. Garstang, J. Phys. B **1,** 847 (1968).

G70 I. P. Grant, Adv. Phys. **19,** 747 (1970).

Ga66 M. K. Gailitis, in *Atomic Collisions. The Theory of Electron-Atom Collisions*, edited by V. Ya. Veldre, R. Ya. Damburg, and R. K. Peterkop, translated by M. V. Kurepa (Butterworth, London, 1966), p. 81, 1.87.

GB65 D. E. Golden and H. W. Bandel, Phys. Rev. **138,** A14 (1965).

GB66 D. E. Golden and H. W. Bandel, Phys. Rev. **149,** 58 (1966).

GBS66 D. E. Golden, H. W. Bandel, and J. A. Salerno, Phys. Rev. **146,** 40 (1966).

GCMH69 D. E. Groce, D. G. Costello, J. W. McGowan, and D. F. Herring, in *Sixth International Conference on the Physics of Electronic and Atomic Collisions: Abstracts of Papers* (*M.I.T.*, Cambridge, Mass., 1969), p. 757.

GD67 A. E. S. Green and S. K. Dutta, J. Geophys. Res. **72,** 3933 (1967).

Ge68 J. Geiger, *Elektronen und Festkörper- Anregungen, Energieverluste, dielektrische Theorie* (Friedr. Vieweg, Braunschweig, 1968).

GH60 A. H. Gabriel and D. W. O. Heddle, Proc. Roy. Soc. (London) **A258,** 124 (1960).

GH67 A. Gaudin and R. Hagemann, J. Chim. Phys. **64,** 1209 (1967).

GI68 A. E. Glassgold and G. Ialongo, Phys. Rev. **175,** (1968).

GM9 H. Geiger and E. Marsden, Proc. Roy. Soc. (London) **A82,** 495 (1909).

GP68 T. A. Green and J. M. Peek, Phys. Rev. **169,** 37 (1968).

GP69 T. A. Green and J. M. Peek, Phys. Rev. **183,** 166 (1969).

Gr66 A. E. S. Green, AIAA J. **4,** 769 (1966).

GS65 J. Geiger and W. Stickel, J. Chem. Phys. **43,** 4535 (1965).

GS68 J. Geiger and B. Schröder, J. Chem. Phys. **49,** 740 (1968).

GS69a J. Geiger and H. Schmoranzer, J. Mol. Spectry. **32,** 39 (1969).

GS69b J. Geiger and B. Schröder, J. Chem. Phys. **50,** 7 (1969).

GT66 J. Geiger and M. Topschowsky, Z. Naturforsch. **21a,** 626 (1966).

GW64 M. L. Goldberger and K. M. Watson, *Collision Theory* (Wiley, New York, 1964).

GW65 J. Geiger and K. Wittmaack, Z. Naturforsch. **20a,** 628 (1965).

H33 W. Henneberg, Z. Physik **86,** 592 (1933).

H69a A. R. Holt, J. Phys. B **2,** 1202 (1969).

H69b A. R. Holt, J. Phys. B **2,** 1209 (1969).

H71 R. D. Hudson, "Critical Review of Photoabsorption Cross Sections for Molecules of Astrophysical and Aeronomic Interest," Rev. Geophys. Space Phys. **9,** (1971).

HBE64 J. O. Hirschfelder, W. B. Brown, and S. T. Epstein, Advan. Quantum Chem. **1,** 256 (1964).

HHMM62 J. W. Hooper, D. S. Harmer, D. W. Martin, and E. W. McDaniel, Phys. Rev. **125,** 2000 (1962).

HL69 H. H. Heckman and P. J. Lindstrom, Phys. Rev. Letters **22,** 871 (1969).

HTL63a R. E. Huffman, Y. Tanaka, and J. C. Larrabee, J. Chem. Phys. **39,** 902 (1963).

HTL63b R. E. Huffman, Y. Tanaka, and J. C. Larrabee, Appl. Opt. **2,** 947 (1963).

HM68a A. R. Holt and B. L. Moiseiwitsch, J. Phys. B **1,** 36 (1968).

HM68b A. R. Holt and B. L. Moiseiwitsch, Advan. At. Mol. Phys. **4,** 143 (1968).

HR68a I. V. Hertel and K. J. Ross, J. Phys. B **1,** 697 (1968).

HR68b I. V. Hertel and K. J. Ross, Phys. Rev. Letters **21,** 1511 (1968).

HR69a I. V. Hertel and K. J. Ross, J. Phys. B **2,** 285 (1969).

HR69b I. V. Hertel and K. J. Ross, in *Sixth International Conference on the Physics of Electronic and Atomic Collisions: Abstracts of Papers* (M. I. T. ,Cambridge, Mass., 1969), p. 280.

Hu69 J. H. Hubbell, Natl. Std. Ref. Data Ser., Natl. Bur. Std. (U.S.) **29** (1969).

I63 M. Inokuti, Argonne National Laboratory Report No. ANL-6769, p. 7 1963.

I66 M. Inokuti, Argonne National Laboratory Report No. ANL-7220, p. 1, 1966.

IK68 M. Inokuti and Y.-K. Kim, Phys. Rev. **173,** 154 (1968).

IK69 M. Inokuti and Y.-K. Kim, Phys. Rev. **186,** 100 (1969).

IKP67 M. Inokuti, Y.-K. Kim, and R. L. Platzman, Phys. Rev. **164,** 55 (1967).

IP65 M. Inokuti and R. L. Platzman, in *Fourth International Conference on the Physics of Electronic and Atomic Collisions: Abstracts of Papers* (Science Bookcrafters, Hastings-on-Hudson, New York, 1965), p. 408; Argonne National Laboratory Report ANL-7060, p. 7, 1965.

J48 E. A. Jones, Ph.D. thesis, Ohio State University, 1948.

JM65 C. J. Joachain and M. H. Mittleman, Phys. Rev. **140,** A432 (1965).

JV70 C. J. Joachain and R. K. van den Eynde, Physica **46,** 8 (1970).

K59 R. Kubo, Lectures Theoret. Phys., **1,** 120.

K61 J. Karle, J. Chem. Phys. **35,** 963 (1961).

K63 C. Kittel, *Quantum Theory of Solids* (Wiley, New York, 1963), Chaps. 6, 19.

K65 A. E. Kingston, Proc. Phys. Soc. (London) **86,** 467 (1965).

K68 C. E. Kuyatt, Methods Exp. Phys. **7,** 1 (1968).

K69 K. G. Kessler, Comments At. Mol. Phys. **1,** 70 (1969).

KCM69 G. S. Khandelwal, B. H. Choi, and E. Merzbacher, Atomic Data **1,** 103 (1969).

KD66 L. J. Kieffer and G. H. Dunn, Rev. Mod. Phys. **38,** 1 (1966).

Ke69 J. Kessler, Rev. Mod. Phys. **41,** 3 (1969).

Ki69 L. J. Kieffer, Atomic Data **1,** 19, 120, 359 (1969).

KI68 Y.-K. Kim and M. Inokuti, Phys. Rev. **175,** 176 (1968).

KI69a Y.-K. Kim and M. Inokuti, Phys. Rev. **181,** 205 (1969).

KI69b Y.-K. Kim and M. Inokuti, Phys. Rev. **184,** 38 (1969).

KI70 Y.-K. Kim and M. Inokuti, Phys. Rev. A **1,** 1132 (1970).

KI71 Y.-K. Kim and M. Inokuti, Phys. Rev. A **3,** 665 (1971).

KICM68 Y.-K. Kim, M. Inokuti, G. E. Chamberlain, and S. R. Mielczarek, Phys. Rev. Letters **21,** 1146 (1968).

KK68 D. J. Kennedy and A. E. Kingston, J. Phys. B **1,** 195 (1968).

KL70 J. Kessler and J. Lorenz, Phys. Rev. Letters **24,** 87 (1970).

KM66a G. S. Khandelwal and E. Merzbacher, Phys. Rev. **144,** 349 (1966).

KM66b G. S. Khandelwal and E. Merzbacher, Phys. Rev. **511,** 12 (1966).

KM69 M. Krauss and S. R. Mielczarek, J. Chem. Phys. **51,** 5241 (1969).

KMC69 L. Kerwin, P. Marmet, and J. D. Carette, in *Case Studies in Atomic Collision Physics I,* edited by E. W. McDaniel and M. R. C. McDowell (North-Holland, Amsterdam, 1969), p. 527.

KMS60 A. E. Kingston, B. L. Moiseiwitsch, and B. G. Skinner, Proc. Roy. Soc. (London) **A258,** 245 (1960).

KS64 C. E. Kuyatt and J. A. Simpson, in *Atomic Collision Processes. The Proceedings of the Third International Conference on the Physics of Electronic and Atomic Collisions,* edited by M. C. R. McDowell (North-Holland, Amsterdam, 1964), p. 191.

KSD65 A. E. Kingston, B. L. Schram, and F. J. de Heer, Proc. Phys. Soc. (London) **86,** 1374 (1965).

KSLCM70 M. C. Krause, F. A. Stevie, L. J. Lewis, T. A. Carlson, and W. E. Moddeman, Phys. Letters **31A,** 81 (1970).

L65 E. N. Lassettre, J. Chem. Phys. **43,** 4479 (1965).

L69 E. N. Lassettre, Can. J. Chem. **47,** 1733 (1969).

L70 E. N. Lassettre, J. Chem. Phys. **53,** 3801 (1970).

LF64 E. N. Lassettre and S. A. Francis, J. Chem. Phys. **40,** 1208 (1964).

LGMS65 E. N. Lassettre, F. M. Glaser, V. D. Meyer, and A. Skerbele, J. Chem. Phys. **42,** 3429 (1965).

LL65 L. D. Landau and E. M. Lifshitz, *Quantum Mechanics. Non-Relativistic Theory,* translated by J. B. Sykes and J. S. Bell (Pergamon, London, 1965), 2nd ed.

LLS61 J. Lawson, W. Lawson, and M. J. Seaton, Proc. Phys. Soc. (London) **77,** 192 (1961).

LJ64 E. N. Lassettre and E. A. Jones, J. Chem. Phys. **40,** 1218 (1964).

LKS64 E. N. Lassettre, M. E. Krasnow, and S. Silverman, J. Chem. Phys. **40,** 1242 (1964).

LMD68 G. M. Lawrence, D. L. Mickey, and K. Dressler, J. Chem. Phys. **48,** 1989 (1968).

LS65 E. N. Lassettre and J. C. Shiloff, J. Chem. Phys. **43,** 560 (1965).

LSD69 E. N. Lassettre, A. Skerbele, and M. A. Dillon, J. Chem. Phys. **50,** 1829 (1969).

LSD70 E. N. Lassettre, A. Skerbele, and M. A. Dillon, J. Chem. Phys. **52,** 2797 (1970).

LSDR68 E. N. Lassettre, A. Skerbele, M. A. Dillon, and K. J. Ross, J. Chem. Phys. **48,** 5066 (1968).

LSM66 E. N. Lassettre, A. Skerbele, and V. D. Meyer, J. Chem. Phys. **45,** 3214 (1966).

LW58 E. N. Lassettre and E. R. White, The Ohio State University Research Foundation Scientific Report No. 12 (AFCRC-TN-58-406), 1958 (unpublished).

M30 N. F. Mott, Proc. Roy. Soc. (London) **A126,** 259 (1930).

M31 N. F. Mott, Proc. Cambridge Phil. Soc. **27,** 553 (1931).

M32 C. Møller, Ann. Physik **14,** 531 (1932).

M53 G. W. McClure, Phys. Rev. **90,** 796 (1953).

M56 W. F. Miller, Ph.D. thesis, Purdue University, 1956 (unpublished).

M65 R. A. Mapleton, J. Chem. Phys. **42,** 1846 (1965).

M66 B. L. Moiseiwitsch, Proc. Phys. Soc. (London) **87,** 885 (1966).

M67 M. H. Mittleman, Phys. Rev. **164,** 48 (1967).

M68 C. B. O. Mohr, Advan. At. Mo. Phys. **4,** 221 (1968).

M69 K. J. Miller, J. Chem. Phys. **51,** 5235 (1969).

M70 J. Macek, Phys. Rev. A **1,** 235 (1970).

M71 K. J. Miller, "Electron Scattering Off Atoms for Excitation to Valence and Rydberg States," Intern. J. Quantum Chem. **5,** (1971).

Ma69 S. T. Manson, in *Sixth International Conference on the Physics of Electronic and Atomic Collisions: Abstracts of Papers* (M. I. T., Cambridge, Mass., 1969), p. 626.

Ma71 S. T. Manson, Phys. Rev. A**3,** 1260 (1971).

MBG69 H. S. W. Massey, E. H. S. Burhop, and H. G. Gilbody, *Electronic and Ionic Impact Phenomena* (Oxford, U. P., London, 1969), 2nd ed.

Mc69 J. C. McConnell, Ph.D. thesis, The Queen's University of Belfast, 1969 (unpublished).

Mc71 E. J. McGuire, Phys. Rev. A **3,** 267 (1971).

MD67 H. R. Moustafa Moussa and F. J. de Heer, Physica **36,** 646 (1967).

MDPM70 G. Missoni, C. E. Dick, R. C. Placious, and J. W. Motz, Phys. Rev. A **2,** 2309 (1970).

MDS69 H. R. Moustafa Moussa, F. J. de Heer, and J. Schutten, Physica **40,** 517 (1969).

MG51 C. J. Mullin and E. Guth, Phys. Rev. **82,** 141 (1951).

MGV63 S. Meyerson, H. M. Grub, and R. W. Vander Haar, J. Chem. Phys. **39,** 1447 (1963).

MK67 K. J. Miller and M. Krauss, J. Chem. Phys. **47,** 3754 (1967).

MK68 K. J. Miller and M. Krauss, J. Chem. Phys. **48,** 2611 (1968).

ML65 V. D. Meyer and E. N. Lassettre, J. Chem. Phys. **42,** 3436 (1965).

ML66 V. D. Meyer and E. N. Lassettre, J. Chem. Phys. **44,** 2535 (1966).

MM31 H. S. W. Massey and C. B. O. Mohr, Proc. Roy. Soc. (London) **A132,** 605 (1931).

MM33 H. S. W. Massey and C. B. O. Mohr, Proc. Roy. Soc. (London) **A140,** 613 (1933).

MM65 N. F. Mott and H. S. W. Massey, *The Theory of Atomic Collisions* (Oxford U. P., London, 1965), 3rd ed.

MMH56 L. Marton, C. Marton, and W. G. Hall, Natl. Bur. Std. Circ. **571,** (1956).

MMK69 K. J. Miller, S. R. Mielczarek, and M. Krauss, J. Chem. Phys. **51,** 26 (1969).

Mo32 P. M. Morse, Physik. Z. **33,** 443 (1932).

MOK64 J. W. Motz, H. Olsen, and H. W. Koch, Rev. Mod. Phys. **36,** 881 (1964).

MP57 W. F. Miller and R. L. Platzman, Proc. Phys. Soc. (London) **A70,** 299 (1957).

MP65 B. L. Moiseiwitsch and R. Perrin, Proc. Phys. Soc. (London) **85,** 51 (1965).

MS41 L. Marton and L. I. Schiff, J. Appl. Phys. **12,** 759 (1941).

MS68 B. L. Moiseiwitsch and S. J. Smith, Rev. Mod. Phys. **40,** 238 (1968); **41,** 574 (1969).

MSL65a V. D. Meyer, A. Skerbele, and E. N. Lassettre, J. Chem. Phys. **43,** 805 (1965).

MSL65b V. D. Meyer, A. Skerbele, and E. N. Lassettre, J. Chem. Phys. **43,** 3769 (1965).

N30 C. E. Normand, Phys. Rev. **35,** 1217 (1930).

N64 P. Nozières, *Theory of Interacting Fermi Systems,* translated by D. Hone (Benjamin, New York, 1964).

O65 W. J. B. Oldham, Jr., Phys. Rev. **140,** A1477 (1965).

O67 W. J. B. Oldham, Jr., Phys. Rev. **161,** 1 (1967).

O68a W. J. B. Oldham, Jr., Phys. Rev. **166,** 34 (1968).

O68b W. J. B. Oldham, Jr., Phys. Rev. **174,** 145 (1968); **181,** 463 (1969).

O69 W. J. B. Oldham, Jr., Phys. Rev. **186,** 52 (1969).

OM71 W. J. B. Oldham, Jr., and B. P. Miller Phys. Rev. A **3,** 948 (1971).

Om65a K. Omidvar, Phys. Rev. **140,** A26 (1965).

Om65b K. Omidvar, Phys. Rev. **140,** A38 (1965).

Om69a K. Omidvar, Phys. Rev. **177,** 212 (1969).

Om69b K. Omidvar, Phys. Rev. **188,** 140 (1969).

ONT70 N. Oda, F. Nishimura, and S. Tahira, Phys. Rev. Letters **24,** 42 (1970).

OPB71 C. B. Opal, W. K. Peterson, and E. C. Beaty "Energy and Angular Distribution of Electrons Ejected in Ionizing Collisions of Electrons with Helium," J. Phys. B (to be published); "Measurement of Secondary Electron Spectra by Electron Impact Ionization of a Number of Simple Gases" Phys. Rev. (to be published).

P52 G. Placzek, Phys. Rev. **86,** 377 (1952).

P56 H. S. Perlman, Proc. Phys. Soc. (London) **A69,** 318 (1956).

P59 C. L. Pekeris, Phys. Rev. **115,** 1216 (1959).

P60 R. L. Platzman, J. Phys. Radium **21,** 853 (1960).

P62 R. L. Platzman, Vortex **23,** 372 (1962).

P63 R. L. Platzman, J. Chem. Phys. **38,** 2775 (1963).

P64 J. M. Peek, Phys. Rev. **134,** A877 (1964).

P65a J. M. Peek, Phys. Rev. **139,** A1429 (1965).

P65b J. M. Peek, Phys. Rev. **140,** A11 (1965).

P67 J. M. Peek, Phys. Rev. **154,** 52 (1967).

P69 J. M. Peek, Phys. Rev. **183,** 193 (1969).

PD71 B. Peart and K. T. Dolder, "Cross Sections for the Production of Protons by Collision Between Electrons and H_2 ions," unpublished.

Pea65 G. Peach, Proc. Phys. Soc. (London) **85,** 709 (1965).

Per65 J. C. Person, J. Chem. Phys. **43,** 2553 (1965).

PG69 J. M. Peek and T. A. Green, Phys. Rev. **183,** 202 (1969).

PGW67 J. M. Peek, T. A. Green, and W. H. Weihofen, Phys. Rev. **160,** 117 (1967).

PL67 L. I. Pivovar and Yu. Z. Levchenko, Zh. Eksp. Teor. Fiz. **52,** 42 (1967) [Sov. Phys. JETP **25,** 27 (1967)].

PN68 J. C. Person and P. P. Nicole, J. Chem. Phys. **49,** 5421 (1968).

PN70 J. C. Person and P. P. Nicole, J. Chem. Phys. **53,** 1767 (1970).

Po67 C. J. Powell, Health Phys. **13,** 1265 (1967).

PS69 J. T. Park and F. D. Schowengerdt, Phys. Rev. **185,** 152 (1969).

PWD69 B. Peart, D. S. Walton, and K. T. Dolder, J. Phys. B **2,** 1347 (1969).

PWD70 B. Peart, D. S. Walton, and K. T. Dolder, J. Phys. B **3,** 1346 (1970).

R11 E. Rutherford, Phil. Mag. **21,** 669 (1911).

R59 F. Rohrlich, Lectures Theoret. Phys. **1,** 1 (1959).

R64 F. H. Read, Proc. Phys. Soc. (London) **83,** 619 (1964).

R65 H. Reather, Springer Tracts in Modern Physics **38,** 84 (1956).

R68 M. R. H. Rudge, Rev. Mod. Phys. **40,** 564 (1968).

RD67 S. Rothenberg and E. R. Davidson, J. Mol. Spectry. **22,** 1 (1967).

RE65 D. Rapp and P. Englander-Golden, J. Chem. Phys. **43,** 1464 (1965).

RF67 A. R. P. Rau and U. Fano, Phys. Rev. **162,** 68 (1967).

RG69 M. E. Rudd and D. Gregoire, in *Physics of the One- and Two-Electron Atoms,* edited by F. Bopp and H. Kleinpoppen (North-Holland, Amsterdam, 1969), p. 795.

RL66 K. J. Ross and E. N. Lassettre, J. Chem. Phys. **44,** 4633 (1966).

RP65–70 F. F. Rieke and W. Prepejchal, Argonne National Laboratory Report ANL-7060, p. 33 (1965); ANL-7220, p. 19 (1966); ANL-7360, p. 50 (1967); ANL-7489, p. 99 (1968); ANL-7615, p. 214 (1969); ANL-7760-I, p. 87, (1970). See also *Sixth International Conference on the Physics of Electronic and Atomic Collisions: Abstracts of Papers* (M. I. T., Cambridge, Mass., 1969), p. 623.

RS68 M. E. Rudd and K. Smith, Phys. Rev. **169,** 79 (1968).

RSB66 M. E. Rudd, C. A. Sautter, and C. L. Bailey, Phys. Rev. **151,** 20 (1966).

RW63 F. W. Read and G. L. Whiterod, Proc. Phys. Soc. (London) **82,** 434 (1963).

RW65 F. H. Read and G. L. Whiterod, Proc. Phys. Soc. (London) **85,** 71 (1965).

S30 P. T. Smith, Phys. Rev. **36,** 1293 (1930).

S51 M. J. Seaton, Proc. Roy. Soc. (London) **A208,** 418 (1951).

S58 S. M. Silverman, Phys. Rev. **111,** 1114 (1958).

S61 M. J. Seaton, Proc. Phys. Soc. (London) **77,** 184 (1961).

S62 M. J. Seaton, Proc. Phys. Soc. (London) **79,** 1105 (1962).

S65 I. H. Sloan, Proc. Phys. Soc. (London) **85,** 435 (1965).

S66 B. L. Schram, Physica **32,** 197 (1966).

S68 L. I. Schiff, *Quantum Mechanics* (McGraw-Hill, New York, 1968), 3rd ed.

S69 A. Salin, J. Phys. B **2,** 631 (1969).

S70 A. F. Starace, Phys. Rev. A **2,** 118 (1970).

S71 A. F. Starace, Phys. Rev. A **3,** 1242 (1971).

SBK66 B. L. Schram, A. J. H. Boerboom, and J. Kistemaker, Physica **32,** 185 (1966).

Sc70 B. Schneider, Phys. Rev. A **2,** 1873 (1970).

SDL67 A. Skerbele, M. A. Dillon, and E. N. Lassettre, J. Chem. Phys. **46,** 4161 (1967).

SDMBK66 J. Schutten, F. J. de Heer, H. R. Moustafa, A. J. H. Boerboom, and J. Kistemaker, J. Chem. Phys. **44,** 3924 (1966).

SDVK65 B. L. Schram, F. J. de Heer, M. J. van der Wiel, and J. Kistemaker, Physica **31,** 94 (1965).

Se70 M. J. Seaton, Comments At. Mol. Phys. **2,** 37 (1970).

Sh71 I. Shimamura, J. Phys. Soc. Japan **30,** 824 (1971).

SKYW70 H. Suzuki, A. Konishi, M. Yamamoto, and K. Wakiya, J. Phys. Soc. Japan **28,** 534 (1970).

SL58 S. M. Silverman and E. N. Lassettre, J. Chem. Phys. **29,** 891 (1958).

SL64 S. M. Silverman and E. N. Lassettre, J. Chem. Phys. **40,** 1265 (1964).

SL66 A. Skerbele and E. N. Lassettre, J. Chem. Phys. **45,** 1077 (1966).

SL70a A. Skerbele and E. N. Lassettre, J. Chem. Phys. **52,** 2708 (1970).

SL70b A. Skerbele and E. N. Lassettre, J. Chem. Phys. **53,** 3806 (1970).

SLi70 J. C. Steelhammer and S. Lipsky, J. Chem. Phys. **53,** 1445 (1970).

SM69 J. A. Simpson and S. R. Mielczarek, in *Sixth International Conference on the Physics of Electronic and Atomic Collisions: Abstracts of Papers* (M. I. T., Cambridge, Mass., 1969), p. 344.

SML64 R. M. St. John, F. L. Miller, and C. C. Lin, Phys. Rev. **134,** A888 (1964).

SMSD66 B. L. Schram, H. R. Moustafa, J. Schutten, and F. J. de Heer, Physica **32,** 734 (1966).

SN70 A. Salop and H. H. Nakano, Phys. Rev. A **2,** 127 (1970).

SP64 B. Schiff and C. L. Pekeris, Phys. Rev. **134,** A638 (1964).

SSLF70 F. A. Sharpton, R. M. St. John, C. C. Lin, and F. E. Fajen, Phys. Rev. A **2,** 1305 (1970).

SVDM66 B. L. Schram, M. J. van der Wiel, F. J. de Heer, and H. R. Moustafa, J. Chem. Phys. **44,** 49 (1966).

T12 J. J. Thomson, Phil. Mag. **23,** 449 (1912).

T67 E. W. Thomas, Phys. Rev. **164,** 151 (1967).

T71 L. H. Toburen, Phys. Rev. A **3,** 216 (1971).

TB69 C. Tavard and R. A. Bonham, J. Chem. Phys. **50,** 1736 (1969).

TBGF70 H. Tai, R. H. Bassel, E. Gerjuoy, and V. Franco, Phys. Rev. A **1,** 1819 (1970).

TCK68 D. G. Truhlar, D. C. Cartwright, and A. Kuppermann, Phys. Rev. **175,** 113 (1968).

TCRBK68 S. Trajmar, D. C. Cartwright, J. K. Rice, R. T. Brinkmann, and A. Kuppermann, J. Chem. Phys. **49,** 5464 (1968).

TRK70 S. Trajmar, J. K. Rice, and A. Kuppermann, Advan. Chem. Phys. **18,** 15 (1970).

TRKTC70 D. G. Truhlar, J. K. Rice, A. Kuppermann, S. Trajmar, and D. C. Cartwright, Phys. Rev. A **1,** 778 (1970).

V31 L. C. Van Atta, Phys. Rev. **38,** 876 (1931).

V54 L. Van Hove, Phys. Rev. **95,** 249 (1954).

V67 L. Vriens, Phys. Rev. **160,** 100 (1967).

V69 L. Vriens, in *Case Studies in Atomic Collision Physics I,* edited by E. W. McDaniel and M. R. C. McDowell (North-Holland, Amsterdam, 1969), p. 337.

V70 R. Vanderpoorten, Physica **48,** 254 (1970).

VC70 L. Vriens and J. D. Carriere, Physica **49,** 517 (1970).

VCM71 D. A. Vroom, A. R. Comeaux, and J. W. McGowan, "Energy and Angular Distributions of Secondary Electrons Ejected from Argon by Fast Electrons," (unpublished).

VD69a D. A. Vroom and F. J. de Heer, J. Chem. Phys. **50,** 573 (1969).

VD69b D. A. Vroom and F. J. de Heer, J. Chem. Phys. **50,** 580 (1969).

VD69c D. A. Vroom and F. J. de Heer, J. Chem. Phys. **50,** 1883 (1969).

VdB69a J. van den Bos, Physica **42,** 245 (1969).

VdB69b J. van den Bos, Phys. Rev. **181,** 191 (1969).

CDJ70 J. van Eck and J. P. de Jongh, Physica **47,** 141 (1970).

VdW70 M. J. van der Wiel, Physica **49,** 411 (1970).

VEV69 M. J. van der Wiel, T. M. El-Sherbini, and L. Vriens, Physica **42,** 411 (1969).

VG61 R. T. Van de Walle and C. C. Grosjean, Nuovo Cimento **19,** 872 (1961).

VK70 R. J. van Brunt and L. J. Kieffer, Phys. Rev. A **2,** 1293 (1970).

VP68 L. A. Vaĭnshteĭn and L. P. Presnyakov, Zh. Eksp. Teor. Fiz. **55,** 297 (1968) [Sov. Phys. JETP **28,** 156 (1969)].

VSM68 L. Vriens, J. A. Simpson, and S. R. Mielczarek, Phys. Rev. **165,** 7 (1968).

VW71 M. J. van der Wiel and G. Wiebes, "Multiple Ionization of Ar by 10 KeV Electrons as a Function of the Energy Loss," Physica (to be published).

VZ68 R. J. Van Brunt and R. N. Zare, J. Chem. Phys. **48,** 4304 (1968).

W29 G. Wentzel, Z. Physik **58,** 348 (1929).

W33 J. A. Wheeler, Phys. Rev. **43,** 258 (1933).

W37 C. F. v. Weizsäcker, Z. Physik **88,** 612 (1937).

W45 E. J. Williams, Rev. Mod. Phys. **17,** 217 (1945).

W51 M. C. Walske, Ph.D. thesis, Cornell University, 1951 (unpublished).

W52 M. C. Walske, Phys. Rev. **88,** 1283 (1952).

W56 M. C. Walske, Phys. Rev. **101,** 940 (1956).

W67 A. W. Weiss, J. Res. Natl. Bur. Std. **71A,** 163 (1967).

W69 K. G. Williams, in *Sixth International Conference on the Physics of Electronic and Atomic Collisions: Abstracts of Papers* (M. I. T., Cambridge, Mass., 1969), p. 731.

W70 G. Wiebes, Physica **48,** 407 (1970).

Wo69 L. Wolniewicz, J. Chem. Phys. **51,** 5002 (1969).

WO62 T.-Y. Wu and T. Ohmura, *Quantum Theory of Scattering* (Prentice-Hall, Englewood Cliffs, N.J., 1962).

WP34 R. Whiddington and H. Priestley, Proc. Roy. Soc. (London) **A145,** 462 (1934).

WT34 R. Whiddington and J. E. Taylor, Proc. Roy. Soc. (London) **A145,** 465 (1934).

WW35 R. Whiddington and E. G. Woodroofe, Phil. Mag. **20,** 1109 (1935).

YS71 M. Yamamoto and H. Suzuki, "Energy Spectra of Electrons Emitted in Autoionization of Ar Excited by Electron Impact" J. Phys. Soc. Japan (to be published).

Z66 I. P. Zapesochnyi, Astron. Zh. **43,** 954 (1966) [Sov. Astron. AJ **10,** 766 (1967)].